THE VOLATILITY SPILLOVERS OF U.S. QUANTITATIVE EASING

EVIDENCE FROM AUSTRALIA

BY

HAMID YAHYAEI

DEPARTMENT OF APPLIED FINANCE

MACQUARIE BUSINESS SCHOOL

A dissertation submitted in partial fulfillment

of the requirements for the degree of

Master of Research in Applied Finance

SUPERVISORS

DR. ABHAY SINGH
DR. LURION DE MELLO

MACQUARIE UNIVERSITY

2020

STATEMENT OF ORIGINALITY

This work has not previously been submitted for a degree or diploma in any university. To the best of my knowledge and belief, the thesis contains no material previously published or written by another person except where due reference is made in the thesis itself.

Hamid Yahyaei

11 November 2020

ACKNOWLEDGEMENTS

"In the name of God, stop a moment, cease your work, look around you." – Leo Tolstoy

In my younger years, I experienced a lack of self-worth. As tragic as this sounds, these feelings of worthlessness are an unfortunate commonality for many. I realised that for those who do not reflect the values they are unquestionably expected to adopt, and for those who wish to voice their opinions in the face of mass conformity, the odds are often stacked against you. Sometimes, the only solace comes from believing in a higher cause. Whether it is divinity or an all-encompassing desire to work for the greater good, one must have something to rely on. It is akin to sailing across the unsteady ocean, holding tightly onto a barely seaworthy vessel, in hopes of reaching the elusive shore. I hope that all of us can remain abroad our vessels, no matter what we perceive them to be, to one day reach the beauty that awaits us.

It is with this thesis that I begin the journey towards the shore. To me, this is not a piece of academic work, but rather, it is a symbol of how far I have been privileged to venture. I must begin by thanking my parents. As immigrants in a foreign country, the hope of a better life for their children is the sweetest of all fruits. To my brothers, I hope that my accomplishments can ignite a fire in yourselves to achieve more than anyone could ever imagine for our family.

To Dr. Abhay Singh and Dr. Lurion De Mello, how could I ever amass the words necessary to thank you for your guidance and friendship. I look forward to our work together. To Professor Tom Smith, I hope that one day I can encompass a small piece of the characteristics you embody as the quintessential professor. To Professor Martina Linnenluecke, Dr. Dan Daugaard, Associate Professor Sean Turnell, Dr. Frank Song, Dr. Prashan Karunaratne, and the 'Systematic Persians', thank you for your unwavering belief in me. To Damien Wood, my mentor and friend, thank you for providing a young analyst his first opportunity to step foot in the world of finance. To Dr. Michael Armstrong, you have changed my life for the better.

Finally, to my love, Chloe, I look forward to what life has planned for us. To me, it is not the completion of this dissertation that is the reward for this journey, but rather, it is meeting you.

– Hamid Yahyaei

Contents

Abstract

This dissertation investigates the cross-market volatility spillovers induced by U.S. Quantitative Easing (QE) programs. Specifically, this study examines the volatility that commences in U.S. financial markets and spreads to Australian equity and government bond markets. The study features the creation of an implied volatility index for the Australian government bond market that is considered alongside other implied volatility indices to create dynamic measures of cross-market spillovers. Data-driven Structural Vector Autoregressive (SVAR) models are then estimated to assess the impact of an unexpected QE shock on volatility transmission. The study finds evidence of an intensification of volatility spillovers that is explained by QE, primarily during the period of policy normalisation. The QE-induced volatility transmission between the U.S. and Australian equity markets is found to be especially pronounced. Furthermore, the results show that contractionary QE shocks promote an increase in volatility spillovers, while expansionary shocks suppress them. This study is among the first to provide a comprehensive analysis of the cross-border effects of U.S. QE programs on Australian financial markets, contributing to a growing set of literature that examines the implications of unconventional monetary policies.

Keywords: Australian Financial Markets; Implied Volatility Indices; Quantitative Easing; Structural Vector Autoregression; Unconventional Monetary Policy; Volatility Spillovers

List of Tables

List of Figures

1. INTRODUCTION

Few events in history are as captivating as the bursting of the U.S. subprime mortgage bubble. Consequently, it comes as little surprise that an extensive corpus of literature examines the effects of this significant economic disturbance. While much emphasis is placed on the actions of the entities considered to have contributed to the crisis, an equally substantial focus is thrust upon the institutions mitigating the fallout. At the heart of the counteraction against the crisis is the U.S. Federal Reserve, who through a series of unconventional monetary policies endeavoured to support dysfunctional financial markets and stimulate economic activity. The most notable, and perhaps most contentious of these policies, termed Quantitative Easing (QE), involves the purchase of trillions worth of financial securities funded by the creation of bank reserves (Joyce et al., 2012).

This dissertation investigates the implications resulting from the Federal Reserve's QE policies, and in doing so, adds to the already considerable evidence that sizeable central bank stimulus can result in cross-market volatility spillovers that transcend the local bounds of the monetary operation. In particular, this study explores the bilateral transmission of QE-induced volatility between equity and government bond markets in the U.S. and Australia, conveying the far-reaching implications of unconventional monetary policy through a previously unexplored Australian dimension.

Section 1 begins with an account of the emergence of QE as an alternative to traditional monetary policy. Specifically, the impotence of the nominal policy rate in the face of a constraining zero lower bound justified the imposition of unorthodox policy measures. The transmission channels, that is, the means through which QE stimulates economic activity and supports financial markets are discussed, and in effect, illustrate the propensity for QE to have implications on a broad array of financial assets. Notably, this study remains agnostic to the channel through which QE affects financial markets, and instead, focuses on presenting evidence of its impacts. Specific features of the Federal Reserve's QE policies, entitled Large Scale Asset Purchases (LSAPs), are also explored, and attention is drawn to the evolution of the policy.

Section 2 then reviews the literature that examines the implications of QE, identifying two recurrent themes. First, a consensus emerges that shows QE promotes declines in government bond yields that resultingly influences a range of asset valuations. Second, recurring evidence is presented that affirms QE-induced volatility in U.S. financial markets can spread to markets in other geographic jurisdictions. Together, these elements serve as the basis on which this study builds, that is, the Federal Reserve's implementation of QE induces volatility spillovers between the U.S. and Australian financial markets. Moreover, since volatility is the second moment of the asset return distribution, volatility spillovers are akin to the spillover of risk, and as such, investigating risk transference is of material importance for the broader set of financial literature.

Section 3 turns to the data used to investigate the volatility spillovers between equity and government bond

markets in both countries. Specifically, a series of implied volatility indices are chosen as the representative market indices as they capture ex-ante volatility dynamics. To address the lack of an existing implied volatility index for the Australian government bond market, a novel index, entitled the AGSVIX, is constructed in a state-preference framework and constitutes one of the methodological contributions of this study. In addition, an implied volatility index that reflects the volatility dynamics in the Australian equity market prior to the onset of the financial crisis is constructed and fused into the existing AVIX series, alleviating a long-standing gap in empirical knowledge. Collectively, the implied volatility indices permit the derivation of aggregate and pairwise spillover indices that demonstrate bilateral risk transmission between the markets throughout time. The spillover indices are constructed using a recursive variant of the Diebold and Yilmaz (2012) framework, and to quantify the influence of the Federal Reserve's QE programs on these indices, a set of linear models that incorporate instruments that proxy the innovations in QE are estimated.

As an additional dimension, this study also examines the ramifications of an unexpected "QE shock" on volatility spillovers, defined as a change in the magnitude of the Federal Reserve's QE program. A series of Structural Vector Autoregressive (SVAR) models are estimated to derive impulse response functions that exhibit the expected short-term volatility transmission between each market. For robustness, three data-driven identification schemes are used to recover the structural shocks.

Section 4 explains the primary findings which are twofold. First, the evidence shows a significant influence of the Federal Reserve's QE programs on volatility spillovers. Notably, the volatility transmitted between the U.S. and Australian equity markets is material and the magnitude of risk spillover is at its greatest during the Federal Reserve's attempts at normalising its QE policies. Moreover, the evidence shows a simultaneous influence stemming from the Australian policy rate in contributing to spillovers, particularly among domestic markets. Second, short-term volatility spillovers are intensified when a contractionary QE shock is imposed, while an expansionary shock suppresses them. The shocks have a substantial influence on spillovers between the equity markets in both countries, shedding light on the codependency between equity markets in advanced economies. Together, the results illustrate the meaningful impact of QE on risk transferral from the U.S. to Australia.

Section 5 considers the policy-relevance of the findings. Specifically, the implications of QE on systemic risk are discussed and future opportunities to extend the study are also proposed. Section 6 concludes.

1.1 The Advent of Quantitative Easing

Before the adoption of unconventional monetary policies, central banks relied on the nominal policy rate as the key instrument to address economic conditions. Specifically, central banks adjusted the policy rate to promote low and stable inflation, fostering price stability, and targeting full employment (Joyce et al., 2012). This process of price-setting was propelled into favour during the 1990s as central banks in advanced economies embraced inflation-targeting frameworks that eliminated the inflationary pressures that plagued much of the 1970s and early 1980s (Svensson, 2000).

In contrast, the economic fallout following the bursting of the subprime mortgage bubble saw conventional monetary policy grow increasingly inadequate as a viable instrument. As nominal policy rates converged towards zero (Figure 1), concerns over the effectiveness of traditional monetary policy in mitigating the crisis served as an impetus for the trial of unconventional measures (Gagnon et al., 2018). Furthermore, the closely linked European Sovereign Debt crisis in 2010 served as additional motivation for the implementation of nonstandard policies, including negative interest rates and direct-lending operations (Meegan et al., 2018). Most prominently, to address dysfunctional financial markets and deflationary pressures, central banks in advanced economies including the Federal Reserve committed vigorously to QE, accumulating large holdings of financial assets (Figure 2). As a result, the adoption of QE instigated a transition away from price-setting, towards a nonstandard regime of actively using the central bank's balance sheet to increase the quantity of bank reserves, prodigiously expanding the monetary base and solidifying a turning point for central bank policy.

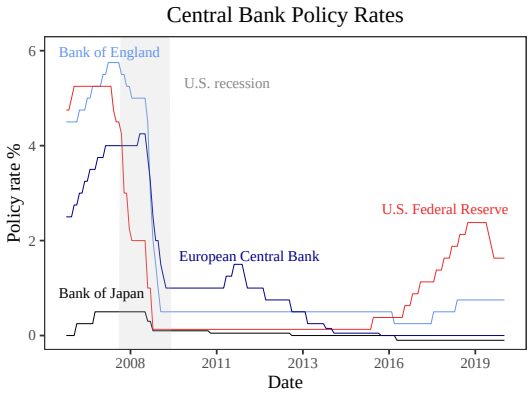

Bank for International Settlements (2020)

Figure 1: Central Bank Policy Rates

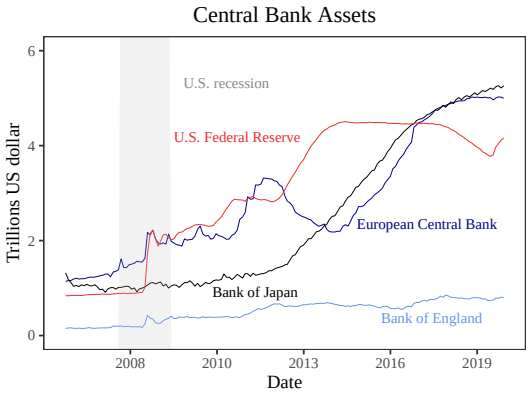

Federal Reserve Bank of St. Louis (2020a)

Figure 2: Central Bank Assets

Note. Central bank asset holdings are in USD at the prevailing spot exchange rate at the end of each month. The Bank of England discontinued publication of its weekly asset holdings in September 2014 and commenced publishing holdings quarterly. As such, monthly holdings from late 2014 are extrapolated between each quarter until March 2019, the most recent publication. Holdings beyond March 2019 are held at the same rate until the end of the year and changes in the value only reflect innovations in the exchange rate. U.S. recession refers to the National Bureau of Economic Research (2020) U.S. Business Cycle Contraction dates.

The concentration of central bank policy towards QE is underpinned by the premise that large-scale asset purchases can engender declines in long-term interest rates, overcoming the constraints of the zero lower bound (Bernanke et al., 2004). By way of exposition, as it purchases financial assets funded by the creation of bank reserves, the central bank grows its balance sheet and increases the broad supply of money to a level beyond the minimum needed to sustain the policy rate close to zero. As a result, the central bank incites further downward pressure on interest rates and overcomes the hindrances of a liquidity trap that renders conventional policy ineffective (Krugman et al., 1998). Ultimately, as bank reserves reach an abundant level, excess reserves, defined as reserves beyond the levels needed for regulatory and liquidity purposes, are expected to spillover to broader lending in the private sector. This spillover of excess reserves into wider lending results in an improvement in the availability and cost of funding, thus stimulating real economic activity (Joyce et al., 2012).

1.2 Transmission Channels

For financial markets, the relevance of QE is illustrated through its impact on the cost of funding when the conventional policy response is no longer efficacious, permitting the central bank to address tight financial conditions that amass during economic distress. In essence, QE allows the central bank to target asset prices and influence their yields (Fratzscher et al., 2018). How then, does the implementation of QE translate into an impact on the cost of funding? The answer to this question is uncovered by identifying the transmission channels that allow QE to influence financial markets. While these channels are multifaceted, there are two contemporaneously linked channels to consider. First, the signalling provided by QE announcements can influence the behaviour of market participants and affect their investment decisions (Bauer and Rudebusch, 2013). As announcements of QE reveal information on the state of the economy, market participants can form expectations on this information and adjust their investment holdings, thus affecting asset prices (Kawai, 2015). Moreover, within these announcements, the central bank can define its monetary policy stance and provide market participants an indication of its reaction function, thus nurturing (or suppressing) expectations for the path of the policy rate.

The second transmission channel that links QE to financial markets is the portfolio balance channel. As the central bank is indiscriminate to the prices of the assets it purchases and instead is focused on fulfilling its capacity as a lender of last resort, it plays the role of a liquidity provider *en masse*. In doing so, the central bank's sizeable purchases reduce the relative supplies of assets available to the private sector (Karadi and Nakov, 2020). This reduction in asset supply encourages market participants to reallocate capital into imperfect substitute securities, such as corporate debt and equity, thus reducing risk premia more broadly (Joyce et al., 2012). As the prices of riskier substitute assets increase, so too does the attractiveness of raising capital and investing, thus stimulating financial market activity. Notably, the premise of the portfolio balance channel is reliant on frictions propagated by market segmentation. Put concretely, the assumption

that market participants are constrained to transact among certain asset classes and within set maturities gives rise to imperfect substitutability (Modigliani and Sutch, 1966), providing a mechanism through which QE impacts broader asset prices.

Additionally, the creation of excess reserves serves as a transmission channel that is independent of the assets the central bank purchases. Christensen and Krogstrup (2019), citing the actions of the Swiss National Bank, show that the creation of excess reserves can impact the direction of long-term government bond yields, regardless of whether the central bank purchases assets outright. The authors illustrate a third, reserve-induced transmission channel that effects the cost of funding.

Together, these transmission channels provide insight into the link between QE and financial markets. This study, however, remains agnostic to the source of the transmission of QE onto financial markets and is instead focused on identifying the resulting impacts. Specifically, each of these channels has the propensity to increase financial market activity, thus triggering volatility. It is this idea of an intensification of volatility that may then spillover across markets that is of interest.

1.3 The U.S. Federal Reserve

The Federal Reserve's QE policies were implemented over a series of iterations, with the first in November 2008. The policies went through three stages of evolution. The first stage was a concentrated imposition of QE, focused on dealing with functionality issues in housing credit markets. The nature of the policy then shifted towards asset purchases to stimulate real economic activity, addressing concerns of lacklustre inflation in mid-2010. The final transformation involves its normalisation from 2013 onward.

The Federal Reserve's initial LSAPs targeted housing credit markets during the early stages of the crisis. Specifically, the Federal Reserve announced purchases of $500 billion in Mortgage-Backed Securities (MBS) and $100 billion in Government-Sponsored Enterprise (GSE) debt to address the elevated risk premia in these markets (Gagnon et al., 2018). In March 2009, the Federal Reserve expanded the size of the program by an additional $750 billion in MBS, $100 billion in GSE debt, and announced purchases of $300 billion in longer-term government securities, constituting its first involvement in the U.S. government bond market.

In contrast to the initial implementation of the policy, the Federal Reserve's subsequent iterations of QE modified the policy to incorporate a larger remit, thus no longer constraining its applicability upon an underlying state of economic distress. Specifically, in mid-2010, quantity targets for asset purchases were removed in preference for a pace of purchases that would sustain the size of the Federal Reserve's balance sheet. Debt that was close to maturity was reinvested into government securities, forcing the composition of the balance sheet towards government bonds (Figure 3). The rationale supporting this shift was based on concerns of continued undershooting of inflation targets and stagnant output growth. The Board of Governors of the Federal Reserve System (2010) emphasised their concerns on inflation in their August 2010 statement: "*Measures of underlying inflation have trended lower in recent quarters and, with substantial*

resource slack continuing to restrain cost pressures and longer-term inflation expectations stable, inflation is likely to be subdued for some time."

While the composition of the Federal Reserve's asset holdings shifted towards government securities, its liabilities also evolved. Specifically, excess reserves continued to increase, reflecting an expansion of the monetary base through the imposition of QE (Figure 3). Several further enlargements of the LSAPs continued into late 2012, culminating in three programs in total.

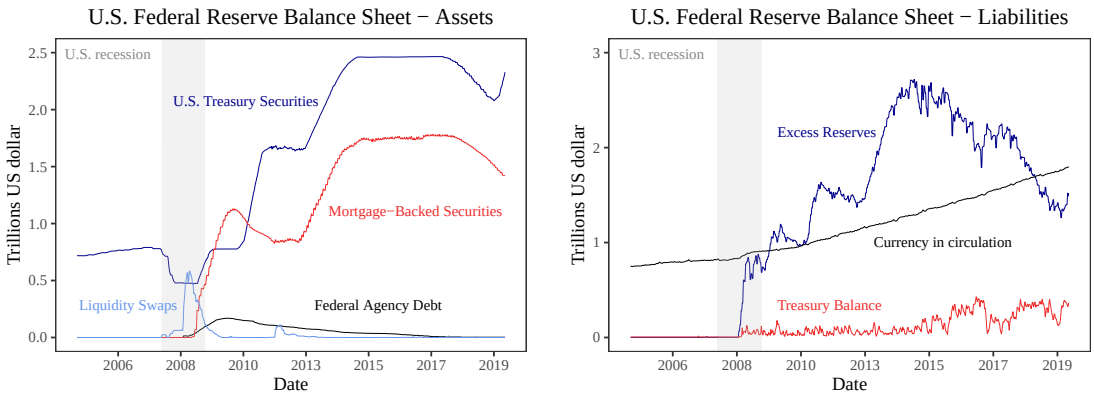

Federal Reserve Bank of St. Louis (2020a)

Figure 3: U.S. Federal Reserve Assets & Liabilities

In May 2013, the first indication of a potential curtailment of the Federal Reserve's LSAPs emerged. Specifically, in testimony to the U.S. Joint Economic Committee, Federal Reserve Chairman Ben Bernanke signalled that continued improvement in economic conditions would justify a moderation of purchases. This statement triggered significant global financial market volatility. Widely regarded as the "Taper tantrum", the reactions observed in asset prices following this announcement paved the way for concerns of financial market contagion as a result of QE (Kawai, 2015). The normalisation of the Federal Reserve's balance sheet would eventually commence in October 2017 and continue into 2019.

However, in late 2019, the Federal Reserve adjusted its policy normalisation process to address tight financial conditions in short-term U.S. dollar funding markets. The Federal Open Market Committee (FOMC) announced asset purchases would restart to ensure that bank reserves remained ample for the efficient implementation of monetary policy[1]. While not necessarily an evolution in the policy, the difficulty faced by the Federal Reserve in its attempts to normalise its balance sheet brings forth an interesting dilemma. Namely, that implications for financial markets may not only be found in the implementation of QE, but also in the normalisation process, much like the volatility experienced in mid-2013.

[1]The Federal Open Market Committee (FOMC) is responsible for directing open market operations. It comprises of 12 members including the 7 members of the Board of Governors of the Federal Reserve System and the 5 Federal Reserve Bank Presidents (Board of Governors of the Federal Reserve System, 2020a).

1.4 QE in the Australian Context

While the Reserve Bank of Australia (RBA) did not pursue unconventional policy measures to counteract the crisis, it did lower the policy rate in tandem with the Federal Reserve (Figure 4). Nevertheless, Australian financial markets are far from immune to the cross-boundary effects of QE as the economic links between the two countries serves as a conduit for volatility transmission. Specifically, both countries are advanced open economies with little capital market frictions between them, increasing the propensity for QE-induced volatility spillovers (MacDonald, 2017). Both countries also share significant cross-investments in debt and equity securities, with the U.S. accounting for the greatest proportion of foreign investment into Australian assets, while outbound Australian investments are likewise concentrated in the U.S. (Figure 5). The deeply liquid Australian dollar has also seen offshore investors, particularly central banks as part of their foreign reserve portfolios, hold an increasing proportion of Australian government securities, such that around 60 per cent of the investor base comprises of offshore agents (Australian Office of Financial Management, 2020a). Collectively, the economic links between the two countries elucidates the propensity for the Federal Reserve's actions to influence Australian financial markets.

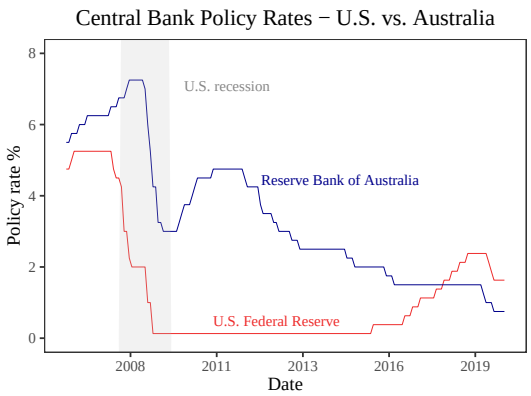

Bank for International Settlements (2020)

Figure 4: U.S. & Australian Policy Rates

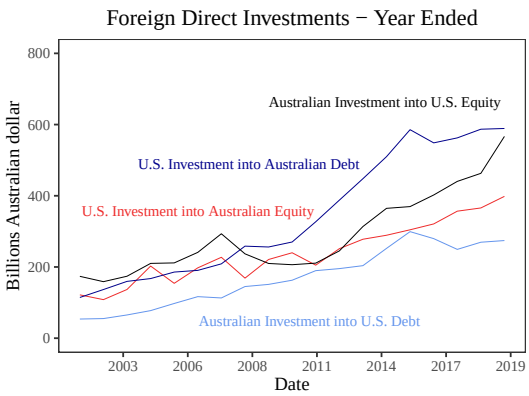

Australian Bureau of Statistics (2020)

Figure 5: Foreign Direct Investments

Despite the economic bonds between the two countries, Australian financial markets have been a non-existent element within studies that have examined cross-border volatility transmission induced by QE. When Australian markets are included in these studies, they are done so under a banner of aggregation. For instance, Bauer and Neely (2014) examine the effects of the Federal Reserve's QE programs on global government bond yields, including Australian government bonds. While the study sheds light on one dimension of the pass-through of QE, that is, through its effect on government bond yields, the study does little to dissect the nuanced dynamics of the Australian government bond market and its reaction to QE. Similarly, Neely (2015) examines government bond yields but solely focuses on movements in the yield of 10 year government bonds, with no consideration of other maturities.

Comparably, Australian markets are also neglected in studies assessing capital flows. For instance, Fratzscher et al. (2018) investigate the effects of the Federal Reserve's LSAPs in inducing portfolio balancing between 53 different markets, compartmentalising them as located in either advanced or emerging economies. While the scale of the study provides insight into the global implications of QE, the volatility spillovers onto the Australian financial markets are clouded through an aggregation of the effects. Likewise, Lavigne et al. (2014) look at capital flows between advanced and emerging economies, combining the effects of QE on Australian markets among eight advanced economies, again presenting the same issue.

2. REVIEW OF LITERATURE

The adoption of unconventional monetary policy has given rise to a new dimension of financial market research. Specifically, evidence of amplified intensity in the moments of asset prices, distinctly, asset price variance, has fuelled a contentious debate on the effects resulting from large-scale central bank stimulus. As such, a series of studies have focused on the variance transmission between financial markets, termed as volatility spillovers. In this section, the relevant literature is reviewed and the central themes among the studies are identified, shedding light on the research gap this study addresses.

At the core of the literature is the work of Bernanke et al. (2004), which although predates the imposition of QE by the Federal Reserve provides an unparalleled foundation for most of the later work in this area, inclusive of this study. The study is a seminal contribution as it contrasts between various forms of unconventional monetary policy, resulting in an unambiguous definition for the boundaries that constitute QE. The study presents QE as being contingent on the creation of bank reserves to fund asset purchases, providing a disentanglement from other monetary operations that result in a net-zero effect on the supply of money. The work also presents evidence, based on the Bank of Japan, that QE does indeed yield implications for asset prices. The findings in this work affirm the critical idea that asset purchases in an environment of elevated excess reserves will see a broad range of asset prices affected.

Owning to findings of Bernanke et al. (2004), two themes are notably present across the literature that has since built on their work. First, as noted by Ait-Sahalia et al. (2012), there is evidence that QE has implications for long-term interest rates, caused by declines in government bond yields that affect broader asset prices such as equities and corporate bonds. Secondly, although the number of studies is limited, there is evidence that the Federal Reserve's QE policies have resulted in cross-border volatility spillovers, exemplified by the covaried decline in global long-term government bond yields (Neely, 2015; Meegan et al., 2018).

2.1 Signalling and Portfolio Balancing

The two recurrent elements in the literature are established on the premise that signalling and portfolio balancing effects are the link between QE and financial markets. In a comprehensive review of QE-related literature, Gagnon (2016) finds that both signalling and portfolio balance effects are drivers of long-term interest rates, often occurring contemporaneously. Nevertheless, there is a bifurcation among the literature whereby researchers have focused solely on each effect.

The signalling effect is explored among event studies that examine the movements in asset prices around QE announcements from the Federal Reserve. These event studies are skewed towards investigating government bond yields, with evidence revealing that a decline in yields can result in increased volatility for a range of assets (Gagnon et al., 2018). Bomfim (2003) shows that asset price movements are contingent on whether

market participants interpret announcements of monetary policy as unexpected shocks, which suggests that less-anticipated QE announcements may cause greater volatility spillovers. Kenourgios et al. (2015) note that currency markets are particularly affected by QE announcements, with heterogeneity exhibited in the degree of volatility transmission across the exchange rates in advanced economies. Likewise, in their assessment of the signalling effect, Bauer and Rudebusch (2013) provide a breakdown between its impact on short and long-term interest rates. The authors show that the greatest evidence of the effect stems from movements in short-term expectations of the future policy rate. Collectively, the research assessing the signalling effect is plentiful, with a clear consensus that QE announcements can affect asset prices.

Among studies exploring portfolio balancing, the research is focused on cross-border capital flows. These transboundary flows are shown to spur volatility spillovers that lead to disproportionate impacts on more financially vulnerable economies (Chen et al., 2016). For instance, substantial outflows of private capital from the U.S. into emerging market economies, particularly across emerging Asian economies, are found to be increased as QE is enacted, potentially triggering exuberant asset price appreciation (Cho and Rhee, 2013). Morgan (2011) provides further insight on the implications of portfolio balancing on emerging Asia, arguing that capital flows are driven by the relatively higher-yielding investment opportunities in emerging markets, especially as QE causes declines in U.S. government bond yields. Collectively, these studies show that portfolio balancing can increase financial market activity and promote volatility spillovers, with the extent of the spillovers being dependent on the market. More insidiously, as capital flows are intensified, the risk of a sudden withdrawal of the capital can leave an economy vulnerable to shocks that undermine financial stability, suggesting QE may also have implications for systemic risk (Hutchison and Noy, 2006).

The normalisation of QE also features as a specific component of the literature, explored under the premise of both signalling and portfolio balancing. In particular, the "taper tantrum" has featured extensively among the literature, with studies focusing on the volatility spillovers that affected emerging markets following this unexpected normalisation announcement (see Sahay et al. (2014), Avdjiev and Takáts (2014), & Ahmed et al. (2017)). Notably, Ghosh and Saggar (2017) use high-frequency data to examine narrow window intervals around the FOMC's announcement in May 2013, showing evidence of a signalling effect that caused intensified volatility among several asset classes. Harmoniously, Kawai (2015) finds evidence of capital outflows from emerging market economies back into the U.S. following the FOMC's normalisation announcement, triggering significant volatility. The author attributes this phenomenon to a reappraisal by investors of the risk and return dynamics in U.S. domiciled assets.

Finally, the literature has also investigated the relationship between economic connectedness and volatility spillovers. Studies that explore this association find evidence of proportionality between volatility spillovers and the degree of flexibility in a country's capital account (Apostolou and Beirne, 2019). Moreover, capital market frictions between economies can influence the extent of volatility spillovers (MacDonald, 2017), with bilateral trade volumes found to exhibit empirical power for explaining the volatility that transmits between

markets, with a greater level of trade contributing to heightened spillovers (Balli et al., 2018). This idea of economic connectedness suggests that a country such as Australia, which shares significant trade linkages with the U.S., may be susceptible to volatility spillovers induced by QE. Likewise, Shogbuyi and Steeley (2017) examine the pairwise correlations between equity markets in the U.S. and the United Kingdom, exhibiting evidence of a strengthening in covariation as central banks in both countries embarked on their QE programs. The authors argue that bilateral links between these advanced economies may explain the strong correlations. Yang and Zhou (2017) similarly look at the pairwise volatility transmission across multiple advanced economies. Their study focuses on the centrality of the U.S. equity market as the core proponent of volatility spillovers, finding that the network of spillovers, derived from assessing ex-ante expectations of volatility, is strongly driven by financial markets in the U.S.

In entirety, although the literature is rich with evidence exhibiting QE-induced signalling and portfolio balancing effects, which increase financial market activity and thus spillovers, little exists in the way of a comprehensive examination of the Australian financial markets. With this research gap in mind, this study turns to identify whether volatility spillovers between the U.S. and Australia can be explained by the Federal Reserve's QE programs.

2.2 Research Questions and Hypotheses

The absence of literature that examines the volatility spillovers induced by the Federal Reserve's QE programs between U.S. and Australian financial markets presents the knowledge gap this study addresses. Specifically, the research questions this study attempts to answer are as follows:

1. *What has been the impact of the Federal Reserve's QE programs on volatility spillovers between financial markets in the U.S. and Australia?*
2. *What is the expected impact of a QE shock on volatility spillovers stemming from financial markets in the U.S. to Australia?*

The first research question aims to explain the historic influence of the Federal Reserve's QE programs on volatility spillovers. Specifically, it seeks to determine whether changes in the magnitude of the Federal Reserve's LSAPs between 2006–2019 have affected the degree of cross-market spillovers. The second research question is forward-looking, as an unexpected change in the dimensions of the Federal Reserve's QE program may cause volatility to intensify between the U.S. and Australia. To test these research questions, the following null hypotheses are proposed:

- H_1 : *The Federal Reserve's QE programs have suppressed volatility spillovers by easing financial conditions.*
- H_2 : *An unexpected contractionary QE shock intensifies short-term volatility spillovers between financial markets in the U.S. and Australia.*

Null hypothesis 1 is developed on the basis that the imposition of QE eases financial conditions and thus suppresses volatility spillovers. Null hypothesis 2 assumes that a contractionary QE shock, identified as a reduction in asset purchases, causes an immediate intensification of volatility spillovers.

3. DATA AND METHODOLOGY

3.1 Methodology Overview

The methodology comprises of three components. The first component outlines the creation of an implied volatility index that provides an ex-ante measure of volatility for the Australian government bond market. The creation of this index permits a cross-comparison with commercially available indices that track the expected volatility for the equity and government bond markets in the U.S. and the equity market in Australia. Collectively, these indices represent the volatility dynamics in each market of interest.

The second component quantifies the spillovers between each implied volatility index to derive a set of spillover indices. These spillover indices illustrate the daily bilateral volatility transmission between each market throughout time. The spillover indices are derived in the same manner as Yang and Zhou (2017) by using a recursive variant of the Diebold and Yilmaz (2012) framework. Upon derivation of the spillover indices, linear regression models are estimated to determine the drivers of volatility spillovers between each market. To isolate the influence of the Federal Reserve's QE programs on cross-market volatility, and thus testing H_1, two instruments that proxy the innovations in QE are used as regressors. The first instrument is the U.S. Shadow Policy Rate composed by Krippner (2013), which measures the effective monetary policy rate if it were not constrained by the zero lower bound. The second variable is a measure of the changes in the Federal Reserve's System Open Market Account (SOMA) portfolio, which houses the assets purchased through open market operations to fulfill the policy mandate.

The final component features three SVAR model specifications to derive impulse response functions to test H_2. These functions trace out the expected impact of an unconventional monetary policy shock on the spillover indices, portraying the short-term volatility spillovers that may unfold if the Federal Reserve alters the dimensions of its QE program. Figure 6 illustrates the interconnection between each component of the methodology[2].

[2] Given the multitude of data used in this study, Appendix A provides a summary of all the sources.

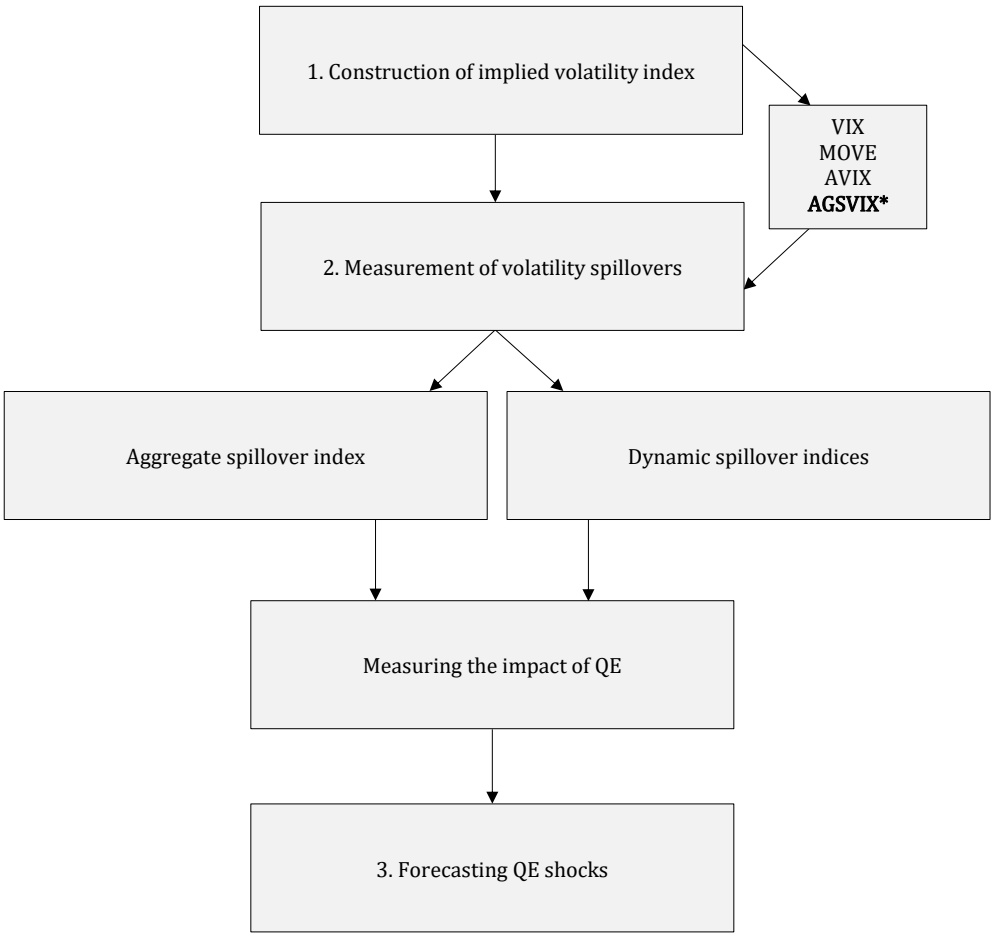

Figure 6: Methodology Overview

3.2 Implied Volatility Indices

The representative market indices in this study are a series of implied volatility indices. In comparison to ex-post volatility measures, implied volatility indices are an ex-ante measure of volatility as they are constructed using the future payoffs on options contracts (Whaley, 2000). Implied volatility indices also illustrate market linkages, subsuming the information available in more computationally demanding models of volatility (Mi and Hodgson, 2018). Yang and Zhou (2017) provide the best example of the use of implied volatility indices to derive spillover measures. The authors use spillover indices to isolate the influence of the Federal Reserve's QE programs, and as such, the sections that follow draw on their work for guidance.

The most widely used implied volatility index in financial market research is the CBOE Market Volatility Index (VIX). The VIX measures the expected volatility of the S&P 500 for the next 30 days and serves as a measure of uncertainty in the U.S. equity market (Whaley, 2009). The popularity of the VIX has given rise to additional volatility indices including the ICE BofAML MOVE Index (MOVE) which tracks the expected volatility on the U.S. government bond market, and the S&P/ASX 200 VIX Index (AVIX), which tracks the expected volatility on the Australian equity market. In this study, the VIX, AVIX, and MOVE

are the representative indices that illustrate the volatility dynamics in each underlying market. Equity and government bond markets are selected due to their relatively enhanced liquidity and their wide-spread use as barometers for economic conditions, capturing a majority of trading activity. The lack of a readily available implied volatility index for the Australian government bond market, however, denies a cross-comparison between each market. To overcome this issue, a novel implied volatility index for the Australian government bond market is constructed in a state-preference framework.

3.2.1 Australian Government Security Volatility Index (AGSVIX)

The state-preference framework of Arrow (1964) & Debreu (1959) is adopted to construct the implied volatility index. The framework is well-grounded in theory, simple to implement, and has been used to create volatility indices for many asset classes. For instance, Mi et al. (2018) use the state-preference framework to create an implied volatility index for the U.S. Real Estate Investment Trust (REIT) market, displaying its ability to serve as a consensus measure of fear for real estate assets. Similarly, Wang (2009) compares the correlations of implied volatility indices against the more computationally demanding volatility model of Fleming et al. (1998), illustrating identical results across the two methods for capturing bilateral volatility dynamics. Many of the elements in this section also follow Pan (2018), who uses the framework to construct an implied volatility index for the U.S. government bond market. The framework equates the price of any asset j at time t as a function of the product sum of the state price, $\phi_{t,s}$, and payoff, $d_{t,s}$, in each state s:

$$P_t^j = \sum_{s=1}^{S} \phi_{t,s} d_{t,s} \tag{1}$$

The framework's applicability expands beyond modelling prices, and as such, the moments of any asset including its variance can also be modelled. Thus, the squared Australian Government Security Volatility Index (AGSVIX) can be expressed as follows:

$$AGSVIX_t^2 = \sum_{s=1}^{S} \phi_{t,s} E\left(M_s | M_t\right) \tag{2}$$

The state price, $\phi_{t,s}$, is a stochastic discount rate that represents the price of a state-contingent claim that pays a single unit of consumption at time t in state s and zero in all other states. The payoff, $E\left(M_s|M_t\right)$, is the expected future return variance of the market in state s, compared to its current level at time t. The underlying market index is an equally weighted portfolio of the daily Australian 3 and 10 Year Treasury Bond Futures prices sourced from Refinitiv Eikon[3]. The prices of the Australian 3 & 10 Year Treasury Bond Futures contracts are employed as they are highly correlated with the prices of the underlying 3 & 10 year Australian government bonds. Furthermore, the 3 & 10 year bonds are the most liquid lines in

[3]The equally weighted portfolio is indexed at 100 on the first day.

the Australian government bond market and are used as pricing benchmarks for other securities, with the majority of issuance concentrated among these tenors (Australian Office of Financial Management, 2020b).

In the same manner, as Pan (2018), the payoff is set equal to the squared natural log of the future and current level of the index. The future level of the index, M_s, represents the set of possible future states in the market spanning between 50 per cent of the minimum and 150 per cent of the maximum level of the equally weighted portfolio from 19 December 2005 to 31 December 2019[4]. Each state is constructed in tick intervals of 0.01, sufficiently covering multiple possibilities for the future return variance[5]. The payoff is then computed for each historic level of the portfolio:

$$E\left(M_s|M_t\right) = \left(\ln\left(\frac{M_s}{M_t}\right)\right)^2 \quad \forall_t \quad t = 1 \ldots N \tag{3}$$

To compute state prices, the delta security method of Breeden and Litzenberger (1978) is followed. The authors estimate state prices as the second derivative of a call option's price using the Black and Scholes (1976) options pricing model:

$$\phi\left(M_s, M_{s+1}\right) = e^{-rt}\left[\mathscr{N}\left(d_2\left(M_s\right)\right) - \mathscr{N}\left(d_2\left(M_{s+1}\right)\right)\right] \tag{4}$$

Where $\mathscr{N}$ represents the standard normal probability density function applied to $d_2\left(M_s\right)$:

$$d_2\left(M_s\right) = \frac{\ln\left(\frac{S_0}{K_t}\right) + \left(r - \frac{1}{2}\sigma^2\right)T}{\sigma\sqrt{T}} \tag{5}$$

In Equation (4), $\phi\left(M_s, M_{s+1}\right)$ is the delta security that gives the price of an asset with a one-unit payoff if the market index is between M_s and M_{s+1} (where $M_{s+1} > M_s$), r is the risk-free rate set equal to the daily RBA Interbank Overnight Cash Rate and t, the time to maturity, is equal to 30/365. In Equation (5), K_t is the strike price, which is the level of the underlying market index for which the state price is being calculated, S_0 is the current level of the market index, T is the time to maturity measured in years as 30/365, and σ is the option implied volatility. To compute σ, the arithmetic average of option implied volatilities derived from 30, 60, and 90 day continuous At-The-Money (ATM) call and put options written on the Australian 3 and 10 Year Treasury Bond Futures contracts are sourced from Bloomberg. The arithmetic average of the option implied volatilities is taken as it alleviates the misspecification that is often found in options pricing models that rely on contracts of certain maturities (Jorion, 1995) and is akin to the methodology used to create the MOVE index, whereby the average yield volatility of different tenor U.S. government bonds is used (Chicago Board Options Exchange, 2015).

As a final calibration, to address the fact that the state prices are constructed in 0.01 intervals, the payoffs are adjusted for the minimum tick size for Australian Treasury Bond Futures contracts of 0.005 per cent,

[4]The starting date of 19 December 2005 aligns to the available data for option implied volatilities for the Australian 3 & 10 Year Treasury Bond Futures contracts.

[5]There are 10,804 possible states spanning between 49.15 and 157.19 in 0.01 increments.

allowing the payoffs to reach the midpoint of the interval. Taking the square root of the sum of the products of the state prices and payoffs gives the AGSVIX:

$$AGSVIX_t = 100 \times \sqrt{\frac{365}{30} \times \sum_{s=1}^{S} \phi_{t,s} \left(\ln \left(\frac{M_s + (\frac{1}{2} \times 0.005)}{M_t} \right) \right)^2} \tag{6}$$

Figure 7 illustrates the AGSVIX in levels and in comparison to the VIX and MOVE on a natural log scale. To interpret the index, a level of 100 signifies that the AGSVIX is expected to increase to 100 in 30 days. Optically, the movements in the AGSVIX closely follow the various market cycles over the past several years including the intensification of market volatility during the financial crisis commencing in late 2007 and the European sovereign debt crisis beginning in 2010. The AGSVIX also illustrates differentiation in behaviour that reflects the idiosyncratic dynamics of the Australian government bond market, especially from 2016 onward as a disparity emerged in the stance of monetary policy between the U.S. and Australia, sparking a divergence among government bond yields.

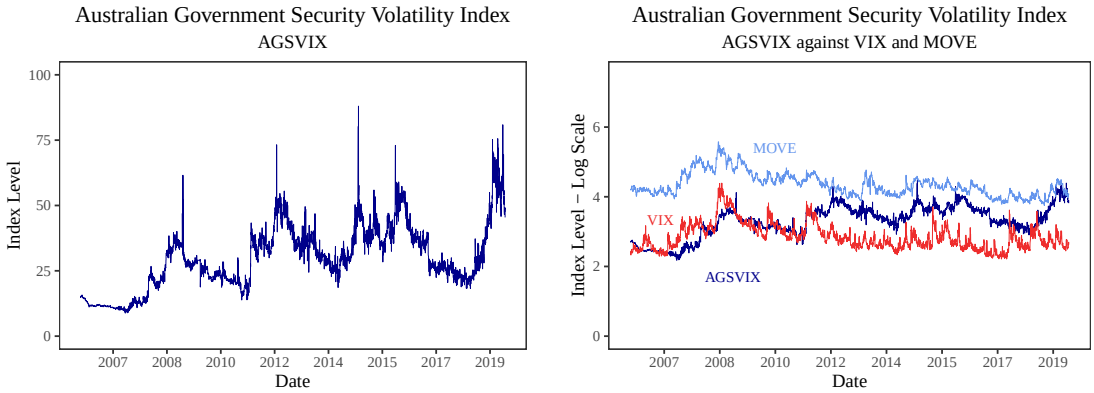

Figure 7: Australian Government Security Volatility Index (AGSVIX)

3.2.2 Robustness Test

To ensure the AGSVIX has been constructed appropriately, this section replicates the state-preference approach to create an implied volatility index for the U.S. equity market as a test of robustness. The purpose of this section is to examine as to whether an implied volatility index constructed in a state-preference framework can mirror the innovations in the commercially available VIX. If the state-preference approach is appropriate, then the innovations between the newly created index should closely follow the VIX, thus validating the suitability of the framework to construct the AGSVIX.

To create this index for the U.S. equity market, continuous 30, 60, and 90 day option implied volatilities derived from ATM call and put options contracts written on the S&P 500 are used. For the risk-free rate, the 1-month constant maturity U.S. Treasury benchmark rate is employed, and the underlying market index is the S&P 500. All the data is sourced from Refinitiv Eikon in daily frequency. Figure 8 displays the state-

preference VIX against the official VIX. The two indices are highly correlated, with a Pearson correlation coefficient equal to 0.99 across the sample, illustrating the effectiveness of the state-preference approach in replicating the VIX. The results in this section echo Liu and O'Neill (2017) and Han et al. (2019), both of which adopt the state-preference framework to create implied volatility indices tracking the S&P 500, illustrating its near-perfect correlation with the official VIX.

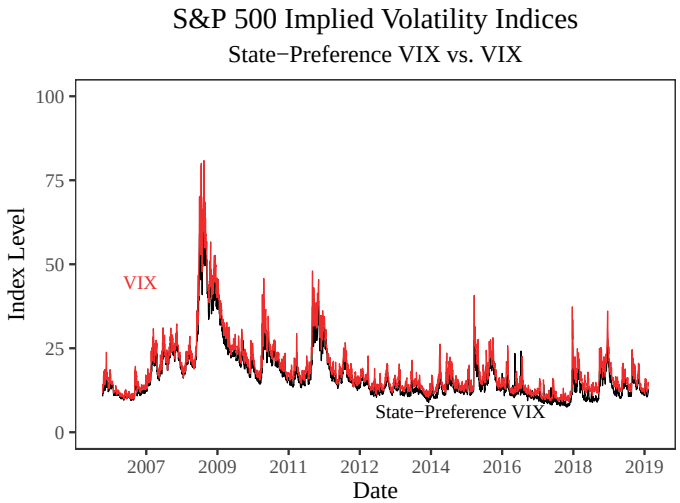

Figure 8: State–Preference VIX vs. VIX

3.2.3 State–Preference AVIX

To ensure consistency among all four indices, an implied volatility index for the Australian equity market between 2006–2007 is constructed. While the AVIX is incorporated into this study, the series commences in January 2008 and omits much of the innovations in ex-ante volatility expectations leading up to the financial crisis. As such, using the arithmetic average of option implied volatilities derived from continuous ATM call and put options written on the S&P/ASX 200, and using the same index as the choice for the underlying market, an implied volatility index is derived in the same manner as the AGSVIX. This index is then fused into the official AVIX series. To illustrate the consistency between the state-preference approach and the official AVIX methodology proposed by S&P Global (2020), this section provides a comparison between the two methods. The official AVIX is constructed in the same manner as the official VIX and is expressed as follows:

$$AVIX = 100 \times \sqrt{\frac{N_y}{N_m}\left(T_1\sigma_1^2\left[\frac{N_{T_2}-N_m}{N_{T_2}-N_{T_1}}\right]+T_2\sigma_2^2\left[\frac{N_m-N_{T_1}}{N_{T_2}-N_{T_1}}\right]\right)} \tag{7}$$

Where N_y is the number of days in one year and N_m represents the number of days in one month, set equal to 365/30. This annualisation is identical to that performed in the state-preference method. The inputs σ_1^2 and σ_2^2 represent the squared option implied volatility derived from near-term call and put options contracts

written on the S&P/ASX 200 that constitutes a 30 day calendar period. The use of close-to-maturity options is the key distinction between the two methods as the state-preference AVIX uses an arithmetic average of option implied volatilities derived from 30, 60, and 90 day ATM call and put contracts. The sole rationale for this choice is to remedy the lack of data available for near-term 30 day option implied volatilities before 2008. The correlated nature of these option implied volatilities, however, eliminates the possibility of mispricing the index by using a mixture of contracts with a slightly longer maturity (Jorion, 1995).

The variables N_{T_2} and N_{T_1} represent the number of days between the current and expiration date of the options, while T_1 and T_2 represent the time to expiration expressed in years. Figure 9 illustrates the state-preference AVIX against the official AVIX. The two indices are again highly correlated, with a Pearson correlation coefficient of 0.98 from 2008 onward. The fusion of the state-preference AVIX into the official AVIX now provides an adequate number of observations to examine ex-ante volatility expectations leading up to the crisis.

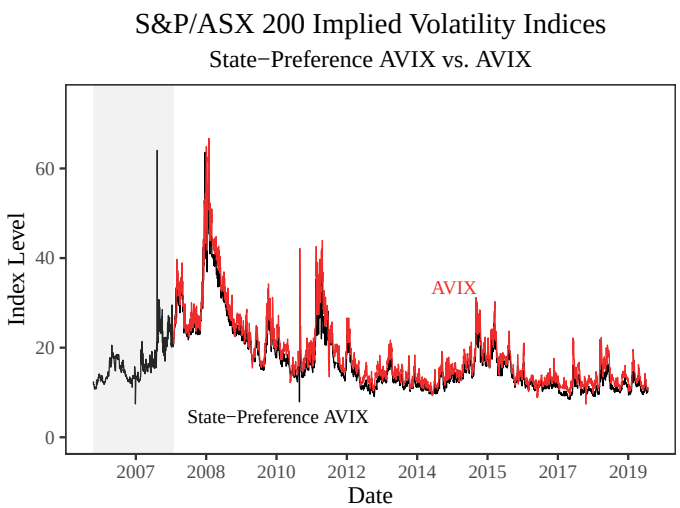

Figure 9: State–Preference AVIX vs. AVIX

3.2.4 Descriptive Statistics

Figure 10 plots all four indices in natural log scale from 2006–2019. Optically, the indices exhibit similar variations across time, especially around key disturbances such as the onset of the crisis. It is also evident that the AGSVIX departs from its close codependency with the VIX and AVIX from around 2016 onward and is subsequently more correlated to the MOVE.

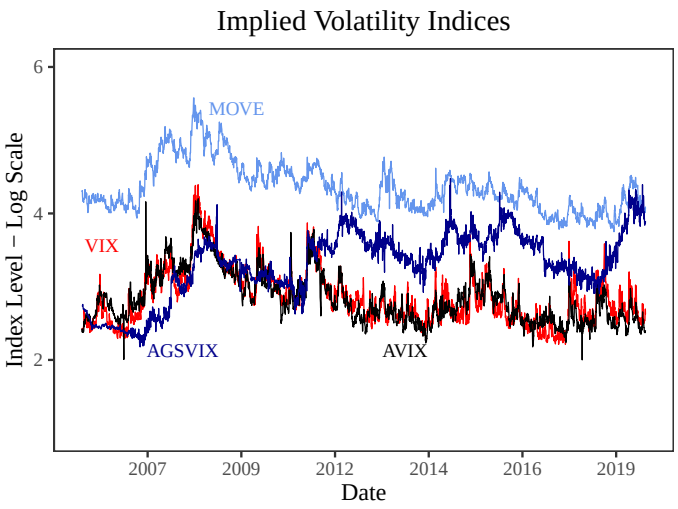

Figure 10: Implied Volatility Indices

Table 1 presents the statistical properties of each index in levels and first differences across all 3523 daily observations. Following Yang and Zhou (2017), first differences are used to remedy the persistent autocorrelation exhibited in volatility indices. The first difference also achieves stationarity, which is an important property required for the creation of the spillover indices in the sections that follow. As shown in Panel (A), the Autocorrelation Functions (ACF) at 1, 5, & 10 lags for each of the indices illustrates persistent serial correlation, which could be problematic for empirical testing. Furthermore, the most volatile of the indices is the MOVE based on standard deviation, although all indices exhibit significant variation across time, as illustrated by the wide difference between the minimum and maximum values. Collectively, the statistics depict a bifurcation of volatility into low and high states. The indices also show evidence of a departure from normality, illustrated by the significant Jarque and Bera (1980) statistics, the presence of excess kurtosis, and positive skewness. The departure from normality speaks to the leptokurtic nature of the volatility captured by these indices.

In Panel (B), the first differences illustrate similar properties although there is no evidence of persistent serial correlation across the same lags, alleviating the likelihood of drawing spurious results in empirical testing. Once again, the MOVE is the most volatile based on standard deviation. A high degree of non-normality is also again present. In particular, the excess kurtosis is greatly elevated and reflects the large fluctuations in the changes in daily volatility.

Levels				
Panel A	VIX	MOVE	AVIX	AGSVIX
Mean	18.801	82.344	18.374	29.782
Median	16.120	72.700	15.863	28.898
Maximum	80.860	264.600	66.721	88.019
Minimum	9.140	45.532	7.394	8.824
Std. Dev	8.991	32.350	7.871	12.312
Skewness	2.566	1.824	2.137	0.504
Excess Kurtosis	9.033	4.011	6.179	0.284
Jarque-Bera χ^2	15842***	4314***	8284***	161***
ACF(1)	0.979	0.993	0.973	0.969
ACF(5)	0.930	0.964	0.930	0.957
ACF(10)	0.893	0.937	0.899	0.939
Observations	3523	3523	3523	3523

First Differences (%)				
Panel B	VIX	MOVE	AVIX	AGSVIX
Mean	0.001	-0.004	0.000	0.010
Median	-0.080	-0.200	-0.043	0.000
Maximum	20.010	41.500	44.805	36.453
Minimum	-17.360	-40.500	-43.009	-33.381
Std. Dev	1.825	3.910	1.825	3.016
Skewness	0.987	0.497	0.968	0.526
Excess Kurtosis	19.559	16.234	205.963	32.023
Jarque-Bera χ^2	56713***	38818***	6225789***	150650***
ACF(1)	-0.125	0.044	-0.269	-0.488
ACF(5)	0.000	-0.065	-0.024	0.049
ACF(10)	0.073	0.032	-0.002	0.004
Observations	3522	3522	3522	3522

Table 1: Descriptive Statistics of Implied Volatility Indices

Note. This table displays the descriptive statistics for each of the four indices in both levels and first differences. The Jarque and Bera (1980) test examines whether the third and fourth moments of the data match those of the normal distribution. ACF(τ) refers to the Autocorrelation Function at each respective lag interval. The levels of significance are defined as follows: '***' implies significance at the 0.1% level, '**' implies significance at the 1% level, and '*' implies significance at the 5% level.

The pairwise correlations between implied volatility indices also embed useful information concerning the dynamics between each market (Wang, 2009). Table 2 illustrates the correlations across the full sample in levels and first differences. Notably, in Panel (A), strong positive correlations between the VIX and AVIX (0.91) & MOVE and AVIX (0.85) suggests the linkage between the U.S. equity and government bond markets to the Australian equity market is significant. These high correlations imply that a shock in one market that intensifies volatility may result in risk spillovers to the Australian equity market. Comparably, a strong positive relationship between the VIX and MOVE (0.81) suggests a high degree of dependence between the U.S. equity and government bond markets, such that a domestic disturbance that triggers volatility may circulate between each market. In contrast, linkages to the AGSVIX are weak between all three markets, suggesting a lack of volatility transmission to the Australian government bond market.

The narrative is different when considering the first differences in Panel (B). While the correlations of levels in Panel (A) show a degree of dependence, the first differences may reflect the true nature of the bilateral dynamics after eliminating the persistent serial correlation. Specifically, the only positive and

significant relationship is between the VIX and MOVE (0.24), while all other correlations are close to zero. The correlation between the VIX and AVIX is significant but is limited to around 5 per cent. However, it must be stated that static correlations fail to account for changes in the relationships between the markets around key disturbances.

Levels				
Panel A	VIX	MOVE	AVIX	AGSVIX
VIX	1.000			
MOVE	0.805***	1.000		
AVIX	0.912***	0.852***	1.000	
AGSVIX	0.007	-0.082***	-0.064***	1.000

First Differences (%)				
Panel B	VIX	MOVE	AVIX	AGSVIX
VIX	1.000			
MOVE	0.235***	1.000		
AVIX	-0.052**	0.014	1.000	
AGSVIX	0.001	-0.002	0.022	1.000

Table 2: Pairwise Pearson Correlation Matrix of Implied Volatility Indices

Note. This table displays the pairwise Pearson correlation coefficients across each pair of markets for the full sample from 2006–2019. The levels of significance are defined as follows: '***' implies significance at the 0.1% level, '**' implies significance at the 1% level, and '*' implies significance at the 5% level.

Following Mi and Hodgson (2018), rolling correlations of each market pair across 500 days are used to examine the relationships around key developments. The authors argue that a rolling window of 500 days is sufficient to eliminate the high variability of shorter-term window lengths, while still being sensitive enough to capture the innovations in volatility, unlike longer-term windows that may be too persistent. Figure 11 illustrates the rolling Pearson correlation coefficient between each combination of the indices, shedding light on multiple interesting trends. First, the correlations are mostly positive, although a few times the relationships have been negative such as between 2012–2014, a period that corresponds to an improving economic outlook that saw asset prices diverge. A sharp rise in correlations between 2007–2008 is also evident and aligns to the onset of the financial crisis. A further change in the relationships occurred around the end of 2014 up until early 2015, potentially explained by the covaried decline in asset prices following the steep drop in global crude oil prices[6].

[6]Between 1 January 2014 and 1 January 2015, the price of West Texas Intermediate (WTI) Crude Oil declined around 45 per cent, causing significant market-wide volatility.

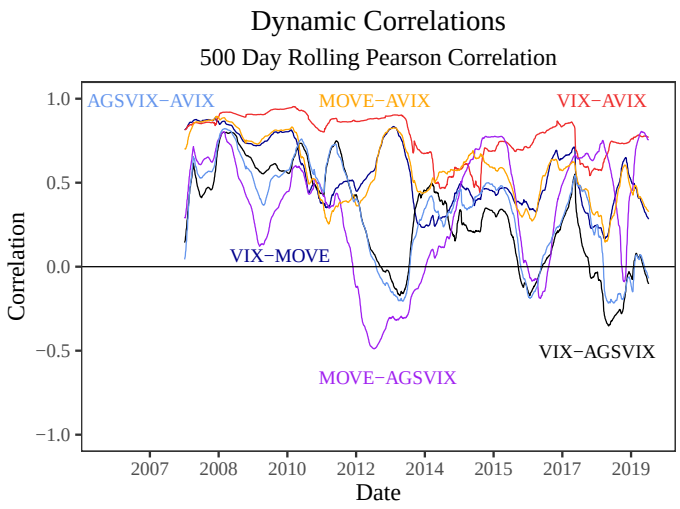

Figure 11: Rolling Correlations

3.3 Measuring Volatility Spillovers

Since implied volatility indices reflect innovations in the second moment of the asset return distribution, measuring spillovers between these indices is akin to illustrating the spillover of risk (Yang and Zhou, 2017). To measure these risk spillovers, the Diebold and Yilmaz (2012) framework is adopted. This framework allows for the construction of dynamic spillover indices based on the forecast error variance decompositions of a VAR model, permitting creation of aggregate and pairwise indices that exhibit the evolution of volatility transference throughout time. The framework is simple to implement and features extensively across the literature examining risk spillovers among financial markets (see Alter and Beyer, 2014, Antonakakis, 2012, & Zhou et al., 2012). To construct the indices, the *'frequencyConnectedness'* R package created by Baruník and Křehlík (2018) is used.

3.3.1 The Spillover Model

The original framework proposed by Diebold and Yilmaz (2009) measures time-varying volatility spillovers by using the forecast error variance decompositions derived from an unrestricted VAR model. The key feature in this framework is the error variance decomposition which reflects the proportion of the H-step-ahead forecast error variance of some variable i that is explained by another variable within the system, j. While useful, the original framework suffers from problematic elements.

Specifically, the original framework employs a Cholesky decomposition identification scheme for estimating the VAR model. This is particularly troublesome as a Cholesky decomposition renders the forecast error variance decompositions contingent on the ordering of the variables. Thus, a different order of the variables in the model may impact the magnitude of the spillovers. In contrast, the extended framework of Diebold and Yilmaz (2012) permits forecast error variance decompositions that are invariant to ordering, achieved

by employing a generalised VAR specification. This specification also permits analysis of the direction and intensity of risk spillovers, capturing further information concerning the dynamics of volatility transmission. To provide an exposition of the framework, an N-variable, covariance-stationary, unrestricted VAR model of order p is first stated as follows:

$$y_t = \sum_{i=1}^{p} \phi_i y_{t-i} + \varepsilon_t \tag{8}$$

Where y_t is the vector of implied volatility indices and ε_t is the vector of identically and independently distributed disturbance terms with distribution $\varepsilon_t \sim (0, \lambda)$. If the assumption of covariance-stationarity is satisfied, Equation (8) can be represented as an infinite moving average process:

$$y_t = \sum_{i=0}^{\infty} A_i \varepsilon_{t-i} \tag{9}$$

Diebold and Yilmaz (2012) assume that the $N \times N$ coefficients, A_i, follow the recursion $A_i = \phi_1 A_{i-1} + \phi_2 A_{i-2} + \cdots \phi_p A_{i-p}$ where A_0 is assumed to be an $N \times N$ identity matrix and $A_i = 0 \; \forall_i < 1$. The moving average coefficients represent the contemporaneous relationships between variables and can be transformed into variance error decompositions to delineate the volatility spillovers. To avoid dependence on the ordering of the variables, the generalised VAR framework of Koop et al. (1996) and Pesaran and Shin (1998) is employed. This generalised framework permits contemporaneously correlated VAR innovations, unlike the Cholesky decomposition scheme which orthogonalises the innovations. The generalised H-step-ahead forecast error variance decompositions are denoted as follows:

$$\theta_{ij}^{g}(H) = \frac{\sigma_{jj}^{-1} \sum\limits_{h=0}^{H-1} (e_i' A_h \lambda e_j)^2}{\sum\limits_{h=0}^{H-1} (e_i' A_h \lambda A_h' e_i)} \tag{10}$$

Where the subscript g represents the generalised framework and λ is the variance-covariance matrix of the disturbance term, ε_t. Furthermore, σ_{jj} is the standard deviation of the error term for the jth equation, and e_i is a vector with 1 as the ith element and zero otherwise. Since the VAR innovations are not orthogonalised, the sum of the contributions of each variable to the total forecast error variance may not equate to unity. To remedy this, each variance decomposition is normalised by diving $\theta_{ij}^{g}(H)$ as follows:

$$\widetilde{\theta}_{ij}^{g}(H) = \frac{\theta_{ij}^{g}(H)}{\sum\limits_{j=1}^{N} \theta_{ij}^{g}(H)} \tag{11}$$

Importantly, by construction the following conditions also hold, further simplifying the creation of the indices:

$$\begin{aligned} \sum_{j=1}^{N} \widetilde{\theta}_{ij}^{g}(H) &= 1 \\ \sum_{i,j=1}^{N} \widetilde{\theta}_{ij}^{g}(H) &= N \end{aligned} \tag{12}$$

From Equation (11), a series of spillover indices are created. The first of these indices is the aggregate spillover index that measures the combined contribution of the variables to the total forecast error variance in the system of markets:

$$S_{Aggregate}^{g}(H) = \frac{\sum_{\substack{i,j=1 \\ i \neq j}}^{N} \widetilde{\theta}_{ij}^{g}(H)}{N} \times 100 \tag{13}$$

The generalised framework also permits the construction of directional spillover indices that illustrate the volatility received by market i from all j markets in the system:

$$S_{i \leftarrow j}^{g}(H) = \frac{\sum_{\substack{j=1 \\ j \neq 1}}^{N} \widetilde{\theta}_{ij}^{g}(H)}{N} \times 100 \tag{14}$$

Similarly, the volatility transmitted by market i to all j markets can be stated as follows:

$$S_{i \rightarrow j}^{g}(H) = \frac{\sum_{\substack{j=1 \\ j \neq 1}}^{N} \widetilde{\theta}_{ji}^{g}(H)}{N} \times 100 \tag{15}$$

Given these directional spillovers, $S_{i \leftarrow j}^{g}(H)$ and $S_{i \rightarrow j}^{g}(H)$, the net transmission of volatility from market i to all j markets is derived as the difference between the two indices:

$$S_{Net}^{g}(H) = S_{i \rightarrow j}^{g}(H) - S_{i \leftarrow j}^{g}(H) \tag{16}$$

Equation (16) is particularly informative as each market can be assessed as to whether it is a net contributor or receiver of volatility. Finally, the net pairwise volatility spillovers between two individual markets i and j can be constructed as follows:

$$S_{ij}^{g}(H) = \left(\frac{\widetilde{\theta}_{ji}^{g}(H) - \widetilde{\theta}_{ij}^{g}(H)}{N} \right) \tag{17}$$

Equation (17) represents the difference between volatility transmitted from market i to market j and vice versa.

3.3.2 Model Calibration

To derive the spillover indices, three requirements must be satisfied. The first requirement is the selection of an optimal lag length for the VAR model that is chosen based on an appropriate information criterion. The second is the selection of the H-step-ahead forecast horizon which dictates whether short-run or long-run volatility dynamics are emphasised in the indices (Diebold and Yılmaz, 2014). Finally, an appropriate window length needs to be defined.

For the optimal lag length, a lag order of 4 is chosen based on the Bayesian (Schwarz) Information Criterion (BIC). While Diebold and Yilmaz (2012) indicate the framework is robust to the choice of the VAR model's lag order, the BIC's recommended lag length is adopted to ensure an accurate specification. Additionally, to ensure the VAR model is robust to spurious results, tests of stationarity are performed. Table 3 reports the results of the Augmented Dickey-Fuller (ADF), Phillip-Peron (PP), and Kwiatkowski–Phillips–Schmidt–Shin (KPSS) tests performed on the first differences of the implied volatility indices. The ADF and PP tests have a null non-stationarity and across all indices, the null hypothesis is significantly rejected ($p < 0.001$). In contrast, the KPSS test has a null of stationarity and for each index, the null hypothesis cannot be rejected. Collectively, these tests validate the stationarity of the variables.

	First Differences (%)			
	VIX	MOVE	AVIX	AGSVIX
ADF	-16.493***	-15.370***	-16.984***	-17.235***
PP	-3325.200***	-2985.900***	-3785.200***	-4449.600***
KPSS	0.021	0.026	0.027	0.018

Table 3: Stationarity Tests of Implied Volatility Indices

Note. This table displays the stationarity test statistics performed on the first differences of each implied volatility index. The ADF & PP tests have a null of non-stationarity, while the KPSS test has a null of stationarity. The levels of significance are defined as follows: '***' implies significance at the 0.1% level, '**' implies significance at the 1% level, and '*' implies significance at the 5% level.

For the H-step-ahead forecast horizon, Diebold and Yilmaz (2012) argue that this choice depends on the nature of the study. Seeing as the daily volatility spillovers between each market is of interest, 1, 3, and 12 day H-step-ahead forecast horizons are estimated in the same manner as Yang and Zhou (2017). The authors argue that the 12 day H-step-ahead forecast horizon permits stabilisation of the forecast error variance decompositions, and as such, this specification is favoured in this study. For the window length, a recursive expanding sample estimation is used. Unlike a rolling window estimation, a recursive estimation provides a Bayesian-like approach to estimate volatility spillovers that are free from the variation that may result from different window lengths (Yang and Zhou, 2017)[7]. To recursively estimate the spillover indices, each volatility index is first broken into subsamples between 2006–2008 (corresponding to the first QE event

[7]For robustness, rolling window estimations across 60, 70, 80, and 90 days are conducted and presented in Appendix C.

on 25 November 2008). These partitioned samples are then used to compute the first set of spillovers. Each spillover index is then expanded as QE-relevant events are realised[8]. In total, 22 events based on the QE-timeline presented in Appendix B are used and constitute the ending period for each expanded sample. The timeline features QE-relevant announcements made by the Board of Governors of the Federal Reserve System (2020b) and is cross-checked against Fawley and Neely (2013), who present a similar list of events.

Finally, to ensure precision, the time difference (12–16 hours) between the closing of the U.S. and Australian markets is addressed. The AVIX and AGSVIX are adjusted such that the closing value recorded at $t+1$ aligns to the closing value of the VIX and MOVE at $t+0$, eliminating the discrepancy resulting from geographically distinct time zones.

3.3.3 Measuring the Influence of QE

This section is concerned with the development of an empirical framework that isolates the influence of the Federal Reserve's QE programs on cross-market volatility spillovers, addressing the first research question of this study and permitting testing of H_1. To accomplish this, the following linear model is estimated using the Ordinary Least Squares (OLS) method with Newey and West (1986) heteroskedasticity and autocorrelation consistent standard errors, which alleviates the maladies of serial correlation:

$$\begin{aligned} S^g_{ij}(H)_t = \alpha_t + \beta_1 QE_{PROXY_t} + \beta_2 D_{QE_t} + \beta_3 SUR_{G_t} + \beta_4 SUR_{US_t} + \beta_5 SUR_{AU_t} + \beta_6 OIS_{AU_t} \\ + \beta_7 CDS_{US_t} + \beta_8 CDS_{AU_t} + \varepsilon_t \end{aligned} \tag{18}$$

The dependent variable, $S^g_{ij}(H)_t$, is the volatility spillover index between market i and j. The regressor, QE_{PROXY_t}, refers to the instrument that proxies innovations in the Federal Reserve's QE program. For robustness, two instruments are used as the QE proxy. The first is the daily U.S. Shadow Policy Rate constructed by Krippner (2013) which builds on the Vasicek (1977) one-factor short-term interest rate model and closely approximates the numerically intensive method of Black (1995) for deriving interest rates in an options pricing framework. Specifically, the Shadow Policy Rate is constructed using non-negative forward rates derived from bond options, measuring the effective monetary policy rate beyond the zero lower bound. The second instrument is a time-series of 716 weekly changes in the Federal Reserve's SOMA portfolio, which houses the dollar-denominated assets acquired by the Federal Reserve Bank of New York as it conducts open market operations to fulfill the policy mandate[9]. In this sense, changes in the magnitude of asset holdings reflect the accumulation (and eventual normalisation) of QE. Table 4 presents the descriptive statistics for both instruments.

[8] As each event is realised, the sample set is increased. The initial sample set is always considered for each subsequent estimation and ultimately all observations are used. The final sample is between 4 January 2006 to 11 October 2019, which corresponds to the final QE event.

[9] The Federal Reserve Bank of New York carries out the trading operations on behalf of the FOMC (Federal Reserve Bank of New York, 2020).

QE Instruments		
	Shadow Policy Rate (%)	SOMA Portfolio (%)
Mean	0.034	0.002
Median	-0.130	0.000
Maximum	5.340	0.293
Minimum	-5.612	-0.074
Std. Dev	2.875	0.016
Skewness	0.059	10.295
Excess Kurtosis	-0.650	164.475
Jarque-Bera χ^2	63.097***	819704***
Observations	3467	716

Table 4: Descriptive Statistics of QE Instruments

Note. This table displays the descriptive statistics for the QE instruments. The Federal Reserve's SOMA portfolio is represented as weekly changes. The Jarque and Bera (1980) test examines whether the third and fourth moments of the data match those of the normal distribution. The levels of significance are defined as follows: '***' implies significance at the 0.1% level, '**' implies significance at the 1% level, and '*' implies significance at the 5% level.

While both instruments proxy the innovations in QE, the SOMA portfolio represents the operational aspect of the policy, that is, the buying and selling of securities. In contrast, the Shadow Policy Rate is indicative of a risk-free rate in the same essence as the Federal Funds Rate, reflecting the cost of funding when the zero lower bound becomes binding[10]. Thus, while both instruments proxy QE, they do so in a different manner. Figure 12 illustrates both the Shadow Policy Rate and the aggregate SOMA portfolio between 2006–2019, notably exhibiting the unconventional policy response during the crisis.

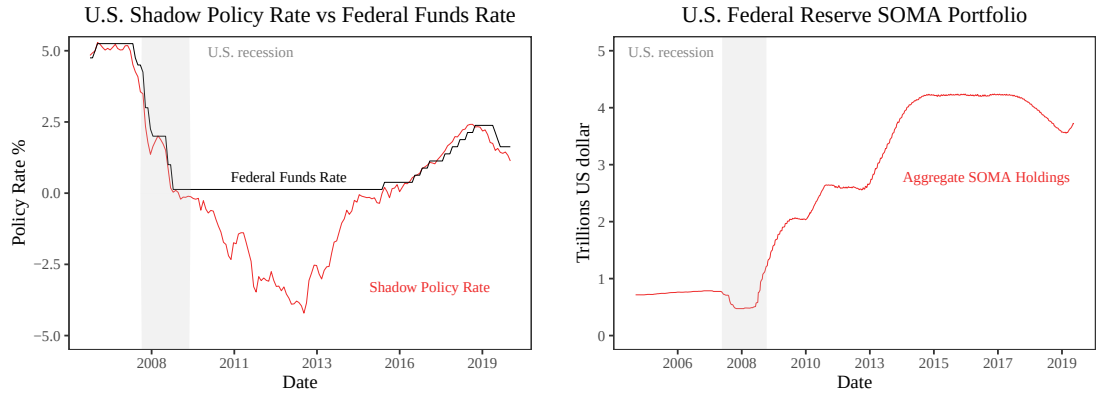

Krippner (2013) Federal Reserve Bank of New York (2020)

Figure 12: QE Instruments

Furthermore, D_{QE_t} is a dichotomous variable that is equal to 1 when QE programs are announced by the Federal Reserve and zero on any other day. This variable captures the immediate signalling effect that the Federal Reserve can inflict on markets when revealing its QE policies and is based on the timeline in Appendix B. To capture the market's anticipation for the Federal Reserve's announcements, the variable is

[10]The Federal Funds Rate is the interest rate at which deposit-taking institutions manage their liquidity in the interbank market and is considered central to the pricing of all other interest rates (Federal Reserve Bank of St. Louis, 2020b).

also equal to 1 one day before and after the announcement, constituting a 3-day window. While this variable is meant to capture the Federal Reserve's announcement effect, higher frequency data may be needed to detect the impact, which is outside the bounds of this study. Moreover, the weekly frequency of the SOMA portfolio forces the dichotomous variable to a weekly frequency as well, with the variable equal to 1 when QE announcements are made in the relevant week and zero on any other week. The preceding and subsequent weeks in this setting are equal to zero as a one week window is deemed of sufficient length.

Alongside the QE variables, control factors are also employed. Firstly, to control for volatility dynamics driven by unexpected economic developments, the daily Citigroup Economic Surprise indices for global, U.S., & Australian economic surprises (SUR_{G_t}, SUR_{US_t}, and SUR_{AU_t}) are sourced from Refinitiv Eikon and employed as part of the framework. Together, these variables act as controls for unexpected economic data readings that may influence volatility. They also are widely used across the literature for controlling for economic data surprises, whereby a positive index value represents a better-than-expected economic data release and vice versa (see for instance Georgiadis and Gräb (2016), Yang and Zhou (2017), & Punzi and Chantapacdepong (2019)).

The variables CDS_{US_t} and CDS_{AU_t} are the daily investment grade Credit Default Swap (CDS) spreads for Australian and U.S. corporates also sourced from Refinitiv Eikon. CDS contracts provide insurance against default in an underlying security and thus the spreads on these instruments reflect the perception of credit risk and the probability of default. In this study, these variables act as a control for the elevated credit risk premia during the onset of the crisis, reflecting the deterioration in risk sentiment as U.S. default rates increased (Galariotis et al., 2016). Finally, OIS_{AU} is the daily rate on the one month Australian Overnight Index Swap sourced from the RBA. This variable reflects the market consensus expectation of the Australian policy rate in the next month, acting as a control for changes in Australian monetary policy[11].

For robustness, the regressions are carried out on subsamples to examine whether the influence of the Federal Reserve's QE programs changes depending on the market cycle. Specifically, the regressions are conducted on the full sample between 2006–2019, during the U.S. and European crisis periods between 2007–2012, and finally, during the period of policy normalisation (which includes the "taper tantrum" of May 2013) between 2013–2019.

3.4 Quantitative Easing Shocks

The final component involves assessing the impact of a QE shock on cross-market volatility spillovers, addressing the second research question of the study and permitting testing of H_2. Specifically, this component is concerned with illustrating the potential short-term impact of a change in the magnitude of the Federal Reserve's QE program. For this analysis, a series of bilateral SVAR models are exploited to derive a set of impulse response functions that exhibit the response of one variable to the shock of another.

[11] Descriptive statistics, Pearson correlation coefficients, and charts for each control variable are provided in Appendix D.

To understand these models, it is important to provide a background on their emergence in macro-financial research. Initially, Sims (1980) promoted the VAR model as an alternative empirical framework to the large-scale and unrealistic macroeconomic models that were heavily relied on. The standard unrestricted VAR model has since featured extensively among literature exploring monetary policy shocks (see Christiano et al. (1994) and Bagliano and Favero (1998)). The atheoretical nature of the unrestricted VAR model, however, results in impulse responses that are difficult to interpret due to a lack of grounding in economic theory (Keating, 1996). Instead, SVAR models are used as they yield impulse responses that represent structural economic shocks, conjoining useful empirical analysis with economic theory (Mangadi and Sheen, 2017). As an exposition, a reduced form VAR model can be expressed as follows:

$$y_t = A_0 + A_1 y_{t-1} + \mu_t \tag{19}$$

Where y_t is the vector of spillover indices, A_0 is the matrix of intercept terms, A_1 is the matrix of coefficients that represent the relationships between the variables, and μ_t houses the disturbance term. To examine structural shocks, the reduced form VAR model is premultiplied by the non-singular matrix, B:

$$\begin{aligned} By_t &= BA_0 + BA_1 y_{t-1} + B\mu_t \\ By_t &= \Gamma_0 + \Gamma_1 y_{t-1} + \varepsilon_t \end{aligned} \tag{20}$$

Where B captures the contemporaneous dynamics between the variables and is known as the matrix of structural impacts. The relationship between the disturbances in the reduced and structural form of the VAR model is shown by the following equality:

$$\mu_t = B^{-1}\varepsilon_t \tag{21}$$

The variance-covariance matrix of the reduced form disturbance term is assumed to be diagonal and is expressed as:

$$\Sigma_\mu = E\left(\mu_t \mu_t'\right) = B^{-1} E\left(\varepsilon_t \varepsilon_t'\right) B^{-1\prime} = B^{-1}\Sigma_\varepsilon B^{-1\prime} \tag{22}$$

To derive the structural impulse response functions, the B matrix must be uniquely identified from the variance-covariance matrix. Under the assumption of normality, however, the structural shocks cannot be recovered unless additional identification restrictions are imposed. The choice of identification scheme, however, can influence the path of the impulse responses. For robustness, three separate schemes are employed.

3.4.1 Identification via Chloesky Decomposition

The Cholesky decomposition is a commonly used scheme that can recover structural shocks in a VAR model. The scheme imposes restrictions on the variance-covariance matrix that permits orthogonalised shocks, resulting in uncorrelated impulse responses. This scheme, however, forces the path of the impulse responses to be contingent on the variable ordering. This implies a Cholesky decomposition results in a recursive structure, which is rarely observed in economic theory (Keating, 1996). As the variable ordering changes, so too does the path of the impulse response, and for an n variable VAR model, a total of $n!$ permutations may exist. The use of a bivariate VAR model, however, can rectify this issue by limiting the permutations to two possibilities. To illustrate this scheme, the variance-covariance matrix for structural shocks, Σ_ε, is assumed to be the identity matrix:

$$\Sigma_\mu = E\left(\mu_t \mu_t'\right) = B^{-1} E\left(\varepsilon_t \varepsilon_t'\right) B^{-1\prime} = B^{-1} I B^{-1\prime} = B^{-1} B^{-1\prime} \tag{23}$$

If Σ_μ is a symmetric positive-definite matrix, it can be decomposed into a lower triangular matrix, P, and its conjugate transpose, P':

$$\Sigma_\mu = PP' \tag{24}$$

Rewriting Equation (23) with the lower triangular decomposition gives:

$$\Sigma_\mu = E\left(\mu_t \mu_t'\right) = P^{-1} E\left(\varepsilon_t \varepsilon_t'\right) P^{-1\prime} = P^{-1} I P^{-1\prime} = P^{-1} P^{-1\prime} \tag{25}$$

Equation (25) is equal to Equation (23), and given this equality, the relationship between the reduced and structural form errors can be expressed as follows:

$$\mu_t = P^{-1} \varepsilon_t \tag{26}$$

This equality permits identification of the structural shocks in the following form:

$$\begin{bmatrix} \mu_{QE_{PROXY_t}} \\ \mu_{S^g_{ij}(H)_t} \end{bmatrix} = \begin{bmatrix} 1 & 0 \\ p_{21} & 1 \end{bmatrix} \begin{bmatrix} \varepsilon_{QE_{PROXY_t}} \\ \varepsilon_{S^g_{ij}(H)_t} \end{bmatrix} \tag{27}$$

The first row in Equation (27) implies that the QE instrument is solely affected by its own lagged innovations, while the second row implies the spillover index is driven by its lagged innovations and the shock imposed on the QE instrument. The magnitude of the shock is captured by the element p_{21}.

3.4.2 Identification via Heteroskedasticity

While the Cholesky decomposition in a bivariate setting simplifies the question of ordering, the scheme does not permit contemporaneously correlated variables. In fact, all identification schemes that depend on *a priori* assumptions fall victim to the same issues. Long-run restrictions pioneered by Blanchard and Quah (1988) or sign restrictions propagated by Uhlig (2005), while popular across the SVAR literature, rely on restrictions that are difficult to reconcile to economic theory. As such, there is a need to consider alternative schemes that allow the characteristics of the data to identify the structural impact matrix without the imposition of constraining restrictions.

One such scheme is the exploitation of the variation exhibited in the spillover indices based on the unconditional changes in the covariance of the VAR residuals. This method, which incorporates exogenously occurring changes in variance as an identification scheme, is pioneered by Rigobon (2003) and extended by Lanne and Lütkepohl (2008). Notably, Herwartz and Plödt (2016) show that this scheme provides more accurate impulse responses compared to identification by Cholesky decomposition or sign restrictions. To apply this scheme, the R package *'svars'* constructed by Lange et al. (2019) is used. The scheme assumes that a single permanent structural break in variance occurs at T_B, where T is the number of observations. This implies that there are two states for the variance-covariance matrix:

$$\Sigma_\mu = E\left(\mu_t \mu_t'\right) = \begin{cases} \Sigma_1 & t = 1, \ldots, T_B - 1 \\ \Sigma_2 & t = T_B, \ldots, T \end{cases} \tag{28}$$

Where $\Sigma_1 \neq \Sigma_2$. The variance-covariance matrices in each state are decomposed as follows:

$$\begin{aligned} \Sigma_1 &= BB' \\ \Sigma_2 &= B\Lambda B' \end{aligned} \tag{29}$$

Where B is an $N \times N$ matrix and Λ is a diagonal matrix with each element $\Lambda_{ii} > 0 \; \forall_i$ where $i = 1, \ldots, N$. The elements of Λ represent the changes in the variances of the shocks after a change occurs in the variance of the data. If the elements are distinct, this implies a change in variance occurs and permits identification of a unique structural impact matrix. In the first state, Σ_1, the structural shocks have unit variance and in the second state, Σ_2, the variances are mapped to Λ_{ii}. If the errors μ_t are assumed to be normally distributed, Lange et al. (2019) show that the log-likelihood function for estimating B and Λ is as follows[12]:

$$\begin{aligned} \log \mathcal{L} = T\tfrac{N}{2}\log 2\pi - \tfrac{T_B-1}{2}\left[\log|(BB')| + trace\left\{\tilde{\Sigma}_1(BB')^{-1}\right\}\right] \\ -\tfrac{T-T_B+1}{2}\left[\log|(B\Lambda B')| + trace\left\{\tilde{\Sigma}_2(B\Lambda B')^{-1}\right\}\right] \end{aligned} \tag{30}$$

[12] Lanne and Lütkepohl (2008) propose a numerical optimisation of the log-likelihood function that relies on an application of the Generalised Least Squares (GLS) method to derive the VAR parameters. The numerical optimisation eventually converges to the analytical function in Equation (30). Given the equality between the results, only the analytical solution is presented here for simplicity.

The variance-covariance matrices, $\tilde{\Sigma}_1$ & $\tilde{\Sigma}_2$, are derived from the estimated residuals $\hat{\mu}$:

$$\begin{aligned} \tilde{\Sigma}_1 &= \tfrac{1}{T_B-1} \textstyle\sum_{t=1}^{T_B-1} \hat{\mu}_t \hat{\mu}_t' \\ \tilde{\Sigma}_2 &= \tfrac{1}{T-T_B+1} \textstyle\sum_{t=T_B}^{T} \hat{\mu}_t \hat{\mu}_t' \end{aligned} \tag{31}$$

To employ this scheme, a structural breakpoint for each spillover index, T_B, must be identified. To identify the breakpoint, this study follows Chow (1960) who proposes a hypothesis test with a null of no structural break. In this test, the alternative hypothesis is specified as a structural break occurring at T_B:

$$H_A : \beta_i = \begin{cases} \beta_A & t = 1, \ldots, T_B - 1 \\ \beta_B & t = T_B, \ldots, T \end{cases} \tag{32}$$

If no structural break occurs, the beta coefficients in both subsamples are equivalent. To test this hypothesis, Chow (1960) proposes estimating regressions in each subsample defined by the predetermined breakpoint and rejecting the null hypothesis whenever the following F statistic is sufficiently large:

$$F_{T_B} = \frac{\hat{\mu}'\hat{\mu} - \hat{\varepsilon}'\hat{\varepsilon}}{\hat{\varepsilon}'\hat{\varepsilon}/(n-2t)} \tag{33}$$

Where $\hat{\varepsilon} = [\hat{\mu}_A, \hat{\mu}_B]'$ and is the vector of residuals from both regressions that are estimated separately, while $\hat{\mu}$ houses the residuals from the restricted model, whereby the parameters are fitted once for all observations. The test statistic, F_{T_B}, is distributed asymptotically as a χ^2 distribution with t degrees of freedom. If the residuals are assumed to be normally distributed, however, $\frac{F_{T_B}}{n}$ has an exact F distribution with degrees of freedom t and $n - 2t$. While the F test is straight forward, the predefined structural breakpoint may not be known. Instead, to permit a data-driven identification of the structural breakpoint, the Chow (1960) test can be applied to the entire sample whereby the test statistic is derived at each observation. To conduct this, the following intercept-only regression is performed:

$$S_{ij}^{g}(H)_t = \alpha_t + \varepsilon_t \tag{34}$$

This regression implies innovations in volatility are constant and permits a sequence of F tests to be derived at each observation. Each separate F statistic can then be aggregated to carry out a significance test, either by computing the arithmetic average, the supremum, or exponentiating the F statistics[13]. Table 5 employs the aggregation methods for the spillover indices (which are discussed in detail in Section 4), illustrating that the null hypothesis of no structural break occurring is significantly rejected.

[13] Appendix F provides an overview of each aggregated F statistic.

Aggregated F Statistics

Volatility Spillover Index	Average F Statistic	Supremum F Statistic	Exponential F Statistic
Aggregate	618.090***	2629.100***	∞***
	(0.000)	(0.000)	(0.000)
VIX to MOVE	504.610***	2887.600***	∞***
	(0.000)	(0.000)	(0.000)
VIX to AVIX	165.370***	1145.800***	565.090***
	(0.000)	(0.000)	(0.000)
VIX to AGSVIX	134.210***	3827.100***	∞***
	(0.000)	(0.000)	(0.000)
MOVE to AVIX	92.974***	961.110***	473.880***
	(0.000)	(0.000)	(0.000)
MOVE to AGSVIX	109.710***	288.240***	139.250***
	(0.000)	(0.000)	(0.000)
AVIX to AGSVIX	901.980***	2473.500***	∞***
	(0.000)	(0.000)	(0.000)

Table 5: Test for Structural Breaks in Volatility Spillover Indices

Note. This table displays the aggregated F statistics for testing the Chow (1960) null hypothesis of no structural breaks throughout the sample for each spillover index. The p-values (in parentheses below the coefficients) are based on Hansen (1997) where '***' implies significance at the 5% level. ∞ implies an exponentially large F statistic that surpasses the bounds of the *'svars'* R package.

To identify the structural breakpoint that constitutes T_B, Zeileis et al. (2003) show that the F statistic which maximises Equation (33) is the optimal point:

$$F^*_{T_B} = \text{argmax}\left(\frac{\hat{\mu}'\hat{\mu} - \hat{\varepsilon}'\hat{\varepsilon}}{\hat{\varepsilon}'\hat{\varepsilon}/(n-2t)}\right) \tag{35}$$

Figure 13 plots the individual and average F statistics for each spillover index using the *'strucchange'* R package constructed by Kleiber et al. (2002). The optimal structural breakpoints are defined both daily and weekly (to accompany the SOMA portfolio) as the vertical lines in each chart.

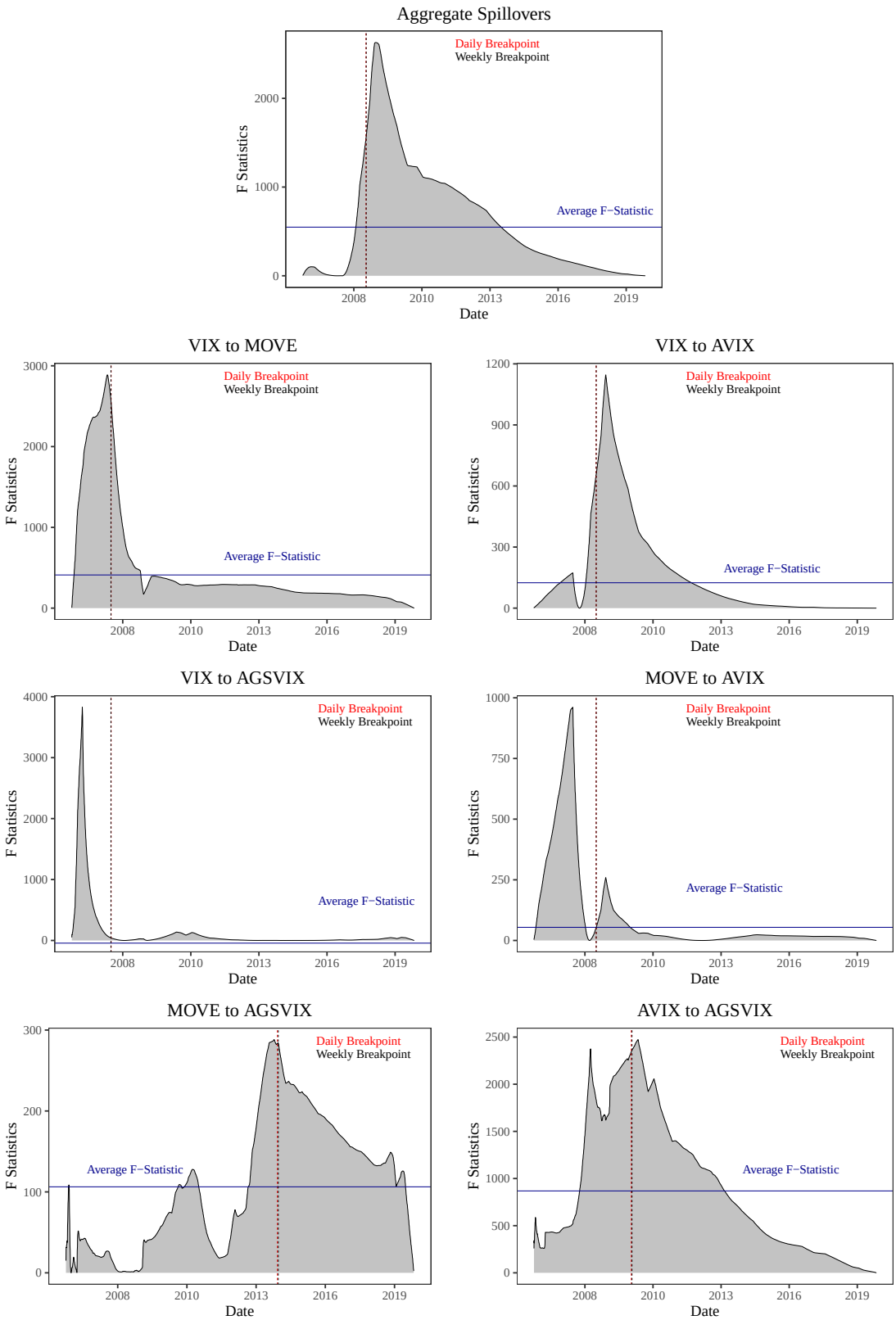

Figure 13: Structural Breaks in Volatility Spillover Indices

Note. These charts display the F statistics calculated at each observation for the spillover indices by performing the intercept-only regression: $S^g_{ij}(H)_t = \alpha_t + \varepsilon_t$. The plots also include the aggregated F statistic defined as the arithmetic average across the sample. The vertical lines are defined as the optimal structural breakpoints which maximise the value of Equation (33) in daily and weekly frequencies. While some lines may not appear to align with the highest point in the charts, identifying a structural breakpoint that is sufficiently in the neighbourhood of the maximum value permits identification of the SVAR models with little differentiation in the path of the impulse response functions. The breakpoints are identified using the *'strucchange'* R package.

Finally, the dates that correspond to the structural breakpoints are identified. Table 6 presents both the daily and weekly breakpoints and notably, there is little differentiation across both frequencies, permitting the structural breaks to occur at the same time in each SVAR model. All the structural break dates align to the crisis period except for the MOVE to AGSVIX and AVIX to AGSVIX indices. For the former, the structural break date aligns closely to the intensification of market volatility following the escalation in tensions between Russia and Ukraine over territorial disputes, while the latter corresponds to the early stages of the European Sovereign Debt crisis[14].

Optimal Break Dates		
	Daily Frequency	Weekly Frequency
Aggregate	2008–12–08	2008–12–03
VIX to MOVE	2008–01–29	2008–01–16
VIX to AVIX	2008–11–24	2008–11–19
VIX to AGSVIX	2008–01–29	2008–01–16
MOVE to AVIX	2008–11–24	2008–11–19
MOVE to AGSVIX	2014–03–28	2014–03–26
AVIX to AGSVIX	2010–03–11	2010–03–10

Table 6: Structural Break Dates

Note. This table reports the structural break dates that are in the neighbourhood of the optimal breakpoint, both daily and weekly. The formatting of the dates is as follows: YYYY/MM/DD.

3.4.3 Identification via Non-Gaussian Maximum Likelihood

Up to this point, the identification schemes discussed have been subject to the assumption of normality. Given the evidence of a departure from normality identified among the implied volatility indices, the use of a scheme that is not limited to normally distributed errors can ensure precision in the impulse response functions[15]. The Non-Gaussian Maximum Likelihood (NGML) identification scheme pioneered by Lanne et al. (2017) is one such method that does not constrain the estimation of the SVAR models to normality. Again, the *'svars'* R package (Lange et al., 2019) is used. The scheme optimises a log-likelihood function of structural shocks that follow a Student t distribution and is applied in three steps. Firstly, the VAR parameters, θ, and the reduced form residuals, μ_t, are estimated using the OLS method:

$$\theta = [\alpha, A_1, \ldots, A_p]' \tag{36}$$

Where α is the intercept term. The reduced form residuals are derived as:

$$\mu_t\left(\hat{\theta}\right) = \left[y_t - \hat{\alpha} - \hat{A}_1 y_{t-1}, \ldots, -\hat{A}_p y_{t-p}\right]' \tag{37}$$

[14]The intensification in market volatility due to the escalation in tensions between Russia and Ukraine is captured by U.S. CDS Spread and thus a specific variable to control for its effects is not required.

[15]Evidence of a departure from normality is also strongly validated for each of the pairwise volatility spillover indices presented in Appendix E.

Secondly, the log-likelihood function is maximised conditional on the estimations in the first step:

$$\log \mathcal{L}(\Theta) = \log \mathcal{L}\left(\hat{\theta}, \Theta\right) = T^{-1} \sum_{t=1}^{T} \omega_t \left(\hat{\theta}, \Theta\right) \tag{38}$$

Where ω_t is defined as:

$$\omega_t \left(\hat{\theta}, \Theta\right) = \sum_{i=1}^{N} \log f_i \left(s_{f_i}^{-1} \hat{i} B(b)^{-1} \mu_t \left(\hat{\theta}\right); d_{f_i}\right) - \log |\{B(b)\}| - \sum_{i=1}^{N} \log s_{f_i} \tag{39}$$

In Equation (39), $\hat{i}$ is the ith unit vector and $\Theta = [b, s_{f_i}, d_{f_i}]'$, with b an $N(N-1) \times 1$ matrix containing the off-diagonal elements of the covariance decomposition of the structural impact (B) matrix. Furthermore, s_{f_i} & d_{f_i} are the scale and the degrees of freedom for the probability density function (f_i) of the Student t distribution. The final step involves replacing Θ by the estimate $\tilde{\Theta}$ which maximises the log-likelihood function and recovers the SVAR parameters:

$$\log \mathcal{L}(\theta) = \log \mathcal{L}\left(\theta, \tilde{\Theta}\right) = T^{-1} \sum_{t=1}^{T} \omega_t \left(\theta, \tilde{\Theta}\right) \tag{40}$$

4. EMPIRICAL RESULTS

4.1 Volatility Spillovers

4.1.1 Static Volatility Spillovers

The first measure of volatility spillovers are the static spillovers that have occurred across the sample from 2006–2019. These spillovers are presented in Table 7 and read as follows. Firstly, the off-diagonal elements represent the proportion of forecast error variance that results from another variable in the system of markets. For instance, the VIX has contributed to roughly 17 per cent of the total variability observed in the AVIX, the most extensive pairwise volatility transmission across all four markets. The 'TO' row represents the volatility transmitted from each of the four variables to the system, while the 'FROM' column captures the volatility received by each variable. The difference between the 'TO' row and the 'FROM' column is the net spillover contributed by each market to the total variability. Finally, the right-lower-diagonal corner of the table, in bold, reflects the total volatility spillover among all four variables and is approximately equal to the grand off-diagonal column sum relative to the grand column sum inclusive of diagonal elements.

Notably, the net spillovers shed considerable light on the volatility transmission between the markets. Firstly, the VIX is the variable of central influence, with the highest net positive contribution to the variability of the system, echoing the findings of Yang and Zhou (2017). The MOVE also contributes positively to the total volatility, albeit, at a lower proportion compared to the VIX. In contrast, the two Australian markets are net volatility receivers as illustrated by the negative spillovers, with the AVIX having received the greatest magnitude of spillovers. Collectively, these dynamics imply that the U.S. equity market, and to a lesser extent, the U.S. government bond market, have contributed to the risk in Australian markets. While the static spillovers add value to understanding the volatility transmission between each market, the dynamic nature of these spillovers throughout time is of greater interest.

Spillover Table (%)

	VIX	MOVE	AVIX	AGSVIX	FROM
VIX	93.470	6.360	0.090	0.080	1.630
MOVE	7.250	92.140	0.390	0.220	1.970
AVIX	17.340	2.280	80.300	0.080	4.920
AGSVIX	0.680	0.310	0.080	98.930	0.270
TO	6.320	2.240	0.140	0.090	–
Net Spillovers	4.690	0.270	-4.780	-0.180	–
Spillover Index					**8.790**

Table 7: Static Volatility Spillovers

Note. This table displays the static spillovers for all four markets from 2006–2019. The off-diagonal elements are the pairwise spillovers between each market. The 'TO' row represents the contribution of volatility from each market to all others, while the 'FROM' column captures the inbound volatility received from all other markets. The net spillovers are the difference between the outbound and inbound volatility between each market, with a positive value indicating the market is a net contributor to volatility and vice versa. The spillover index, indicated in bold, is the total variability in the system across the sample.

4.1.2 Dynamic Aggregate Volatility Spillovers

Figure 14 presents the recursively constructed dynamic aggregate spillover index based on an H-step-ahead forecast horizon of 12 days. This index captures the total variability in the system of markets throughout time. The most significant characteristic depicted by the index is the exponential increase in daily spillovers during the onset of the financial crisis in 2007, which remains elevated until 2009. Spillovers also intensify around 2010, aligning to the European Sovereign Debt crisis, yet are far lesser than the volatility illustrated between 2007–2009. The volatility transmission since the crisis, however, has been relatively benign. While copious economic disturbances have occurred since the crisis, the busting of the U.S. subprime mortgage bubble had a sizable impact on the volatility across all four markets.

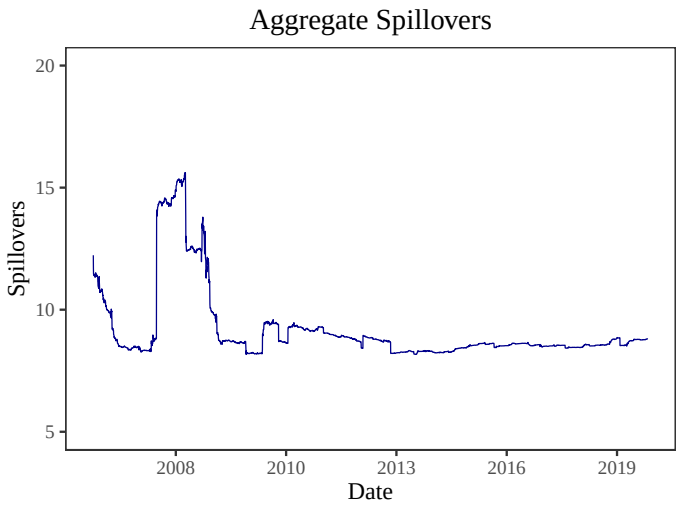

Figure 14: Dynamic Aggregate Volatility Spillovers

Note. This chart illustrates the recursively constructed dynamic aggregate spillover index with an H-step-ahead forecast horizon of 12 days.

4.1.3 Directional Volatility Spillovers

The directional spillover indices display the volatility dynamics of each market and their interaction with the broader system. The first set of indices measures the degree to which each market transmits volatility to all others, permitting identification of the market of greatest influence. Figure 15 shows that the market which contributes the most to the volatility of the system is the VIX, suggesting the U.S. equity market has a central role in the transmission of volatility. The volatility contribution of the VIX is also again magnified around the onset of the crisis. Similarly, the MOVE contributes to the total variability of the system at around half the proportion of the VIX. In contrast, the AVIX and AGSVIX contribute very little to the total volatility, highlighting the lack of influence the Australian financial markets have on U.S. markets.

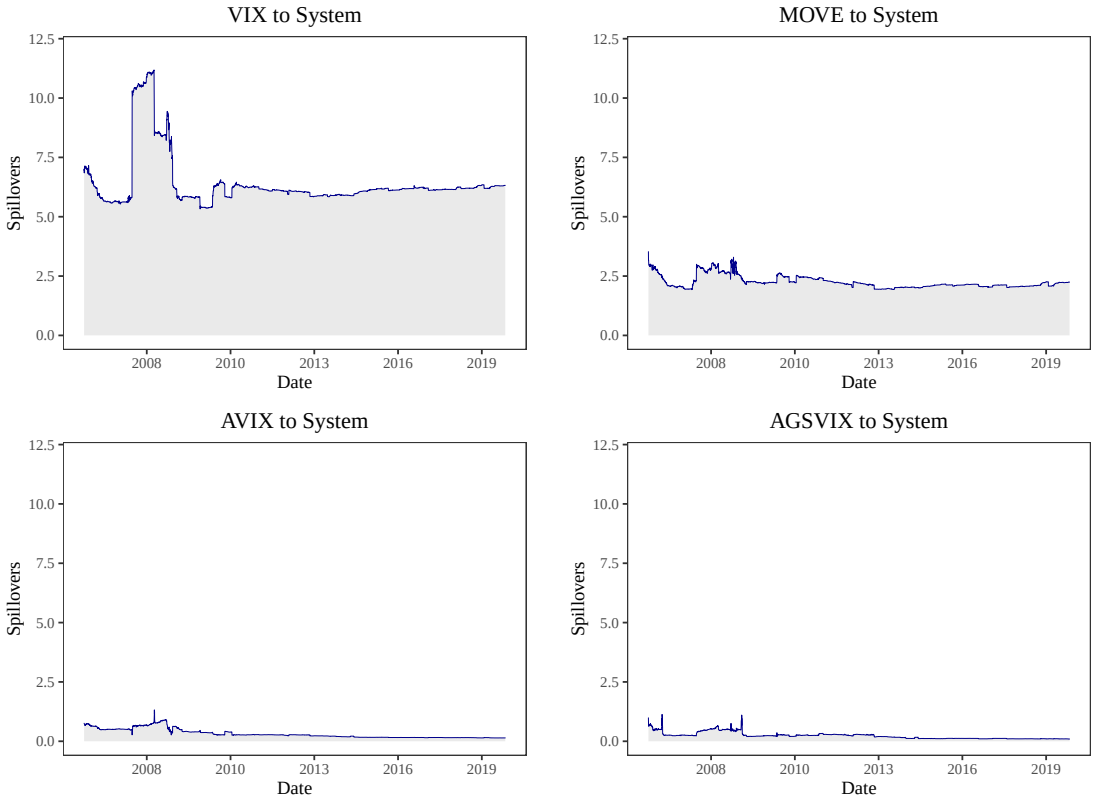

Figure 15: Volatility Spillover Contribution to All Markets

Note. These charts illustrate the recursively constructed dynamic spillover indices with an H-step-ahead forecast horizon of 12 days. The charts depict the daily volatility contributed by each market to all others in the system.

The indices illustrated in Figure 16 exhibit the volatility received by each market from all others. These indices portray the markets that have been the most susceptible to receiving volatility, and clearly, the AVIX has been the most vulnerable. The magnitude of volatility received by the AVIX suggests risk in the Australian equity market has been significantly driven by the U.S. markets. Furthermore, while the

VIX and MOVE receive some inbound volatility, the extent of these spillovers is limited and stable over time. In contrast, the AGSVIX receives little inbound volatility, suggesting that volatility in the Australian government bond market may be driven by idiosyncratic factors that are not captured in this model.

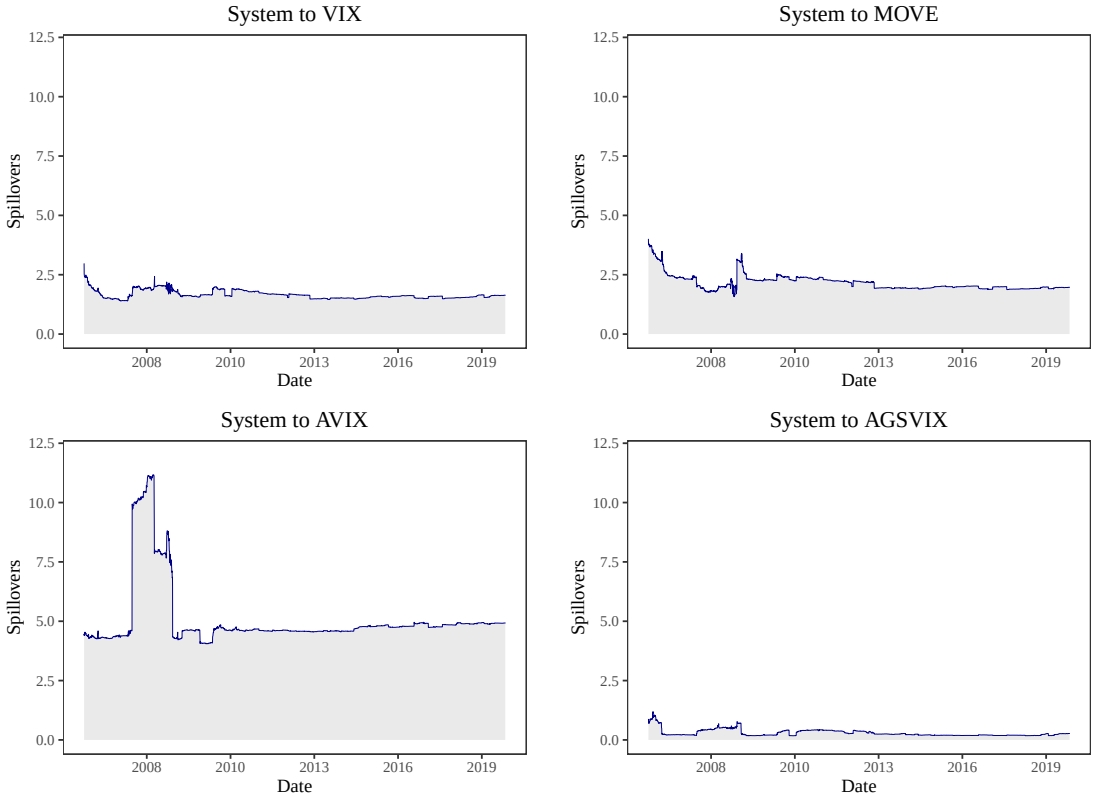

Figure 16: Volatility Spillover Contribution from All Markets

Note. These charts illustrate the recursively constructed dynamic spillover indices with an H-step-ahead forecast horizon of 12 days. The charts depict the daily volatility received by each market from all others in the system.

Upon identifying the volatility each market contributes, and the volatility each market receives, a measure of the net spillovers is attained. This measure provides an illustration of the markets that are net transmitters and those that are net receivers of volatility. Figure 17 displays the centrality of the VIX in being a net transmitter throughout the entire sample, and when compared to the aggregate volatility index in Figure 14, it is clear that the VIX is the largest net contributor of volatility to all other markets. The MOVE's net contributions are negative before the crisis, yet significantly swing to a net positive contribution in late 2007, suggesting the onset of the crisis saw the U.S. government bond market transmit volatility to all others.

In contrast, the AVIX has been a net volatility receiver throughout the entire sample. Moreover, the dynamics of the AVIX resemble an inverse relationship to that of the net contributions of the VIX, suggesting the U.S. equity market has had a significant contribution to the risk received by the Australian equity market. The AGSVIX depicts net volatility dynamics that appear to be inversely related to the MOVE, suggesting a nuanced relationship between government bond markets in both countries. However, the magnitude of

net daily spillovers received by the AGSVIX is limited, indicating both the U.S. markets and the Australian equity market have had little influence on its volatility dynamics.

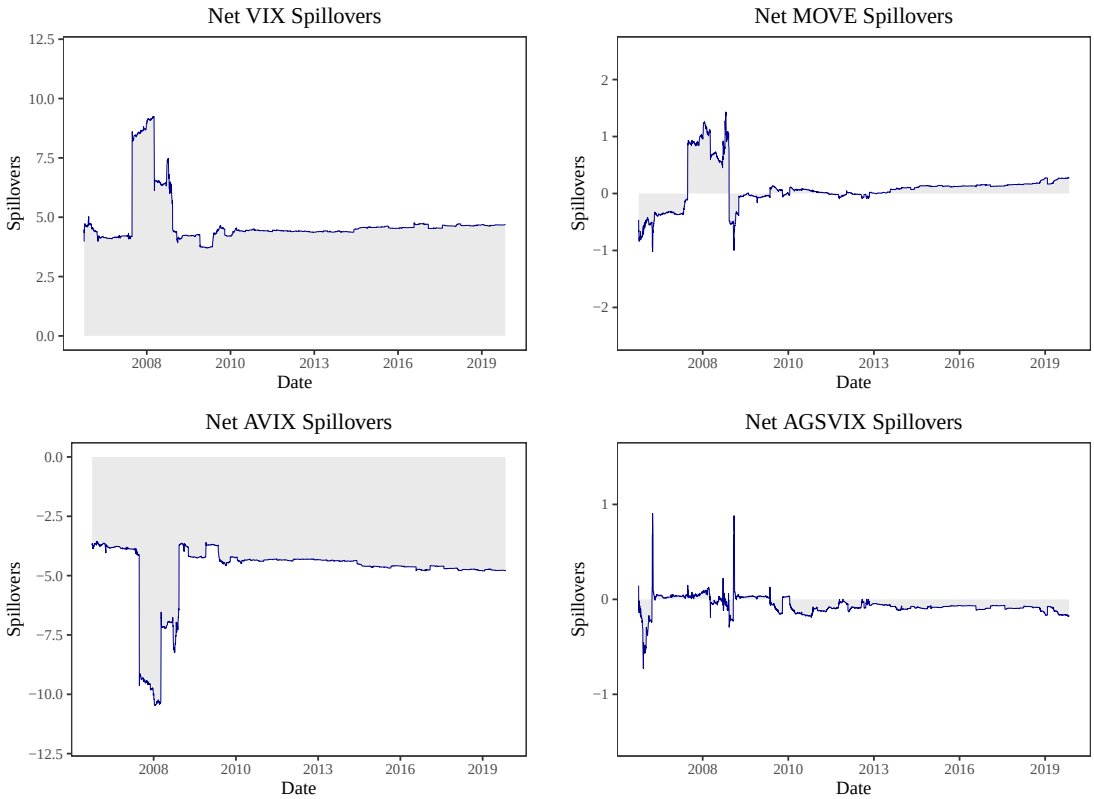

Figure 17: Net Volatility Spillovers

Note. These charts illustrate the recursively constructed dynamic net spillover indices with an H-step-ahead forecast horizon of 12 days.

4.1.4 Pairwise Volatility Spillovers

The pairwise spillover indices are the most important element of the methodology as they illustrate the cross-market volatility dynamics that are used to examine the influence of QE in the section that follows. Figure 18 illustrates these indices, of which multiple elements warrant an exposition. Firstly, the volatility transmission between the U.S. and Australian equity markets is substantial. As shown by the spillovers between the VIX and AVIX, this pairwise relationship accounts for most of the variability in the system. The spillovers between the equity markets in both countries also peak during the onset of the financial crisis, with spillovers remaining steady since. Similarly, the volatility transmission between the U.S. government bond and Australian equity markets is elevated, with intensified spillovers observed during the crisis. While the spillovers between the MOVE and AVIX are lower in comparison to the contribution of the VIX, collectively, it can be contended that the U.S. markets have had considerable effects on the risk in the Australian equity market.

Secondly, the relationship between the VIX and AGSVIX depicts an intensification of volatility at the onset of the crisis and a continued net positive contribution throughout time. While the magnitude of

daily spillovers is considerably small, it is shown that the Australian government bond market has been a net receiver of volatility from the U.S. equity market. In contrast, the spillovers between the MOVE and AGSVIX illustrate a differing narrative. Specifically, around the key disturbance events between 2007–2009, the Australian government bond market appears to have transmitted volatility to the U.S. government bond market, thus reversing the nature of the relationship. The initial reversal occurs in June 2006, corresponding to a global market sell-off following concerns of higher monetary policy rates amid inflationary pressures[16]. The second reversal occurred in September 2008, corresponding to the collapse of Lehman Brothers, the Federal Reserve's bailout of American International Group, and the rejection of the U.S. Government's planned $700 billion Emergency Economic Stabilization Act by the U.S. Congress, which saw severe market dislocation and intensified volatility[17]. While spillovers during these reversals are small, the negative decline in volatility transmission (and thus reversal in the relationship) sheds light on the interconnected nature of these markets, such that even markets at the centre of influence are not immune from risk spillovers from markets in other geographic jurisdictions.

Finally, the relationships between the domestic equity and government bond markets in each country provide insight into the local volatility dynamics. Specifically, the VIX appears to induce volatility in the MOVE throughout the sample, except for the reversal of transmission in late 2008, again corresponding to the collapse of Lehman Brothers. This reversal highlights the fact that for a brief period, the U.S. government bond market had a considerable influence on the volatility in the U.S. equity market. Similarly, the AVIX plays a role much like the VIX when it comes to its influence over the AGSVIX, contributing a net positive volatility transmission throughout the sample. A reversal in the relationship also occurs in March 2008, aligning to the Federal Reserve's bailout of Bear Sterns that improved market sentiment and saw equity indices globally appreciate until the end of May 2008.

[16]On 29 June 2006, the FOMC increased the target for the Federal Funds Rate by 25 basis points to 5.25 per cent in response to elevated core inflation readings. Several central banks including the European Central Bank also increased their policy rates in June, further intensifying global financial market activity.

[17]The Emergency Economic Stabilization Act of 2008 would eventually pass into law on 3 October 2008, giving rise to the Troubled Asset Relief Program (TARP).

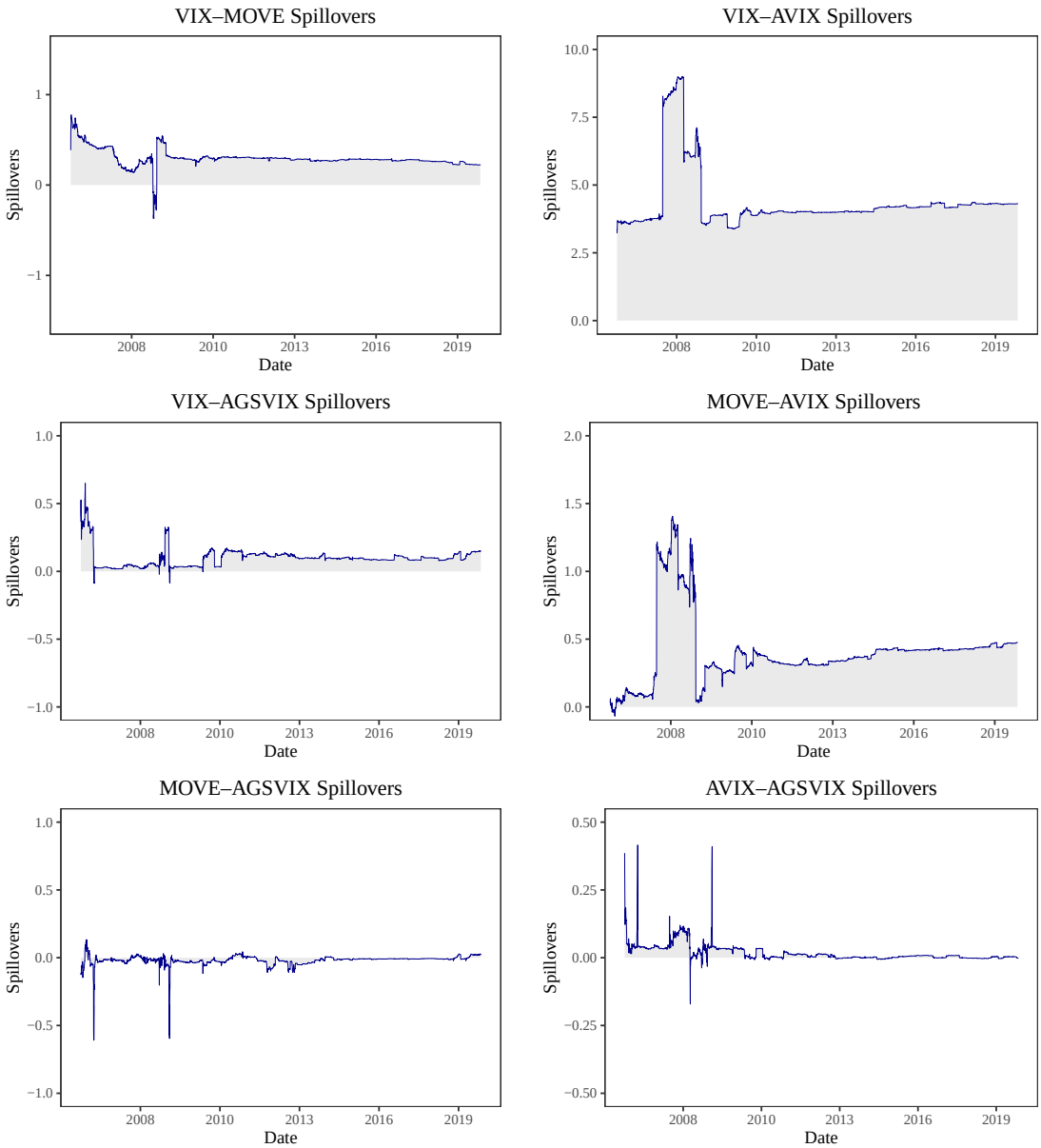

Figure 18: Pairwise Volatility Spillovers

Note. These charts illustrate the recursively constructed dynamic pairwise spillover indices with an H-step-ahead forecast horizon of 12 days. Descriptive statistics and Pearson correlation coefficients for each pairwise spillover index are provided in Appendix E.

In sum, the creation of these spillover indices, while valuable for understanding the bilateral risk transference between equity and government bond markets in both countries, does not specifically draw insight on the effects stemming from the Federal Reserve's QE programs. Instead, the section that follows reports the results of the empirical framework outlined in Section 3.3.3, which when applied to these indices, isolates the Federal Reserve's influence on cross-market volatility.

4.2 Determinants of Volatility Spillovers

4.2.1 U.S. Shadow Policy Rate

Table 8 presents the first set of findings for the determinants of volatility spillovers. Specifically, the framework is sequentially applied to examine the aggregate index, with control variables introduced in each iteration marked as Model 1, 2, & 3 respectively. Model 1 begins by solely testing the influence of the Shadow Policy Rate and the dichotomous variable, D_{QE_t}. The results illustrate the reasonable influence of the Shadow Policy Rate, which explains between 9–22 per cent (Adjusted R^2) of the aggregate spillovers. The positive coefficient on the rate also supports H_1, such that an increase in the rate (reduction in the magnitude of QE) intensifies volatility spillovers by reversing the loose policy settings. In contrast, the dichotomous variable provides little evidence of volatility transmission across the markets from the Federal Reserve's announcements. In comparison to this result, Rosa (2014) finds that high-frequency intraday prices show evidence of a signalling effect, suggesting that at lower frequencies the dichotomous variable may be insufficient to capture this phenomenon.

The results are consistent in Model 2 as the macroeconomic surprise indices are added. The power of the results increases, ranging between 14–32 per cent with the crisis period exhibiting the highest power (0.32). The Shadow Policy Rate is again significant across all three periods, exhibits positive coefficients, and is especially significant in the crisis period ($p < 0.001$). The dichotomous variable again fails to show evidence of signalling effects.

Model 3 introduces the control variables for Australian monetary policy and credit risk, constituting the full framework. The imposition of these variables amplifies the power of the results, ranging between 58–67 per cent with the crisis period again exhibiting the greatest power (0.67). In contrast to the results of Models 1 and 2, the Shadow Policy Rate is only significant across the full sample and the normalisation subperiod ($p < 0.01$), with little evidence that it has a substantial influence over spillovers during the crisis. Instead, the spillovers during the crisis appear to be driven by the Australian policy rate and CDS Spreads[18].

There are several elements within the results of Model 3 that require an exposition. Firstly, the coefficient for the Shadow Policy Rate in the full sample is positive, consistent with H_1. The full sample results also depict the high significance of the Australian macroeconomic surprise index, Australian policy rate, and CDS spreads ($p < 0.001$). The Australian macroeconomic surprise index has a negative coefficient, suggesting that as economic surprises increase, volatility spillovers decrease. This result is consistent with intuition given that an increase in the index suggests better-than-expected macroeconomic performance. The Australian policy rate has a positive coefficient, which aligns with H_1 that tighter monetary policy settings increase volatility spillovers. Likewise, the U.S. CDS spread has a positive coefficient, indicating that an increase in the perception of credit risk leads to greater spillovers. Surprisingly, the Australian CDS spread has a negative coefficient, suggesting that as the perception of Australian credit risk increases, volatility spillovers

[18]These results are consistent among the 60, 70, 80, and 90 day rolling window specification of the aggregate spillover index, with an H-step-ahead forecast horizon of 3 days illustrating the most significant results.

decrease. To meaningfully decompose this result is difficult without first assessing the results of each pairwise spillover index. However, it can be argued that as Australian CDS spreads increase to a level in concert with spreads in the U.S., the expectation of a future widening in credit spreads is reduced and thus suppresses spillovers by resembling a fairer value[19].

In the normalisation period, the narrative differs. In particular, the Shadow and Australian policy rates exhibit negative coefficients, signifying an inverse relationship between them and aggregate spillovers[20]. Specifically, the negative coefficients imply that as the stance of monetary policy in both Australia and the U.S. is tightened, aggregate volatility spillovers decrease. While this result rejects H_1, the normalisation period refers to an environment of improved economic performance, such that reversing extremely loose monetary settings signals economic fundamentals that warrant a return to policy normality (Chari et al., 2020). Thus, it can be contended that as policy rates increased during this period, market participants may have felt more confident in the economic outlook, and thus spillovers were less intense as the appetite to rebalance portfolio holdings was repressed. This conjecture is consistent with the literature that finds the intensity of portfolio balancing is contingent on the underlying state of the economy, and in the absence of economic distress, volatility spillovers are subdued (see for instance Beber et al. (2011) & Baruník et al. (2016)).

[19]The results from the rolling window specifications similarly display significant (albeit at a lower power) results for the U.S. and Australian CDS spread and macroeconomic surprise variables with consistent signs. In contrast, the Australian policy rate, although significant across these results, displays a negative coefficient which rejects H_1. Yang and Zhou (2017) argue that a recursive estimation is more appropriate for modelling the dynamics of volatility, as the rolling window estimations may be biased towards the 'flow' effect, rather than the 'stock' effect of QE. Thus, the inconsistency in the results for the Australian policy rate may be due to the nature of the estimation. Nevertheless, the results are reported for transparency in Appendix C.

[20]Similarly, the negative coefficients are consistent among the rolling window estimations, with the Australian policy rate highly significant across each model ($p < 0.001$). While the Shadow Policy Rate is significant, it exhibits a lesser level of significance than in the recursive estimation results.

	Full Sample: 2006–2019			*Crisis Period: 2007–2012*			*Normalisation Period: 2013–2019*		
	Model 1	Model 2	Model 3	Model 1	Model 2	Model 3	Model 1	Model 2	Model 3
QE_{SHDW}	0.166**	0.179**	0.126***	0.319**	0.365***	0.022	0.030*	0.030*	-0.044**
	(0.006)	(0.004)	(0.000)	(0.004)	(0.001)	(0.767)	(0.042)	(0.036)	(0.008)
D_{QE}	-0.218	-0.096	0.037	-0.127	-0.165	-0.380	0.043	0.053	0.027
	(0.150)	(0.531)	(0.799)	(0.580)	(0.548)	(0.163)	(0.320)	(0.118)	(0.223)
SUR_G		0.003	-0.005		-0.002	0.001		-0.001	-0.001
		(0.785)	(0.374)		(0.858)	(0.908)		(0.443)	(0.220)
SUR_{US}		-0.007	-0.002		-0.011	-0.001		-0.001	-0.001
		(0.335)	(0.633)		(0.164)	(0.852)		(0.189)	(0.072)
SUR_{AU}		-0.007*	-0.008***		-0.011**	-0.006		-0.001	0.000
		(0.025)	(0.001)		(0.005)	(0.109)		(0.379)	(0.268)
OIS_{AU}			0.319***			1.045***			-0.311***
			(0.000)			(0.000)			(0.000)
CDS_{US}			0.047***			0.038***			0.012***
			(0.000)			(0.000)			(0.001)
CDS_{AU}			-0.023***			-0.013*			-0.005**
			(0.000)			(0.021)			(0.007)
Intercept	9.204***	9.282***	6.747***	10.110***	10.289***	2.614**	8.513***	8.514***	8.770***
	(0.000)	(0.000)	(0.000)	(0.000)	(0.000)	(0.010)	(0.000)	(0.000)	(0.000)
Adj. R^2	0.092	0.135	0.615	0.218	0.316	0.674	0.152	0.207	0.579
Obs.	3467	3467	3467	1510	1510	1510	1707	1707	1707

Table 8: Results of Aggregate Volatility Spillover Index

Note. This table displays the result of the following regression estimated using OLS: $S^g_{ij}(H)_t = \alpha_t + \beta_1 QE_{SHDW_t} + \beta_2 D_{QE_t} + \beta_3 SUR_{G_t} + \beta_4 SUR_{US_t} + \beta_5 SUR_{AU_t} + \beta_6 OIS_{AU_t} + \beta_7 CDS_{US_t} + \beta_8 CDS_{AU_t} + \varepsilon_t$. The p-values (in parentheses below the coefficients) are derived from Newey and West (1986) heteroskedasticity and autocorrelation consistent standard errors. The levels of significance are defined as follows: '***' implies significance at the 0.1% level, '**' implies significance at the 1% level, and '*' implies significance at the 5% level.

Table 9 reports the results of the pairwise spillover indices across the entire sample. In these results, the Shadow Policy Rate is only significant ($p < 0.001$) in explaining the volatility transmission between the AVIX and AGSVIX, suggesting that alongside the equally significant Australian policy rate, domestic spillovers between the Australian equity and government bond markets have been driven by the policy settings in both countries. The coefficient is again positive and supports H_1[21].

The other pairwise indices show little evidence of the Shadow Policy Rate in influencing spillovers across the entire sample. Instead, the VIX to MOVE, VIX to AVIX, and MOVE to AVIX highlight the dominant role of CDS spreads, and thus the perception of credit risk, in influencing spillovers. The dichotomous variable again presents no confirmation of a signalling effect, consistent with the results of Bauer and Neely (2014) who find little evidence of this effect among Australian markets[22].

[21] In the rolling window estimations, only the 70 day specification shows a significant effect stemming from the Shadow Policy Rate on the AVIX to AGSVIX spillovers.

[22] Even with the narrower window lengths provided by the rolling window estimations, no evidence of a significant influence is found resulting from the dichotomous variable.

Full Sample: 2006–2019

	VIX/MOVE	VIX/AVIX	VIX/AGSVIX	MOVE/AVIX	MOVE/AGSVIX	AVIX/AGSVIX
QE_{SHDW}	0.006	0.081*	-0.001	0.007	0.002*	0.004***
	(0.083)	(0.012)	(0.665)	(0.354)	(0.048)	(0.000)
D_{QE}	0.005	0.011	0.004	-0.016	0.003	0.002
	(0.657)	(0.919)	(0.584)	(0.576)	(0.499)	(0.541)
SUR_G	0.000	-0.004	0.000	-0.001	0.000	0.000
	(0.451)	(0.476)	(0.274)	(0.500)	(0.725)	(0.356)
SUR_{US}	0.000	-0.001	0.000	0.000	0.000*	0.000
	(0.735)	(0.730)	(0.273)	(0.958)	(0.033)	(0.594)
SUR_{AU}	0.000	-0.005*	0.000*	-0.001	0.000***	0.000
	(0.782)	(0.046)	(0.036)	(0.081)	(0.001)	(0.782)
OIS_{AU}	0.024***	0.082	-0.001	-0.017	-0.003**	0.007***
	(0.000)	(0.201)	(0.762)	(0.265)	(0.010)	(0.000)
CDS_{US}	-0.003***	0.033***	0.000	0.010***	0.000	0.000
	(0.000)	(0.000)	(0.690)	(0.000)	(0.722)	(0.602)
CDS_{AU}	0.002***	-0.018***	0.000	-0.006***	0.000	0.000
	(0.000)	(0.000)	(0.971)	(0.000)	(0.294)	(0.469)
Intercept	0.291***	3.245***	0.126***	0.216***	0.001	-0.020***
	(0.000)	(0.000)	(0.000)	(0.001)	(0.883)	(0.000)
Adjusted R^2	0.253	0.354	0.104	0.292	0.116	0.373
Obs.	3467	3467	3467	3467	3467	3467

Table 9: Results of Pairwise Volatility Spillover Indicies – Full Sample

Note. This table displays the result of the following regression estimated using OLS: $S^g_{ij}(H)_t = \alpha_t + \beta_1 QE_{SHDW_t} + \beta_2 D_{QE_t} + \beta_3 SUR_{G_t} + \beta_4 SUR_{US_t} + \beta_5 SUR_{AU_t} + \beta_6 OIS_{AU_t} + \beta_7 CDS_{US_t} + \beta_8 CDS_{AU_t} + \varepsilon_t$. The p-values (in parentheses below the coefficients) are derived from Newey and West (1986) heteroskedasticity and autocorrelation consistent standard errors. The levels of significance are defined as follows: '***' implies significance at the 0.1% level, '**' implies significance at the 1% level, and '*' implies significance at the 5% level.

While the results in Table 8 show little evidence of an influence stemming from the Shadow Policy Rate on aggregate spillovers during the crisis period, the results in Table 10 illustrate the more nuanced volatility dynamics among the pairwise indices. Specifically, the Shadow Policy Rate is the only significant variable ($p < 0.001$) that explains the domestic AVIX to AGSVIX spillovers during the crisis.

Similarly, the Shadow Policy Rate is the lone significant variable ($p < 0.001$) that explains the spillovers between the VIX & AGSVIX. The negative coefficient on this result, however, provides evidence against H_1. In particular, the negative coefficient indicates that as the Shadow Policy Rate increases, volatility spillovers decrease between the two markets. This result may speak to the distinct interaction between QE, government bond yields, and equity risk premia. Specifically, a higher Shadow Policy Rate encourages higher U.S. government bond yields, creating trading opportunities as yield differentials emerge in the global government bond market (Georgiadis and Gräb, 2016). To match returns on offer from U.S. government bonds, Australian government bond yields would subsequently increase and in turn, the relative value they offer against the U.S. equity market improves. As such, a higher return on offer from investing in Australian government bonds may attenuate the volatility between the markets by reducing the propensity for portfolio balancing, whereby investors liquidate low yielding positions in search of higher returns in riskier assets. Gagnon et al. (2018) provide insight into this result by showing evidence that the Federal Reserve's initial

QE program reduced the U.S. equity risk premium during the onset of the crisis. This reduction in equity risk premia corresponds to evidence of global fund flows into U.S. equity funds following the imposition of LSAP 1, suggesting portfolio balancing may have contributed to a rotation out of Australian securities which intensifies volatility (Fratzscher et al., 2018). Thus, an increasing Shadow Policy Rate may suppress spillovers between equity and government securities by alleviating the propensity for portfolio balancing.

As a final note, the Australian policy rate is highly significant ($p < 0.001$) in explaining the spillovers between the VIX & AVIX and MOVE & AVIX[23]. The positive coefficients in both tests supports H_1, indicating that a tightening in the stance of Australian monetary policy can induce increased spillovers between the markets by undoing easy financial conditions.

Crisis Period: 2007–2012

	VIX/MOVE	VIX/AVIX	VIX/AGSVIX	MOVE/AVIX	MOVE/AGSVIX	AVIX/AGSVIX
QE_{SHDW}	0.006	0.038	-0.012***	-0.017	-0.001	0.007***
	(0.168)	(0.547)	(0.000)	(0.226)	(0.417)	(0.000)
D_{QE}	0.003	-0.160	-0.015	-0.068	0.008	0.000
	(0.914)	(0.478)	(0.264)	(0.176)	(0.324)	(0.950)
SUR_G	0.000	0.004	0.000	0.001	0.000	0.000
	(0.375)	(0.631)	(0.559)	(0.474)	(0.140)	(0.826)
SUR_{US}	0.000	-0.002	0.000	0.000	0.000	0.000
	(0.647)	(0.605)	(0.516)	(0.773)	(0.279)	(0.442)
SUR_{AU}	0.000	-0.005	0.000	-0.001	0.000**	0.000
	(0.275)	(0.126)	(0.633)	(0.210)	(0.006)	(0.361)
OIS_{AU}	-0.016*	0.741***	0.009	0.180***	0.010*	-0.004
	(0.050)	(0.000)	(0.117)	(0.000)	(0.025)	(0.263)
CDS_{US}	-0.002***	0.024**	0.000	0.008***	0.000	0.000
	(0.000)	(0.003)	(0.623)	(0.000)	(0.154)	(0.163)
CDS_{AU}	0.001***	-0.008	0.000	-0.003**	0.000	0.000
	(0.000)	(0.084)	(0.608)	(0.005)	(0.115)	(0.338)
Intercept	0.478***	-0.320	0.037	-0.841***	-0.065**	0.039
	(0.000)	(0.723)	(0.241)	(0.000)	(0.006)	(0.091)
Adjusted R^2	0.242	0.593	0.364	0.622	0.173	0.300
Obs.	1510	1510	1510	1510	1510	1510

Table 10: Results of Pairwise Volatility Spillover Indicies – Crisis Period

Note. This table displays the result of the following regression estimated using OLS: $S^g_{ij}(H)_t = \alpha_t + \beta_1 QE_{SHDW_t} + \beta_2 D_{QE_t} + \beta_3 SUR_{G_t} + \beta_4 SUR_{US_t} + \beta_5 SUR_{AU_t} + \beta_6 OIS_{AU_t} + \beta_7 CDS_{US_t} + \beta_8 CDS_{AU_t} + \varepsilon_t$. The p-values (in parentheses below the coefficients) are derived from Newey and West (1986) heteroskedasticity and autocorrelation consistent standard errors. The levels of significance are defined as follows: '***' implies significance at the 0.1% level, '**' implies significance at the 1% level, and '*' implies significance at the 5% level.

Table 11 presents the results from the normalisation period, which provides the strongest evidence of an influence stemming from Federal Reserve's QE programs on volatility spillovers. These set of results are among the best specified, representing between 29–92 per cent of the variation. In particular, the Shadow Policy Rate significantly explains the spillovers between the VIX to AVIX, VIX to AGSVIX, and MOVE to AVIX ($p < 0.001$). The results for the AVIX to AGSVIX spillovers are also significant, albeit, at a smaller

[23]While the rolling window regressions show some significance for the VIX to AVIX spillovers stemming from the Shadow Policy Rate, the coefficients on these results are at odds with H_1. Notably, the power of the results is also relatively low, ranging between 28–43 per cent.

magnitude compared to the other indices ($p < 0.01$). There are again multiple elements of interest that require elucidation.

Firstly, the VIX to AVIX and MOVE to AVIX tests have the highest powers in the study, with 86 and 92 per cent of the variation explained, respectively. Both results exhibit positive coefficients on the Shadow Policy Rate, supporting H_1, and providing evidence of intensified spillovers as the magnitude of QE is reduced throughout this period. In contrast, the Australian policy rate has a negative coefficient for both tests. This divergence in the signs between the two coefficients may be explained by the fact that the normalisation period captures the division in the stance of monetary policy from 2016 onwards, as both countries enacted different policy settings. Specifically, the Federal Reserve normalised policy and curtailed their QE program, while the RBA held policy rates steady from August 2016 to May 2019. As such, an increase in the Australian policy rate would be expected to quell volatility spillovers as it would equilibrate asset returns on offer in Australia to those in the U.S., eliminating trading opportunities. Concretely, if the Australian policy were to increase it would suppress the appetite for portfolio balancing into higher-yielding assets and effectively counteract the effects of a global yield search.

Secondly, the VIX to AGSVIX spillovers are also significant ($p < 0.001$) although the power of the result pales in comparison to the two aforementioned indices (0.29). Nevertheless, this result is of interest due to the negative coefficient on the Shadow Policy Rate, which is consistent with the results depicted during the crisis period[24]. Specifically, the relationship between monetary policy, equity risk premia, and government bond yields may yet again have a role to play in this result. For the sake of brevity, as monetary policy rates converge, so do the rates of return on offer between asset classes across countries, and as such, the appetency for portfolio balancing may satiate and thus suppress spillovers.

Finally, the domestic AVIX to AGSVIX spillovers portrays a similar narrative in terms of a negative coefficient, such that a normalisation in policy suppresses spillovers between the markets on a domestic basis. Again, it is important to note that the normalisation period saw improving economic fundamentals in the U.S., thus increasing monetary policy rates may signal an improved economic outlook that alleviates the desire to search for higher-yielding securities.

[24]The 60-day rolling window regression results also show a significant negative impact stemming from the Shadow Policy Rate on the VIX to AGSVIX spillovers.

Normalisation Period: 2013–2019

	VIX/MOVE	VIX/AVIX	VIX/AGSVIX	MOVE/AVIX	MOVE/AGSVIX	AVIX/AGSVIX
QE_{SHDW}	-0.001	0.029***	-0.008***	0.014***	0.006*	-0.001**
	(0.566)	(0.000)	(0.001)	(0.000)	(0.012)	(0.002)
D_{QE}	0.004	-0.001	-0.004	-0.004	-0.003	0.001
	(0.111)	(0.885)	(0.246)	(0.142)	(0.329)	(0.174)
SUR_G	0.001***	0.000	0.000	0.000	0.000	0.000
	(0.000)	(0.341)	(0.071)	(0.610)	(0.626)	(0.164)
SUR_{US}	0.000**	0.000	0.000	0.000	0.000	0.000*
	(0.003)	(0.886)	(0.526)	(0.106)	(0.308)	(0.016)
SUR_{AU}	0.000	0.000	0.000	0.000	0.000	0.000
	(0.715)	(0.075)	(0.756)	(0.988)	(0.536)	(0.794)
OIS_{AU}	0.016*	-0.090***	-0.026*	-0.027**	-0.004	-0.006***
	(0.033)	(0.000)	(0.011)	(0.004)	(0.672)	(0.000)
CDS_{US}	0.000	0.003***	0.001	0.000	0.000	0.000
	(0.989)	(0.000)	(0.081)	(0.372)	(0.284)	(0.115)
CDS_{AU}	0.000	-0.001***	-0.001***	0.000	0.000	0.000
	(0.074)	(0.000)	(0.001)	(0.366)	(0.522)	(0.821)
Intercept	0.220***	4.277***	0.161***	0.442***	0.005	0.004
	(0.000)	(0.000)	(0.000)	(0.000)	(0.793)	(0.165)
Adj. R^2	0.633	0.862	0.292	0.916	0.580	0.364
Obs.	1707	1707	1707	1707	1707	1707

Table 11: Results of Pairwise Volatility Spillover Indicies – Normalisation Period

Note. This table displays the result of the following regression estimated using OLS: $S^g_{ij}(H)_t = \alpha_t + \beta_1 QE_{SHDW_t} + \beta_2 D_{QE_t} + \beta_3 SUR_{G_t} + \beta_4 SUR_{US_t} + \beta_5 SUR_{AU_t} + \beta_6 OIS_{AU_t} + \beta_7 CDS_{US_t} + \beta_8 CDS_{AU_t} + \varepsilon_t$. The p-values (in parentheses below the coefficients) are derived from Newey and West (1986) heteroskedasticity and autocorrelation consistent standard errors. The levels of significance are defined as follows: '***' implies significance at the 0.1% level, '**' implies significance at the 1% level, and '*' implies significance at the 5% level.

4.2.2 SOMA Portfolio

For robustness, this section uses changes in the Federal Reserve's SOMA portfolio as the QE instrument. As the SOMA portfolio holdings are disclosed weekly, the results in this section are depicted over a weekly frequency. Table 12 reports the first set of results. In these results, the SOMA portfolio fails to explain spillovers across the three iterations of the models and among each of the three periods. The variables that do explain the spillovers, however, are the highly significant Australian monetary policy and CDS spread controls[25].

Much like the results in Section 4.2.1, the U.S. CDS spread is highly significant in explaining spillovers across each period, albeit, with a diminishing power over the subsamples. Interestingly, the Australian CDS spread again depicts a negative coefficient, which is difficult to adequately explain without assessing the pairwise results first. In sum, the lack of significant influence inflicted on the spillovers from changes in the SOMA portfolio may be due to the nature of what this instrument measures. Specifically, the weekly changes in the SOMA portfolio reflect the operational aspect of implementing QE, unlike the Shadow Policy Rate

[25]These results are consistent with the outcomes shown in the rolling window regressions for the SOMA portfolio. Specifically, the SOMA portfolio is found to be insignificant, while the 3 day H-step-ahead forecast horizon exhibits the most significant results for the Australian monetary policy and CDS Spread control variables.

which is a more encompassing measure of the policy environment. Thus, the lack of significance within these results may speak to the inability of the Federal Reserve's weekly operations to spur spillovers, which may be occurring at higher frequencies such as those captured by the daily Shadow Policy Rate.

	Full Sample: 2006–2019			*Crisis Period: 2007–2012*			*Normalisation Period: 2013–2019*		
	Model 1	Model 2	Model 3	Model 1	Model 2	Model 3	Model 1	Model 2	Model 3
QE_{SOMA}	-18.393	-15.278	-11.095	-23.301*	-20.339	-2.365	-9.103*	-8.092	3.377
	(0.148)	(0.229)	(0.148)	(0.049)	(0.097)	(0.569)	(0.034)	(0.155)	(0.133)
D_{QE}	-0.277	-0.242	-0.049	-0.187	-0.438	-0.497	0.063	0.075	0.066
	(0.126)	(0.217)	(0.818)	(0.728)	(0.372)	(0.170)	(0.176)	(0.060)	(0.066)
SUR_G		0.006	-0.008		0.001	0.000		0.000	-0.001
		(0.588)	(0.246)		(0.940)	(0.978)		(0.784)	(0.512)
SUR_{US}		-0.007	0.000		-0.009	0.000		-0.001	-0.001
		(0.363)	(0.898)		(0.426)	(0.962)		(0.125)	(0.091)
SUR_{AU}		-0.004	-0.005*		-0.003	-0.005		-0.001	-0.001
		(0.249)	(0.050)		(0.611)	(0.254)		(0.320)	(0.185)
OIS_{AU}			0.364**			1.060***			-0.172*
			(0.002)			(0.000)			(0.011)
CDS_{US}			0.047***			0.039**			0.012*
			(0.000)			(0.005)			(0.019)
CDS_{AU}			-0.026***			-0.014			-0.005
			(0.000)			(0.074)			(0.066)
Intercept	9.259***	9.284***	6.841***	10.036***	10.072***	2.539*	8.513***	8.515***	8.477***
	(0.000)	(0.000)	(0.000)	(0.000)	(0.000)	(0.020)	(0.000)	(0.000)	(0.000)
Adj. R^2	0.036	0.056	0.592	0.067	0.094	0.670	0.054	0.103	0.517
Obs.	716	716	716	313	313	313	351	351	351

Table 12: Results of Aggregate Volatility Spillover Index – SOMA Portfolio

Note. This table displays the result of the following regression estimated using OLS: $S^g_{ij}(H)_t = \alpha_t + \beta_1 QE_{SOMA_t} + \beta_2 D_{QE_t} + \beta_3 SUR_{G_t} + \beta_4 SUR_{US_t} + \beta_5 SUR_{AU_t} + \beta_6 OIS_{AU_t} + \beta_7 CDS_{US_t} + \beta_8 CDS_{AU_t} + \varepsilon_t$. The p-values (in parentheses below the coefficients) are derived from Newey and West (1986) heteroskedasticity and autocorrelation consistent standard errors. The levels of significance are defined as follows: '***' implies significance at the 0.1% level, '**' implies significance at the 1% level, and '*' implies significance at the 5% level.

When assessing the SOMA portfolio against the pairwise indices across the full sample, a lack of explanatory power is again evident. Across each of the spillover indices, the SOMA portfolio fails to exhibit significance. While there is some evidence the SOMA portfolio influences the spillovers between the VIX and MOVE ($p < 0.05$), this evidence pales in comparison against the highly significant CDS spread variables ($p < 0.001$). Likewise, the Australian policy rate is significant in explaining spillovers, especially across the domestic spillovers occurring between the VIX to MOVE and AVIX to AGSVIX ($p < 0.001$)[26].

[26]Similarily, the significance of the Australian policy rate is validated across all the rolling window regression results for the SOMA portfolio.

Full Sample: 2006–2019

	VIX/MOVE	VIX/AVIX	VIX/AGSVIX	MOVE/AVIX	MOVE/AGSVIX	AVIX/AGSVIX
QE_{SOMA}	0.965*	-11.170	-0.162	-3.013	-0.001	0.087
	(0.015)	(0.153)	(0.591)	(0.098)	(0.990)	(0.226)
D_{QE}	0.006	-0.032	0.009	-0.016	0.000	0.000
	(0.704)	(0.844)	(0.416)	(0.680)	(0.990)	(0.920)
SUR_G	0.000	-0.006	0.000	-0.001	0.000	0.000
	(0.694)	(0.357)	(0.235)	(0.451)	(0.898)	(0.685)
SUR_{US}	0.000	0.000	0.000	0.000	0.000	0.000
	(0.402)	(0.999)	(0.407)	(0.761)	(0.074)	(0.513)
SUR_{AU}	0.000	-0.003	0.000*	-0.001	0.000**	0.000
	(0.583)	(0.235)	(0.033)	(0.212)	(0.009)	(0.838)
OIS_{AU}	0.027***	0.109	-0.002	-0.015	-0.003	0.008***
	(0.000)	(0.239)	(0.779)	(0.484)	(0.059)	(0.000)
CDS_{US}	-0.003***	0.034**	0.000	0.010***	0.000	0.000
	(0.000)	(0.002)	(0.763)	(0.000)	(0.553)	(0.421)
CDS_{AU}	0.002***	-0.019**	0.000	-0.005***	0.000	0.000
	(0.000)	(0.002)	(0.910)	(0.000)	(0.159)	(0.480)
Intercept	0.298***	3.290***	0.123***	0.216**	0.002	-0.016*
	(0.000)	(0.000)	(0.000)	(0.006)	(0.718)	(0.020)
Adj. R^2	0.244	0.346	0.093	0.316	0.088	0.325
Obs.	716	716	716	716	716	716

Table 13: Results of Pairwise Volatility Spillover Indices – Full Sample (SOMA Portfolio)

Note. This table displays the result of the following regression estimated using OLS: $S^g_{ij}(H)_t = \alpha_t + \beta_1 QE_{SOMA_t} + \beta_2 D_{QE_t} + \beta_3 SUR_{G_t} + \beta_4 SUR_{US_t} + \beta_5 SUR_{AU_t} + \beta_6 OIS_{AU_t} + \beta_7 CDS_{US_t} + \beta_8 CDS_{AU_t} + \varepsilon_t$. The p-values (in parentheses below the coefficients) are derived from Newey and West (1986) heteroskedasticity and autocorrelation consistent standard errors. The levels of significance are defined as follows: '***' implies significance at the 0.1% level, '**' implies significance at the 1% level, and '*' implies significance at the 5% level.

In the crisis period, the SOMA portfolio is the only significant explanatory variable for the spillovers between the VIX and AGSVIX, echoing the results reported for the Shadow Policy Rate. In contrast, however, the negative coefficient on this result supports H_1. Specifically, a contraction in the size of the SOMA portfolio (a negative weekly change) is akin to a reduction in the magnitude of QE. Thus, the act of reducing asset holdings promotes intensified volatility spillovers by tightening the policy stance. Unlike the Shadow Policy Rate, however, the SOMA portfolio fails to adequately explain the domestic spillovers between the AVIX to AGSVIX, with no variables at all deemed as significant for this test.

Crisis Period: 2007–2012

	VIX/MOVE	VIX/AVIX	VIX/AGSVIX	MOVE/AVIX	MOVE/AGSVIX	AVIX/AGSVIX
QE_{SOMA}	0.314	-1.273	-0.523***	-0.568	0.129	0.066
	(0.172)	(0.738)	(0.001)	(0.495)	(0.171)	(0.300)
D_{QE}	0.043	-0.343	0.015	-0.106	0.008	0.001
	(0.316)	(0.291)	(0.605)	(0.168)	(0.491)	(0.851)
SUR_G	0.000	0.003	0.000	0.001	0.000	0.000
	(0.480)	(0.752)	(0.472)	(0.573)	(0.127)	(0.970)
SUR_{US}	0.000	-0.001	0.000	0.000	0.000	0.000
	(0.670)	(0.782)	(0.470)	(0.856)	(0.244)	(0.774)
SUR_{AU}	0.000	-0.004	0.000	-0.001	0.000***	0.000
	(0.063)	(0.291)	(0.053)	(0.135)	(0.001)	(0.187)
OIS_{AU}	-0.004	0.791***	-0.014*	0.147***	0.008**	0.008
	(0.644)	(0.000)	(0.024)	(0.000)	(0.002)	(0.066)
CDS_{US}	-0.003***	0.024*	0.000	0.008**	0.000	0.000
	(0.001)	(0.028)	(0.698)	(0.003)	(0.143)	(0.581)
CDS_{AU}	0.001***	-0.008	0.000	-0.003*	0.000	0.000
	(0.000)	(0.177)	(0.997)	(0.026)	(0.108)	(0.658)
Intercept	0.418***	-0.553	0.140***	-0.689***	-0.057**	-0.017
	(0.000)	(0.579)	(0.000)	(0.000)	(0.003)	(0.527)
Adj. R^2	0.225	0.584	0.232	0.609	0.187	0.171
Obs.	313	313	313	313	313	313

Table 14: Results of Pairwise Volatility Spillover Indices – Crisis Period (SOMA Portfolio)

Note. This table displays the result of the following regression estimated using OLS: $S^g_{ij}(H)_t = \alpha_t + \beta_1 QE_{SOMA_t} + \beta_2 D_{QE_t} + \beta_3 SUR_{G_t} + \beta_4 SUR_{US_t} + \beta_5 SUR_{AU_t} + \beta_6 OIS_{AU_t} + \beta_7 CDS_{US_t} + \beta_8 CDS_{AU_t} + \varepsilon_t$. The p-values (in parentheses below the coefficients) are derived from Newey and West (1986) heteroskedasticity and autocorrelation consistent standard errors. The levels of significance are defined as follows: '***' implies significance at the 0.1% level, '**' implies significance at the 1% level, and '*' implies significance at the 5% level.

The normalisation period again illustrates the strongest evidence of the Federal Reserve's actions on volatility spillovers, with the results explaining between 14–85 per cent of the variation. Across the VIX to AVIX, MOVE to AVIX, and the MOVE to AGSVIX, the SOMA portfolio is significant in explaining spillovers, although, the level of significance is lower compared to the results reported when using the Shadow Policy Rate as the QE instrument.

The most well-specified result is that of MOVE to AVIX, with 85 per cent of the variation explained. The negative coefficient on this result supports H_1, such that a reduction in the extent of asset holdings can spur volatility spillovers[27]. The spillovers between the MOVE to AGSVIX and VIX to AVIX are also highly specified, with 54 to 82 per cent of the variation explained, respectively. The coefficients on these results are again negative, supporting H_1 and providing a well-rounded illustration of the interaction between QE and volatility spillovers during the normalisation period. In essence, reducing asset holdings causes a tightening in the monetary policy stance, increasing risk spillovers.

[27]The results of the 70 day rolling window regression similarly show a significant negative influence stemming from the SOMA portfolio, albeit, at a lower power compared to the recursively constructed index ($p < 0.05$).

Normalisation Period: 2013–2019

	VIX/MOVE	VIX/AVIX	VIX/AGSVIX	MOVE/AVIX	MOVE/AGSVIX	AVIX/AGSVIX
QE_{SOMA}	0.027	-3.335**	0.789*	-1.574***	-0.926**	0.085
	(0.883)	(0.007)	(0.026)	(0.000)	(0.006)	(0.223)
D_{QE}	0.005	-0.011	0.000	-0.008	-0.006	0.001
	(0.203)	(0.456)	(0.992)	(0.122)	(0.287)	(0.214)
SUR_G	0.001***	0.000	0.000	0.000	0.000	0.000
	(0.000)	(0.662)	(0.303)	(0.267)	(0.403)	(0.123)
SUR_{US}	0.000*	0.000	0.000	0.000	0.000	0.000*
	(0.019)	(0.808)	(0.700)	(0.359)	(0.458)	(0.033)
SUR_{AU}	0.000	0.000	0.000	0.000	0.000	0.000
	(0.781)	(0.165)	(0.918)	(0.636)	(0.752)	(0.535)
OIS_{AU}	0.019***	-0.179***	-0.002	-0.069***	-0.021***	-0.002
	(0.000)	(0.000)	(0.845)	(0.000)	(0.000)	(0.227)
CDS_{US}	0.000	0.003***	0.001	0.000	0.000	0.000
	(0.855)	(0.000)	(0.177)	(0.987)	(0.267)	(0.264)
CDS_{AU}	0.000	-0.001***	0.000*	0.000	0.000	0.000
	(0.109)	(0.001)	(0.029)	(0.729)	(0.600)	(0.719)
Intercept	0.211***	4.469***	0.110***	0.534***	0.042***	-0.005
	(0.000)	(0.000)	(0.000)	(0.000)	(0.000)	(0.251)
Adj. R^2	0.623	0.822	0.141	0.850	0.540	0.285
Obs.	351	351	351	351	351	351

Table 15: Results of Pairwise Volatility Spillover Indices – Normalisation Period (SOMA Portfolio)

Note. This table displays the result of the following regression estimated using OLS: $S^g_{ij}(H)_t = \alpha_t + \beta_1 QE_{SOMA_t} + \beta_2 D_{QE_t} + \beta_3 SUR_{G_t} + \beta_4 SUR_{US_t} + \beta_5 SUR_{AU_t} + \beta_6 OIS_{AU_t} + \beta_7 CDS_{US_t} + \beta_8 CDS_{AU_t} + \varepsilon_t$. The p-values (in parentheses below the coefficients) are derived from Newey and West (1986) heteroskedasticity and autocorrelation consistent standard errors. The levels of significance are defined as follows: '***' implies significance at the 0.1% level, '**' implies significance at the 1% level, and '*' implies significance at the 5% level.

4.3 Impulse Response Functions

This section presents the impulse response functions that project the short-term impact resulting from a QE shock. The shocks are defined as a one standard deviation increase in the Shadow Policy Rate and the SOMA portfolio, respectively. An increase in the Shadow Policy Rate is akin to a tightening in monetary policy and a reduction in the magnitude of the Federal Reserve's QE program. Conversely, an increase in the SOMA portfolio resembles an expansion in asset purchases and easier policy settings. Together, the QE instruments depict a contractionary and expansionary shock. The shocks are also imposed across different frequencies. The Shadow Policy Rate shows the impulse response over 30 trading days while the SOMA portfolio exhibits the impact across 30 trading weeks. The responses are presented alongside 95 per cent confidence intervals, depicted around the median response of 500 bootstrapped Monte Carlo simulations.

To ensure the SVAR models are free from misspecification, Table 16 reports the ADF, PP, and KPSS stationarity tests on the first differences of the QE variables and spillover indices. In Panel (A), the ADF and PP tests significantly reject the null hypothesis of non-stationarity for the QE variables. In contrast, the null of stationarity for the KPSS test is rejected for both instruments. This result is not surprising, as stationarity tests can derive results that contradict one another, especially when the models have unit roots close to unity (Caner and Kilian, 2001). Nevertheless, given the strong evidence of stationarity proposed by the ADF and PP tests ($p < 0.001$), the models are estimated without any further manipulation of the QE instruments beyond the first difference. In Panel (B), stationarity is verified for each spillover index, as depicted by the rejection of non-stationarity in the ADF and PP tests and the inability to reject the null of stationarity in the KPSS test.

First Difference of QE Instruments

Panel A	U.S. Shadow Policy Rate	SOMA Portfolio
ADF	-11.059***	-4.369***
PP	-1260.700***	-795.260***
KPSS	1.129***	0.525*

First Difference of Volatility Spillover Indices

Panel B	ADF	PP	KPSS
Aggregate	-14.245***	-2367.700***	0.080
VIX to MOVE	-16.115***	-3619.300***	0.008
VIX to AVIX	-14.053***	-1814.200***	0.056
VIX to AGSVIX	-16.074***	-3611.800***	0.082
MOVE to AVIX	-14.193***	-2832.900***	0.048
MOVE to AGSVIX	-19.368***	-3995.500***	0.007
AVIX to AGSVIX	-19.747***	-2326.600***	0.180

Table 16: Stationarity Tests of QE Instruments & Volatility Spillover Indices

Note. The following table displays the test statistics of each stationarity test performed on the first differences of the QE instruments and implied volatility indices. The ADF & PP tests have a null of non-stationarity, while the KPSS test has a null of stationarity. The levels of significance are defined as follows: '***' implies significance at the 0.1% level, '**' implies significance at the 1% level, and '*' implies significance at the 5% level. Charts illustrating each of the first differences are presented in Appendix G.

4.3.1 U.S. Shadow Policy Rate Shocks

Figure 19 illustrates the impulse response of the aggregate spillover index to a one standard deviation increase in the Shadow Policy Rate over 30 trading days. Initially, the aggregate spillovers are contemporaneously elevated following the shock, with spillovers increasing by around 0.25 to 0.50 per cent across the system of markets. After 5 days, the volatility spillovers decline an equivalent –0.25 to –0.50 per cent, reversing much of the initial spillovers after the markets adjust to the change. After 10 days, the spillovers are no longer significant and diminish to zero. The results are broadly similar across all three SVAR specifications, with the greatest response depicted by the Cholesky decomposition scheme and the tamest response illustrated by the heteroskedasticity scheme. The results for the aggregate spillover index support H_2, that is, that an unexpected contractionary QE shock causes an intensification of short-term volatility in the initial days of trading.

The VIX to MOVE spillovers illustrates a similar path to that of the aggregate spillovers. Initially, the spillovers intensify before displaying a sharp reversal of the volatility transmission the following trading day. This reversal is then followed by a further intensification of spillovers on the third day, before an eventual decline to zero. While the impulse responses depicted in the Cholesky decomposition and NGML schemes show spillovers of a relatively small magnitude, the heteroskedasticity scheme displays a much greater spillover on the first trading day of just under 1 per cent.

Likewise, the response of the VIX to AVIX spillovers exhibits a comparable path. Initially, the spillovers increase over the first two days with a peak daily transmission of 0.25 per cent. The following two days see a decline in spillovers, reversing much of the response, before diminishing until they are no longer significant beyond the 10 day point. The impulse responses are largely equivalent across all three specifications, although, the heteroskedasticity scheme depicts an immediate response that is approximately twice the magnitude of the Cholesky decomposition and NGML schemes at around 0.5 per cent. Across all the indices, the impulse response of the VIX to AVIX spillovers illustrates the single largest magnitude of volatility transmission. This amplified spillover following the shock aligns with the strong influence and centrality of the U.S. equity market on Australian markets.

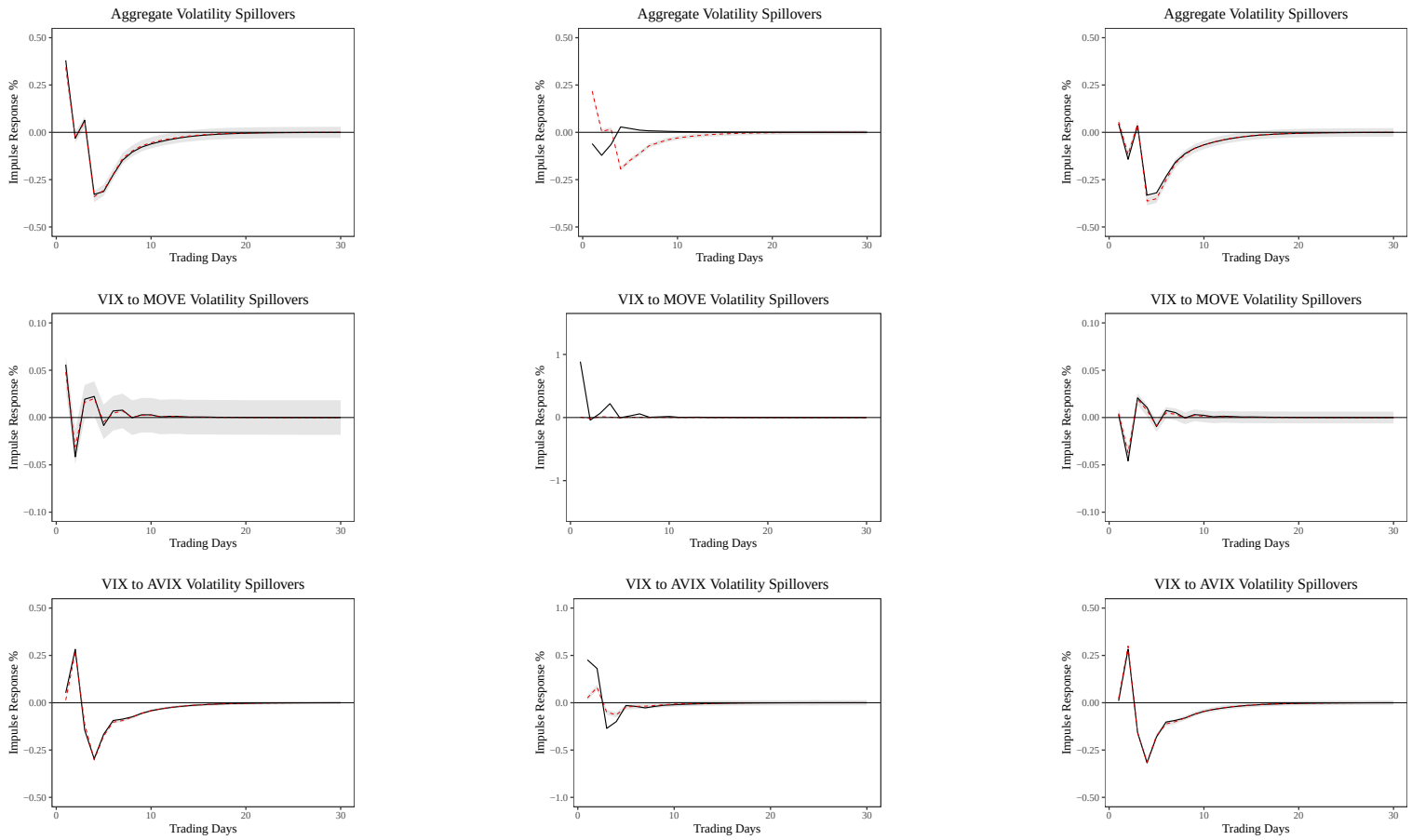

Identification via Cholesky Decomposition | Identification via Heteroskedasticity | Identification via NGML

Figure 19: Response of the Aggregate, VIX to MOVE, & VIX to AVIX Spillover Indices

Note. The following figures display the impulse response of the Aggregate, VIX to MOVE, and VIX to AVIX spillover indices to a one standard deviation increase in the U.S. Shadow Rate over 30 trading days. The black line is the estimated impulse response, the red dashed line measures the median impulse response derived from 500 bootstrapped Monte Carlo simulations, and the shaded grey area is the 95 per cent confidence intervals around the median.

Figure 20 illustrates the impulse response of the VIX to AGSVIX, MOVE to AVIX, and MOVE to AGSVIX spillovers. The response of the VIX to AGSVIX echoes the response of the VIX to AVIX, albeit, at a smaller magnitude. Initially, spillovers are intensified on the first trading day, increasing around 0.025 to 0.05 per cent. Again, a reversal in the spillovers occurs, offsetting the initial day's movements such that the net effect over two days is equal to zero before a slight intensification occurs on the third day. The spillovers transcend to zero following 4–5 days, which is consistent with the dynamics in the previously examined indices.

The MOVE to AGSVIX spillovers exhibit a similar trend, albeit, with volatility remaining intensified until around 15 days. This result illustrates the longest response of all indices, suggesting that the volatility transmission between the government bond markets in the U.S. and Australia remains relatively elevated following the shock. This result is not surprising, given the sensitive nature of government bond yields to the effects of unconventional monetary policy (Neely, 2015).

In contrast, the MOVE to AVIX spillovers illustrates a different behaviour, breaking the pattern exhibited in the other indices following the shock. Namely, spillovers contemporaneously decline, before increasing towards zero and no longer display significance by the 10 day mark. The magnitude of these daily spillovers, however, is remarkably small such that they can be classified as insignificant. In particular, the contemporaneous decline is only around –0.010 to –0.025 per cent, which shows very limited sensitivity between the MOVE and AVIX following the shock.

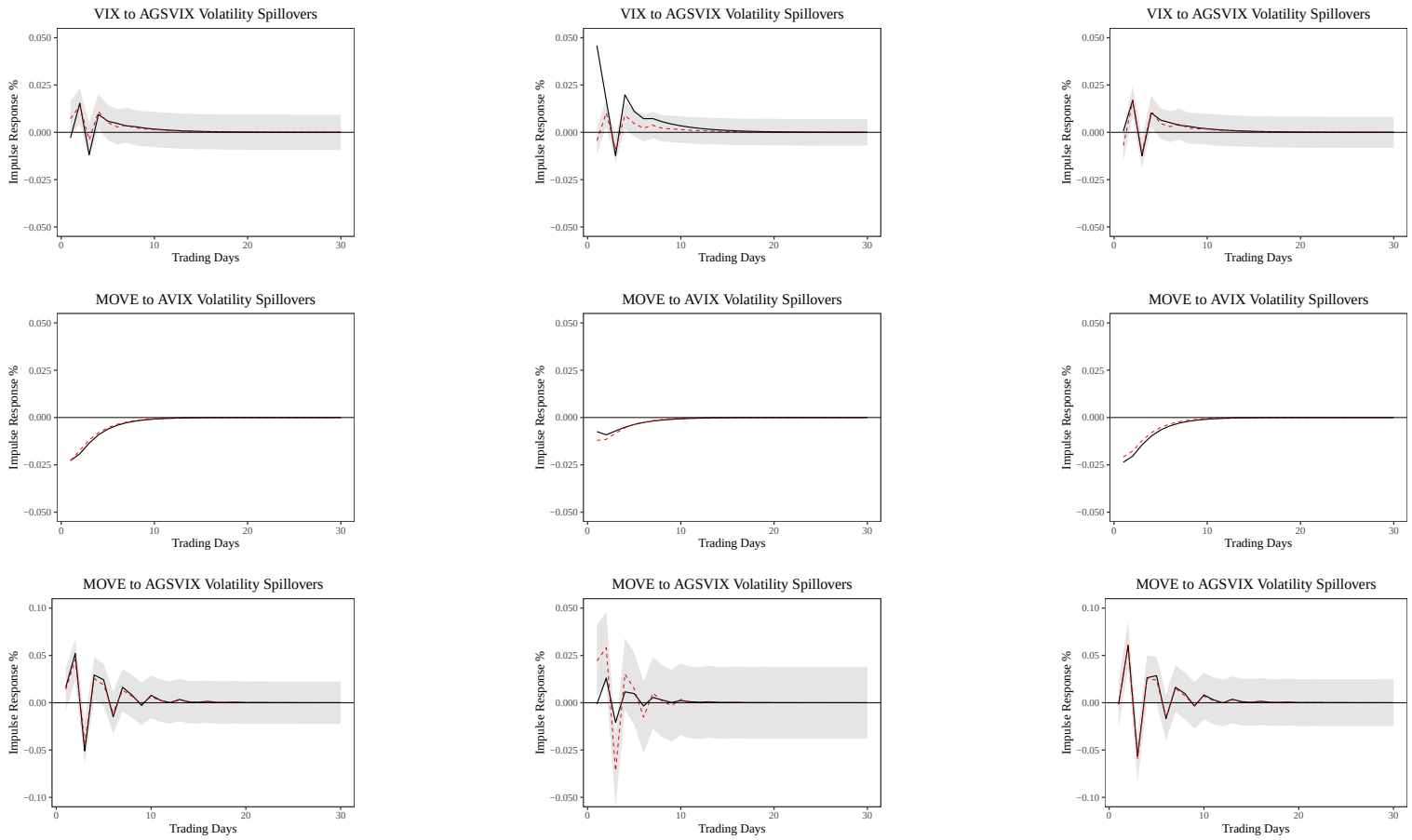

Identification via Cholesky Decomposition | Identification via Heteroskedasticity | Identification via NGML

Figure 20: Response of the VIX to AGSVIX, MOVE to AVIX, & MOVE to AGSVIX Spillover Indices

Note. The following figures display the impulse response of the VIX to AGSVIX, MOVE to AVIX, and MOVE to AGSVIX spillover indices to a one standard deviation increase in the U.S. Shadow Rate over 30 trading days. The black line is the estimated impulse response, the red dashed line measures the median impulse response derived from 500 bootstrapped Monte Carlo simulations, and the shaded grey area is the 95 per cent confidence intervals around the median.

Finally, Figure 21 illustrates the domestic spillovers between the AVIX and AGSVIX following the shock. Again, the impulse responses align with the patterns exhibited by the other spillover indices, supporting H_2. Specifically, the QE shock promotes an initial intensification of volatility on the first trading day. By the second trading day, the spillovers decline and culminate in a zero-sum effect. This is followed by a third day of intensification before the response declines to insignificance.

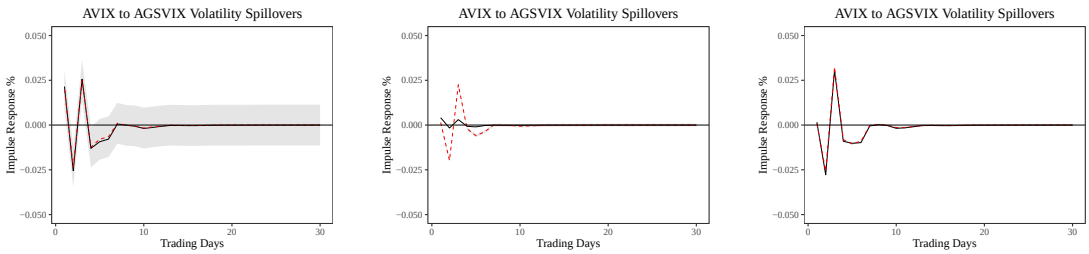

Cholesky Decomposition | Heteroskedasticity | NGML

Figure 21: Response of the AVIX to AGSVIX Volatility Spillover Index

Note. The following figures display the dynamic response of the AVIX to AGSVIX Volatility Spillver Index to a one standard deviation increase in the U.S. Shadow Rate over 30 trading days. The black line is the estimated impulse response, the red dashed line measures the median impulse response derived from 500 bootstrapped Monte Carlo simulations, and the shaded grey area is the 95 per cent confidence intervals around the median.

In sum, the patterns exhibited by the spillover indices following the unexpected increase in the Shadow Policy Rate provide insight into the short-term volatility dynamics that may unfold if the Federal Reserve revises the dimensions of its QE program. Specifically, aside from the insignificant response of the MOVE to AVIX, all other indices support H_2 and show that a one standard deviation increase in the Shadow Policy Rate causes an immediate intensification in volatility spillovers on the first trading day. The spillovers are reversed on the second day and begin to deteriorate into insignificance around the 5 day mark. By 10 days, the spillovers are no longer responsive to the shock. The greatest response is illustrated by the VIX to AVIX spillovers, a result that aligns to the strong relationship between the U.S. and Australian equity markets. Another notable result is the path of the spillovers between the MOVE to AGSVIX which depicts a slightly longer response horizon of around 15 days, shedding light on the persistent effect that changes in monetary policy have on government bond yields.

4.3.2 SOMA Portfolio Shocks

The previous set of impulse responses illustrate the dynamics of volatility spillovers over 30 trading days. The QE shock, however, may have the propensity to cause a more persistent impact on spillovers that is captured by data with a longer-term frequency. This section recomputes the impulse responses by imposing an unexpected QE shock in the form of a one standard deviation increase in the Federal Reserve's SOMA portfolio. Given the SOMA portfolio represents the weekly operations of implementing QE, these impulse responses demonstrate the expected impact on volatility spillovers following the buying of securities over 30 trading weeks. In contrast to the Shadow Policy Rate, a one standard deviation increase in the SOMA portfolio aligns with an expansionary monetary policy shock. As such, the responses are expected to initially depict a contemporaneous decline, which is the inverse logic of H_2 and indicates looser policy settings.

Figure 22 begins by displaying the impulse responses of the aggregate, VIX to MOVE, and VIX to AVIX spillovers. Consistent with the inverse inference of H_2, aggregate spillovers decline over the first trading week. The magnitude of the decline during the first week varies depending on the identification scheme with responses ranging between –0.25 to –6 per cent. This outcome is not surprising, given the variation in impulse responses that can occur at longer-term horizons (Phillips, 1998). The aggregate spillovers also remain persistent until the end of 30 trading weeks, with oscillations in the magnitude of spillovers occurring throughout the horizon.

Similarly, the VIX to MOVE spillovers decline in the first two weeks following the shock, with spillovers again showing wide variation depending on the identification scheme. Specifically, spillovers decrease by around –0.5 to –2.5 per cent, with the greatest degree depicted by the NGML scheme. These spillovers also exhibit an oscillating pattern that is persistently fluctuating between increases and reversals of volatility until the end of 30 trading weeks, with most of the variation shown in the first weeks of trading.

Finally, the response of the VIX to AVIX index again exhibits the greatest extent of pairwise spillovers, echoing the daily impulse response examined previously. The spillovers range between –0.5 to –5.0 per cent in the first trading week, with oscillations in the spillovers between these two markets making up the bulk of the movements in the aggregate index. This result comes as no surprise due to the centrality of the VIX among the markets, highlighting its dominant influence on the volatility in Australian markets.

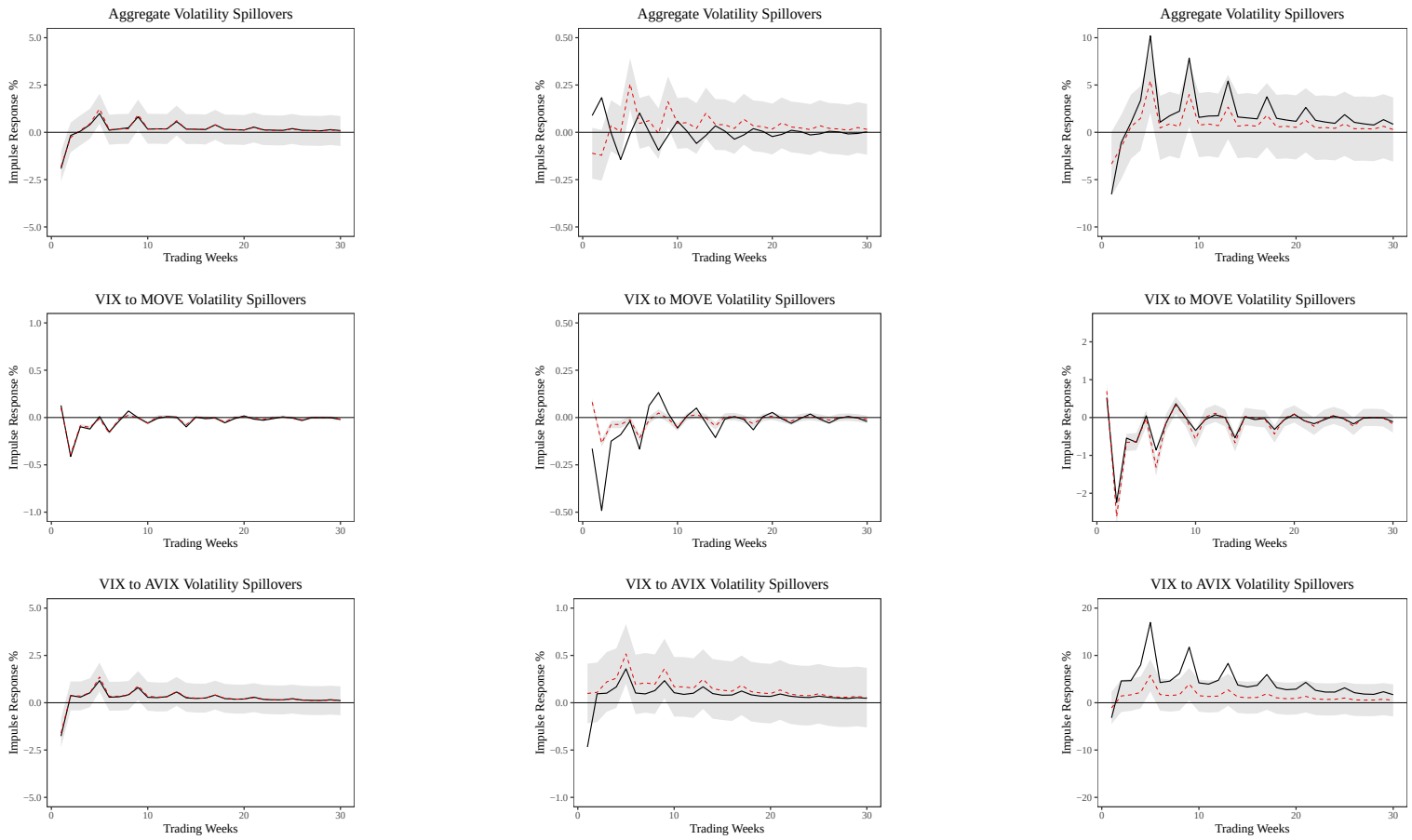

Identification via Cholesky Decomposition | Identification via Heteroskedasticity | Identification via NGML

Figure 22: Response of the Aggregate, VIX to MOVE, & VIX to AVIX Spillover Indices (SOMA Portfolio)

Note. The following figures display the impulse response of the Aggregate, VIX to MOVE, and VIX to AVIX spillover indices to a one standard deviation increase in the Federal Reserve's SOMA Portfolio over 30 trading weeks. The black line is the estimated impulse response, the red dashed line measures the median impulse response derived from 500 bootstrapped Monte Carlo simulations, and the shaded grey area is the 95 per cent confidence intervals around the median.

The impulse responses depicted in Figure 23 also draw noteworthy results. Firstly, unlike the daily responses of the aforementioned indices in Section 4.3.1, the spillovers between the VIX to AGSVIX only decline after around 5 weeks, the slowest of all indices. The response also fades into insignificance by around 15 weeks, the shortest of all response horizons. This lagged response and faster-than-average decline illustrates the insignificance of the spillovers between the U.S. equity and the Australian government bond market, highlighting the lack of historic volatility transmission.

Secondly, the MOVE to AVIX depicts a sharp decline in spillovers in the first trading week. Although the magnitude of the spillovers is small, the response remains significant up until around 20 weeks and ranges between –0.1 to –0.5 per cent. More importantly, this result is at odds with the impulse response of these markets following the Shadow Policy Rate shock, which highlighted a largely insignificant response in daily frequency. In contrast, the shock imposed in weekly frequency displays the relatively longer-term implications of the unexpected alteration in the Federal Reserve's QE program.

The spillovers between the MOVE to AGSVIX depict a comparable path. Initially, spillovers decline over the first two weeks with oscillations occurring until the shock fades into insignificance by around 20 weeks. Notably, the heteroskedasticity scheme depicts the greatest decline in spillovers of about –0.25 per cent in the first two trading weeks.

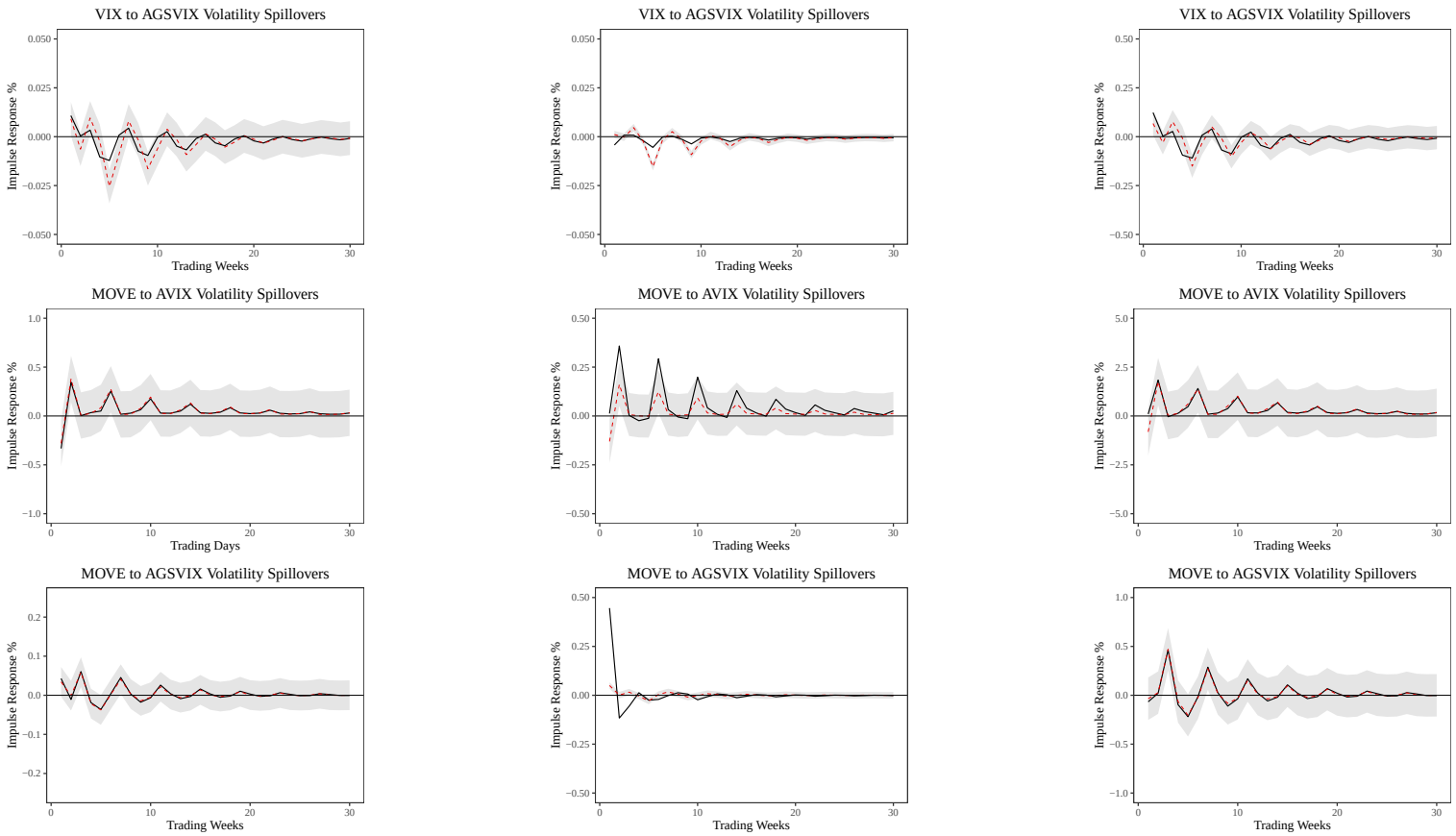

Identification via Cholesky Decomposition | Identification via Heteroskedasticity | Identification via NGML

Figure 23: Response of the VIX to AGSVIX, MOVE to AVIX, & MOVE to AGSVIX Spillover Indices (SOMA Portfolio)

Note. The following figures display the impulse response of the VIX to AGSVIX, MOVE to AVIX, and MOVE to AGSVIX spillover indices to a one standard deviation increase in the Federal Reserve's SOMA Portfolio over 30 trading weeks. The black line is the estimated impulse response, the red dashed line measures the median impulse response derived from 500 bootstrapped Monte Carlo simulations, and the shaded grey area is the 95 per cent confidence intervals around the median.

Finally, the impulse response of the AVIX to AGSVIX illustrated in Figure 24 depicts a similar trend to the other indices. Specifically, an immediate decline in spillovers transpires during the first trading week of around –0.005 to –0.50 per cent and supports the inverse logic of H_2, such that an unexpected expansionary shock alleviates volatility spillovers. The NGML scheme, however, depicts an insignificant response following the shock, as illustrated by the wide confidence intervals that are on either side of the line of origin.

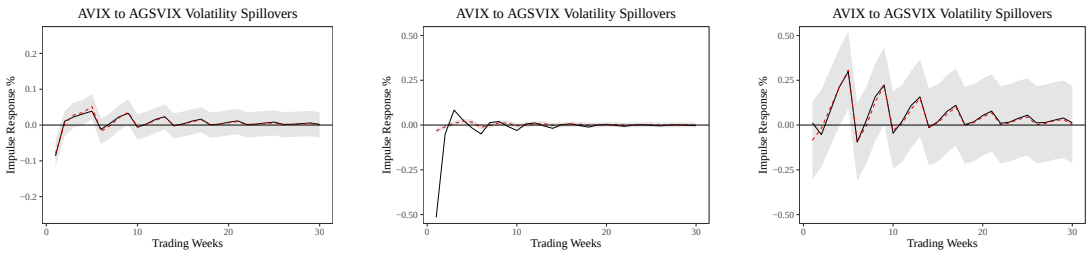

Cholesky Decomposition | Heteroskedasticity | NGML

Figure 24: Response of the AVIX to AGSVIX Volatility Spillover Index (SOMA Portfolio)

Note. The following figures display the dynamic response of the AVIX to AGSVIX Volatility Spillver Index to a one standard deviation increase in the Federal Reserve's SOMA Portfolio over 30 trading weeks. The black line is the estimated impulse response, the red dashed line measures the median impulse response derived from 500 bootstrapped Monte Carlo simulations, and the shaded grey area is the 95 per cent confidence intervals around the median.

In short, the effects conveyed by the SOMA portfolio shock support H_2. As assets holdings unexpectedly increase, volatility spillovers on an aggregate and pairwise basis decline in the first one-to-two trading weeks. Unlike the dynamics exhibited in the responses following the Shadow Policy Rate shock, the behaviour of the indices following the SOMA portfolio shock show a more persistent oscillation of volatility over 30 trading weeks, depicting a longer response horizon. The greatest response is depicted by the spillovers between the equity markets in both countries, which again comes as no surprise due to the strong connection between these markets and the centrality of the VIX.

5. DISCUSSION AND POLICY IMPLICATIONS

5.1 Summary of Results

The results in the preceding section can be summarised as follows. In addressing the first research question, the results show that the Federal Reserve's QE programs have influenced volatility spillovers in two distinct ways. First, during the crisis period, innovations in QE are shown to explain volatility spillovers, with explanatory power particularly elevated for equity markets in both countries, suggesting that the Federal Reserve's actions have had a meaningful effect on the nature of risk transference. The results in this period also support H_1, such that the imposition of QE is shown to suppress spillovers. This result is exemplified by the mostly positive coefficients on the U.S. Shadow Policy Rate, which suggests any reduction in the magnitude of QE intensifies spillovers, presumably by undoing easy financial conditions. The SOMA portfolio conveys results along the same line, represented by mostly negative coefficients. In essence, an increase in SOMA portfolio holdings, and thus a greater magnitude of QE, suppresses spillovers by easing financial conditions. Amidst the crisis, the results convey the benefits of LSAP 1 in alleviating risk spillovers, which if left with no intervention, may have been drastically greater.

During the normalisation period, the curtailment of QE is shown to similarly alleviate volatility spillovers. Although this outcome is at odds with H_1 (as a curtailment of QE is conjectured to tighten financial conditions and increase spillovers), the results in this period provide a powerful inference for the effects of QE amid the backdrop of an improving economic environment. Specifically, a positive economic outlook, such as that experienced between 2013–2019, suggests policy normalisation serves as a signal of improving economic fundamentals, potentially lessening portfolio balancing effects and reducing spillovers.

In addressing the second research question, the results demonstrated by the impulse response functions are germane to intuition. Specifically, the expected impact of a QE shock on volatility spillovers between financial markets in the U.S. and Australia depends on the direction of the shock. An unexpected contractionary shock, defined as a reduction in the magnitude of QE, causes an immediate intensification of short-term volatility spillovers between the markets, supporting H_2. An expansionary shock shows that an increase in the magnitude of QE causes an immediate suppression of short-term volatility spillovers, supporting the inverse logic of H_2. No matter the direction of the shock, it is obvious that unexpected changes in unconventional monetary policy can have substantial effects on cross-market volatility spillovers.

Taken together, the results convey an important narrative that although, in part, supports the Federal Reserve's actions during the height of the crisis, simultaneously emphasise the substantial influence central banks can have on the nature of risk within financial markets. On one hand, the imposition of QE amid elevated risk premia and illiquidity during the crisis may have alleviated further risk transference between

markets in both countries. This alleviation of risk transference may have supported financial stability and limited cross-market contagion, that if left unchecked, could have seen a greater destabilisation of market functioning. Conversely, while the positive short-term effects of QE are exemplified during the crisis, the deeply involved nature of central bank intervention into financial markets may instigate maladies that arise over the long-term. Specifically, in the absence of a positive economic outlook, policy normalisation may be difficult to achieve without spurring significant volatility that may undermine financial stability. With these findings in mind, the section that follows attempts to draw light on the potential side effects resulting from QE on systemic risk, and in doing so, highlights the policy-relevance of the findings.

5.2 Systemic Risk

At the forefront of the concerns that stem from the Federal Reserve's actions is the potential for QE to cause an increase in systemic risk. Undoubtedly, the evidence presented in this study conveying intensified spillovers between U.S. and Australian markets draws light on this very plausible side effect. One significant indication of an increase in systemic risk since the adoption of QE is the covaried and rapid acceleration in asset prices. This effect occurs as the central bank's sizeable purchases may force investors to seek riskier securities to sustain their required rates of return. Consequentially, these investments across riskier and less liquid financial markets may result in asset price appreciation *en masse* (Joyce et al., 2012).

This rapid surge in asset prices can evolve into asset price bubbles, which if were to burst, would cause significant volatility across markets, a hallmark of increased systemic risk. Huston and Spencer (2018) provide some colour on this consequence, arguing that asset purchases that are held long-term on central bank balance sheets can cause these price bubbles by inducing supply scarcity. In particular, the authors find evidence of an explosive increase in government bond prices since the onset of QE, which corresponds to the equivalently dramatic collapse in yields. Given the evidence of spillovers between government bond markets in both countries presented in this study, Australian government bonds may have increased in price concurrently with the U.S., suggesting investors holding these securities are vulnerable to significant losses if financial conditions were to unexpectedly tighten. The potential vulnerability faced by investors who are forced to bear risks beyond their desire for the sake of meeting return objectives reiterates the importance of careful policy analysis. Specifically, much like the empirical investigation presented in this study, the Federal Reserve would benefit from considering the bilateral implications of their QE programs.

In a similar vein, seeing as QE may force investors to seek out riskier securities in the search for higher returns, the policy may result in an environment of excessive risk-taking. If investors are forced to allocate capital to assets that surpass the bounds of their risk appetite due to a lack of supply, they may underappreciate the risk they bear (Gern et al., 2015). A lack of understanding of the financial securities they invest in, or an underappreciation for price volatility, may see investors react more fiercely to any tightening in financial conditions, promoting portfolio balancing to a much greater degree. As conveyed in the results of this study,

an unexpected contractionary QE shock causes an immediate intensification of volatility spillovers between the U.S. and Australia. In an environment of excessive risk-taking and elevated asset prices, an unexpected QE shock may cause far greater volatility spillovers than can be captured in historically focused models. As such, the Federal Reserve must be cognisant of their influence on investor preferences and the effects that their QE programs can inflict on the supply of assets available in public markets.

An increase in systemic risk can also result in impacts on economic agents that rely on financial markets for raising capital. Diamond et al. (2020) argue that loose monetary policy settings promote cross-border capital flows that entice corporates in capital-receiving countries to increase borrowings. A sudden reversal in the monetary policy stance, however, can engender a deterioration in liquidity and corporate funding costs that make it difficult to service elevated debt loads. As conveyed in the results of this study, it may be likely that a sudden reversal in financial conditions in the U.S. may spur an equally significant impact on conditions in Australia, putting pressure on Australian corporates. This possibility of indirectly inflicting financial pressure on corporates outside the bounds of the U.S. puts into perspective the importance of considering the multifaceted implications of QE.

When viewed collectively, the consequences of an increase in systemic risk for financial markets are significant. Asset price bubbles, excessive risk-taking, and an inability to service elevated debt loads if financial conditions suddenly tighten suggests a cautious approach to unconventional monetary policy is warranted. Alongside the evidence presented in this study that finds QE has contributed to an increase in bidimensional spillovers between U.S. and Australian markets, if generalised, the findings can apply for most advanced economies that have strong economic ties with the U.S. As such, the Federal Reserve can benefit from considering the propensity for risk spillovers that result from their policy decisions, and in doing so, they can mitigate their influence on systemic risk.

5.3 Contributions and Future Research

This study makes several contributions to the literature exploring the implications of the Federal Reserve's QE policies. First, the focus on Australian markets sets this study apart from similar efforts that have examined the cross-border implications resulting from QE. Specifically, multiple studies reviewed in this dissertation have investigated the implications of QE on financial markets in the U.S., Europe, and emerging economies. As such, this study addresses a gap in the literature by examining the implications of QE from an Australian perspective. Second, the study adds to the evidence that shows, in consensus, a significant impact resulting from QE on volatility spillovers. Alongside the work of Bernanke et al. (2004), Yang and Zhou (2017), & Fratzscher et al. (2018) among others, this study has presented further evidence of volatility spillovers that can be partly explained by the Federal Reserve's imposition of QE. Finally, the use of implied volatility indices and the creation of a novel index for the Australian government bond market (and extension of observations for the official AVIX) constitutes the methodological contributions made by this study. Unlike

commonly used ex-post calculations, this study displays the merit of using ex-ante instruments that provide a forward-looking measure of volatility.

For future research opportunities, none are more obvious than the extension of the framework and methodology used in this dissertation to examine QE enacted by other central banks. For instance, QE programs by the European Central Bank and Bank of Japan are two examples that remain unexplored in the context of Australia. Furthermore, the availability of various implied volatility indices suggests future studies can include indices that track ex-ante volatility expectations on a range of asset classes, including commodity, currency, and money markets. Similarly, the availability of high-frequency data for Australian markets permits examination of QE in intra-day or real-time frequencies, which may find evidence of a signalling effect that failed to emerge in the lower-frequency results presented in this study.

Finally, the outbreak of the novel Coronavirus (COVID–19) in late 2019 and its subsequent economic impacts have seen a renewed effort among policymakers to use unconventional monetary policies to counteract its devastating effects. Some research has already been conducted in this space, with Hartley and Rebucci (2020) performing an event study that examines 21 central banks and the impact of their QE policies on government bond yields. The study finds declines in yields following the QE announcements, and a rapid increase in the size of central bank balance sheets, with the Federal Reserve accumulating around $3 trillion worth of assets in 2020. While the study explores the actions of the RBA and the effects of QE on Australian government bonds, there is scope to expand the work and examine the implications of COVID–19 on additional markets in Australia.

6. CONCLUDING REMARKS

The advent of unconventional monetary policy marks one of the most significant changes in central bank policy over the past few decades. Most notably, accumulating sizeable holdings of financial securities funded by the creation of bank reserves has resulted in profound consequences for financial markets, among which intensified cross-border volatility spillovers present vehemently. While a rich body of literature has examined many implications stemming from the Federal Reserve's QE policies, this study has addressed a distinct gap that is found in the lack of research investigating volatility spillovers between markets in the U.S. and Australia. In addressing this knowledge gap, this study has presented evidence of intensified spillovers between equity and government bond markets in both countries, with the former pair of markets exhibiting noticeably increased volatility transmission due to the policy.

A key theme in this dissertation centres on the ramifications of the Federal Reserve's attempt at normalising its QE programs, with evidence showing that policy normalisation in the absence of a positive economic outlook can cause intensified spillovers. Indeed, the question remains as to whether the Federal Reserve can ever normalise its balance sheet without triggering significant market volatility as it historically has. Collectively, the findings point to intensified spillovers, with unexpected changes in the dimensions of the Federal Reserve's QE programs shown to illustrate substantial impacts on volatility transmission.

This study makes several contributions, including the methodological innovations presented in the creation of a novel implied volatility index, the derivation of spillover indices, and the use of data-driven identification schemes to assess QE shocks. Much is left open for future exploration, notwithstanding the extension of the study to examine QE by other central banks.

In sum, this study has sought to bring into focus the implications of the Federal Reserve's QE programs in a previously unexplored Australian dimension, and in doing so, has expanded knowledge of the consequences that stem from this important economic policy.

References

Ahmed, S., Coulibaly, B., and Zlate, A. (2017). International financial spillovers to emerging market economies: How important are economic fundamentals? *Journal of International Money and Finance*, 76:133–152.

Ait-Sahalia, Y., Andritzky, J., Jobst, A., Nowak, S., and Tamirisa, N. (2012). Market response to policy initiatives during the global financial crisis. *Journal of International Economics*, 87(1):162–177.

Alter, A. and Beyer, A. (2014). The dynamics of spillover effects during the european sovereign debt turmoil. *Journal of Banking & Finance*, 42:134–153.

Andrews, D. W. (1993). Tests for parameter instability and structural change with unknown change point. *Econometrica: Journal of the Econometric Society*, pages 821–856.

Andrews, D. W. and Ploberger, W. (1994). Optimal tests when a nuisance parameter is present only under the alternative. *Econometrica: Journal of the Econometric Society*, pages 1383–1414.

Antonakakis, N. (2012). Exchange return co-movements and volatility spillovers before and after the introduction of euro. *Journal of International Financial Markets, Institutions and Money*, 22(5):1091–1109.

Apostolou, A. and Beirne, J. (2019). Volatility spillovers of unconventional monetary policy to emerging market economies. *Economic Modelling*, 79:118–129.

Arrow, K. J. (1964). The role of securities in the optimal allocation of risk-bearing. *The Review of Economic Studies*, 31(2):91–96.

Australian Bureau of Statistics (2020). International investment position, australia: Supplementary statistics. `https://www.abs.gov.au/statistics/economy/international-trade/international-investment-position-australia-supplementary-statistics/latest-release`.

Australian Office of Financial Management (2020a). The australian government securities investor base. `https://www.aofm.gov.au/investors/wholesale-investors/investor-insights/australian-government-securities-investor-base`.

Australian Office of Financial Management (2020b). Liquidity of the treasury bond market. `https://www.aofm.gov.au/investors/wholesale-investors/investor-insights/liquidity-treasury-bond-market`.

Avdjiev, S. and Takáts, E. (2014). Cross-border bank lending during the taper tantrum: the role of emerging market fundamentals. *BIS Quarterly Review September*.

Bagliano, F. C. and Favero, C. A. (1998). Measuring monetary policy with var models: An evaluation. *European Economic Review*, 42(6):1069–1112.

Balli, F., Hu, X., and Rana, F. (2018). Bond market integration of emerging economies and bilateral linkages. *Accounting & Finance*.

Bank for International Settlements (2020). Central bank policy rates. `https://www.bis.org/statistics/cbpol.htm`.

Baruník, J., Kočenda, E., and Vácha, L. (2016). Asymmetric connectedness on the us stock market: Bad and good volatility spillovers. *Journal of Financial Markets*, 27:55–78.

Baruník, J. and Křehlík, T. (2018). Measuring the frequency dynamics of financial connectedness and systemic risk. *Journal of Financial Econometrics*, 16(2):271–296.

Bauer, M. D. and Neely, C. J. (2014). International channels of the fed's unconventional monetary policy. *Journal of International Money and Finance*, 44:24–46.

Bauer, M. D. and Rudebusch, G. D. (2013). The signaling channel for federal reserve bond purchases. *International Journal of Central Banking*.

Beber, A., Brandt, M. W., and Kavajecz, K. A. (2011). What does equity sector orderflow tell us about the economy? *The Review of Financial Studies*, 24(11):3688–3730.

Bernanke, B., Reinhart, V., and Sack, B. (2004). Monetary policy alternatives at the zero bound: An empirical assessment. *Brookings Papers on Economic Activity*, 2004(2):1–100.

Black, F. (1995). Interest rates as options. *The Journal of Finance*, 50(5):1371–1376.

Black, F. and Scholes, M. (1976). Taxes and the pricing of options. *The Journal of Finance*, 31(2):319–332.

Blanchard, O. J. and Quah, D. (1988). The dynamic effects of aggregate demand and supply disturbances. Technical report, Brookings Papers on Economic Activity.

Board of Governors of the Federal Reserve System (2010). Fomc statement. `https://www.federalreserve.gov/newsevents/pressreleases/monetary20100921a.htm`.

Board of Governors of the Federal Reserve System (2020a). Federal open market committee. `https://www.federalreserve.gov/monetarypolicy/fomc.htm`.

Board of Governors of the Federal Reserve System (2020b). Timelines of policy actions and communications: Balance sheet policies. `https://www.federalreserve.gov/monetarypolicy/timeline-balance-sheet-policies.htm`.

Bomfim, A. N. (2003). Pre-announcement effects, news effects, and volatility: Monetary policy and the stock market. *Journal of Banking & Finance*, 27(1):133–151.

Breeden, D. T. and Litzenberger, R. H. (1978). Prices of state-contingent claims implicit in option prices. *Journal of Business*, pages 621–651.

Caner, M. and Kilian, L. (2001). Size distortions of tests of the null hypothesis of stationarity: evidence and implications for the ppp debate. *Journal of International Money and Finance*, 20(5):639–657.

Chari, A., Stedman, K. D., and Lundblad, C. (2020). Taper tantrums: Quantitative easing, its aftermath, and emerging market capital flows. *The Review of Financial Studies*.

Chen, Q., Filardo, A., He, D., and Zhu, F. (2016). Financial crisis, us unconventional monetary policy and international spillovers. *Journal of International Money and Finance*, 67:62–81.

Chicago Board Options Exchange (2015). Guide to the cboe / cbot 10 year treasury note volatility index (tyvix index). `http://www.cboe.com/micro/volatility/tyvix/pdf/tyvixguidepart1.pdf`.

Cho, D. and Rhee, C. (2013). Effects of quantitative easing on asia: capital flows and financial markets. *ADBI Working Paper*, (350).

Chow, G. C. (1960). Tests of equality between sets of coefficients in two linear regressions. *Econometrica: Journal of the Econometric Society*, pages 591–605.

Christensen, J. H. and Krogstrup, S. (2019). Transmission of quantitative easing: The role of central bank reserves. *The Economic Journal*, 129(617):249–272.

Christiano, L. J., Eichenbaum, M., and Evans, C. (1994). The effects of monetary policy shocks: some evidence from the flow of funds. Technical report, National Bureau of Economic Research.

Debreu, G. (1959). *Theory of value: An axiomatic analysis of economic equilibrium*. Number 17. Yale University Press.

Diamond, D. W., Hu, Y., and Rajan, R. G. (2020). The spillovers from easy liquidity and the implications for multilateralism. *IMF Economic Review*, 68(1):4–34.

Diebold, F. X. and Yilmaz, K. (2009). Measuring financial asset return and volatility spillovers, with application to global equity markets. *The Economic Journal*, 119(534):158–171.

Diebold, F. X. and Yilmaz, K. (2012). Better to give than to receive: Predictive directional measurement of volatility spillovers. *International Journal of Forecasting*, 28(1):57–66.

Diebold, F. X. and Yılmaz, K. (2014). On the network topology of variance decompositions: Measuring the connectedness of financial firms. *Journal of Econometrics*, 182(1):119–134.

Fawley, B. and Neely, C. (2013). Four stories of quantitative easing. *Federal Reserve Bank of St. Louis Review*, 95(1):51–88.

Federal Reserve Bank of New York (2020). System open market account holdings of domestic securities. `https://www.newyorkfed.org/markets/soma/sysopen_accholdings`.

Federal Reserve Bank of St. Louis (2020a). Board of governors of the federal reserve system total assets. `https://fred.stlouisfed.org/series/WALCL`.

Federal Reserve Bank of St. Louis (2020b). Effective federal funds rate. `https://fred.stlouisfed.org/series/FEDFUNDS`.

Fleming, J., Kirby, C., and Ostdiek, B. (1998). Information and volatility linkages in the stock, bond, and money markets. *Journal of Financial Economics*, 49(1):111–137.

Fratzscher, M., Lo Duca, M., and Straub, R. (2018). On the international spillovers of us quantitative easing. *The Economic Journal*, 128(608):330–377.

Gagnon, J. (2016). Quantitative easing: An underappreciated success. *PIIE Policy Brief*, 16.

Gagnon, J., Raskin, M., Remache, J., and Sack, B. (2018). The financial market effects of the federal reserve's large-scale asset purchases. *International Journal of Central Banking*, 7.

Galariotis, E. C., Makrichoriti, P., and Spyrou, S. (2016). Sovereign cds spread determinants and spill-over effects during financial crisis: A panel var approach. *Journal of Financial Stability*, 26:62–77.

Georgiadis, G. and Gräb, J. (2016). Global financial market impact of the announcement of the ecb's asset purchase programme. *Journal of Financial Stability*, 26:257–265.

Gern, K.-J., Jannsen, N., Kooths, S., and Wolters, M. (2015). Quantitative easing in the euro area: Transmission channels and risks. *Intereconomics*, 50(4):206–212.

Ghosh, S. and Saggar, M. (2017). Volatility spillovers to the emerging financial markets during taper talk and actual tapering. *Applied Economics Letters*, 24(2):122–127.

Han, J., Linnenluecke, M., Liu, Z., Pan, Z., and Smith, T. (2019). A general equilibrium approach to pricing volatility risk. *PloS one*, 14(4):e0215032.

Hansen, B. E. (1997). Approximate asymptotic p values for structuras-change tests. *Journal of Business & Economic Statistics*, 15(1):60–67.

Hartley, J. S. and Rebucci, A. (2020). An event study of covid-19 central bank quantitative easing in advanced and emerging economies. Technical report, National Bureau of Economic Research.

Herwartz, H. and Plödt, M. (2016). Simulation evidence on theory-based and statistical identification under volatility breaks. *Oxford Bulletin of Economics and Statistics*, 78(1):94–112.

Huston, J. H. and Spencer, R. W. (2018). Quantitative easing and asset bubbles. *Applied Economics Letters*, 25(6):369–374.

Hutchison, M. M. and Noy, I. (2006). Sudden stops and the mexican wave: Currency crises, capital flow reversals and output loss in emerging markets. *Journal of Development Economics*, 79(1):225–248.

Jarque, C. M. and Bera, A. K. (1980). Efficient tests for normality, homoscedasticity and serial independence of regression residuals. *Economics letters*, 6(3):255–259.

Jorion, P. (1995). Predicting volatility in the foreign exchange market. *The Journal of Finance*, 50(2):507–528.

Joyce, M., Miles, D., Scott, A., and Vayanos, D. (2012). Quantitative easing and unconventional monetary policy–an introduction. *The Economic Journal*, 122(564):F271–F288.

Karadi, P. and Nakov, A. (2020). Effectiveness and addictiveness of quantitative easing. *Journal of Monetary Economics*.

Kawai, M. (2015). International spillovers of monetary policy: Us federal reserve's quantitative easing and bank of japan's quantitative and qualitative easing. *ADBI Working Paper*.

Keating, J. W. (1996). Structural information in recursive var orderings. *Journal of Economic Dynamics and Control*, 20(9-10):1557–1580.

Kenourgios, D., Papadamou, S., and Dimitriou, D. (2015). Intraday exchange rate volatility transmissions across qe announcements. *Finance Research Letters*, 14:128–134.

Kleiber, C., Hornik, K., Leisch, F., and Zeileis, A. (2002). strucchange: An r package for testing for structural change in linear regression models. *Journal of Statistical Software*, 7(2):1–38.

Koop, G., Pesaran, M. H., and Potter, S. M. (1996). Impulse response analysis in nonlinear multivariate models. *Journal of Econometrics*, 74(1):119–147.

Krippner, L. (2013). Measuring the stance of monetary policy in zero lower bound environments. *Economics Letters*, 118(1):135–138.

Krugman, P. R., Dominquez, K. M., and Rogoff, K. (1998). It's baaack: Japan's slump and the return of the liquidity trap. *Brookings Papers on Economic Activity*, 1998(2):137–205.

Lange, A., Dalheimer, B., Herwartz, H., and Maxand, S. (2019). svars: An r package for data-driven identification in multivariate time series analysis. *Journal of Statistical Software*.

Lanne, M. and Lütkepohl, H. (2008). Identifying monetary policy shocks via changes in volatility. *Journal of Money, Credit and Banking*, 40(6):1131–1149.

Lanne, M., Meitz, M., and Saikkonen, P. (2017). Identification and estimation of non-gaussian structural vector autoregressions. *Journal of Econometrics*, 196(2):288–304.

Lavigne, R., Sarker, S., Vasishtha, G., et al. (2014). Spillover effects of quantitative easing on emerging-market economies. *Bank of Canada Review*, 2014(Autumn):23–33.

Liu, Z. and O'Neill, M. J. (2017). State-preference pricing and volatility indices. *Accounting & Finance*, 57(3):815–836.

MacDonald, M. (2017). International capital market frictions and spillovers from quantitative easing. *Journal of International Money and Finance*, 70:135–156.

Mangadi, K. and Sheen, J. (2017). Identifying terms of trade shocks in a developing country using a sign restrictions approach. *Applied Economics*, 49(24):2298–2315.

Meegan, A., Corbet, S., and Larkin, C. (2018). Financial market spillovers during the quantitative easing programmes of the global financial crisis (2007–2009) and the european debt crisis. *Journal of International Financial Markets, Institutions and Money*, 56:128–148.

Mi, L., Benson, K., and Faff, R. (2018). A specialised volatility index for the new gics sector-real estate. *Economic Modelling*, 70:438–446.

Mi, L. and Hodgson, A. (2018). Real estate's information and volatility links with stock, bond and money markets. *Accounting & Finance*, 58:465–491.

Modigliani, F. and Sutch, R. (1966). Innovations in interest rate policy. *The American Economic Review*, 56(1/2):178–197.

Morgan, P. (2011). Impact of us quantitative easing policy on emerging asia. *ADBI Working Paper*.

National Bureau of Economic Research (2020). Us business cycle expansions and contractions. `https://www.nber.org/cycles.html`.

Neely, C. J. (2015). Unconventional monetary policy had large international effects. *Journal of Banking & Finance*, 52:101–111.

Newey, W. K. and West, K. D. (1986). A simple, positive semi-definite, heteroskedasticity and autocorrelationconsistent covariance matrix. Technical report, National Bureau of Economic Research.

Pan, Z. (2018). A state-price volatility index for the us government bond market. *Accounting & Finance*, 58:573–597.

Pesaran, H. H. and Shin, Y. (1998). Generalized impulse response analysis in linear multivariate models. *Economics Letters*, 58(1):17–29.

Phillips, P. C. (1998). Impulse response and forecast error variance asymptotics in nonstationary vars. *Journal of Econometrics*, 83(1-2):21–56.

Punzi, M. T. and Chantapacdepong, P. (2019). Spillover effects of unconventional monetary policy on asia and the pacific. *Macroeconomic Shocks and Unconventional Monetary Policy: Impacts on Emerging Markets*, 182.

Rigobon, R. (2003). Identification through heteroskedasticity. *Review of Economics and Statistics*, 85(4):777–792.

Rosa, C. (2014). The high-frequency response of energy prices to us monetary policy: Understanding the empirical evidence. *Energy Economics*, 45:295–303.

Sahay, M. R., Arora, M. V. B., Arvanitis, M. A. V., Faruqee, M. H., N'Diaye, M. P., and Griffoli, M. T. M. (2014). *Emerging market volatility: Lessons from the taper tantrum.* Number 14-19. International Monetary Fund.

Shogbuyi, A. and Steeley, J. M. (2017). The effect of quantitative easing on the variance and covariance of the uk and us equity markets. *International Review of Financial Analysis*, 52:281–291.

Sims, C. A. (1980). Macroeconomics and reality. *Econometrica: Journal of the Econometric Society*, 48:1–48.

S&P Global (2020). S&p/asx 200 vix methodology. `https://www.spglobal.com/spdji/en/indices/strategy/sp-asx-200-vix/#overview`.

Svensson, L. E. (2000). Open-economy inflation targeting. *Journal of International Economics*, 50(1):155–183.

Uhlig, H. (2005). What are the effects of monetary policy on output? results from an agnostic identification procedure. *Journal of Monetary Economics*, 52(2):381–419.

Vasicek, O. (1977). An equilibrium characterization of the term structure. *Journal of Financial Economics*, 5(2):177–188.

Wang, K. (2009). Volatility linkages of the equity, bond and money markets: an implied volatility approach. *Accounting & Finance*, 49(1):207–219.

Whaley, R. E. (2000). The investor fear gauge. *The Journal of Portfolio Management*, 26(3):12–17.

Whaley, R. E. (2009). Understanding the vix. *The Journal of Portfolio Management*, 35(3):98–105.

Yang, Z. and Zhou, Y. (2017). Quantitative easing and volatility spillovers across countries and asset classes. *Management Science*, 63(2):333–354.

Zeileis, A., Kleiber, C., Krämer, W., and Hornik, K. (2003). Testing and dating of structural changes in practice. *Computational Statistics & Data Analysis*, 44(1-2):109–123.

Zhou, X., Zhang, W., and Zhang, J. (2012). Volatility spillovers between the chinese and world equity markets. *Pacific-Basin Finance Journal*, 20(2):247–270.

APPENDICES

Appendix A: Data Summary

Data Summary

	Source	Vendor
Central Bank Policy Rates	Bank for International Settlements	Bank for International Settlements
Central Bank Assets	Federal Reserve Bank of St. Louis	Federal Reserve Bank of St. Louis
Federal Reserve Assets & Liabilities	Federal Reserve Bank of St. Louis	Federal Reserve Bank of St. Louis
Foreign Direct Investments	Australian Bureau of Statistics	Australian Bureau of Statistics
CBOE Market Volatility Index	Chicago Board Options Exchange	Refinitiv Eikon
ICE BofAML MOVE Index	Intercontinental Exchange (ICE)	Refinitiv Eikon
S&P/ASX 200 VIX Index	S&P Global	Refinitiv Eikon
AUS Treasury Bond Futures Prices	Australian Securities Exchange	Refinitiv Eikon
AUS Treasury Bond Futures Volatilities*	Australian Securities Exchange	Bloomberg
RBA Interbank Overnight Cash Rate	Reserve Bank of Australia	Reserve Bank of Australia
S&P 500 Index	S&P Global	Refinitiv Eikon
S&P 500 Volatilities*	S&P Global	Refinitiv Eikon
1 Month U.S. Treasury Rate	Federal Reserve Bank of St. Louis	Refinitiv Eikon
ASX/S&P 200 Index	S&P Global	Refinitiv Eikon
S&P/ASX 200 Volatilities*	S&P Global	Refinitiv Eikon
Shadow Policy Rate	Leo Krippner (LJK Limited)	Leo Krippner (LJK Limited)
Federal Reserve SOMA Portfolio	Federal Reserve Bank of New York	Federal Reserve Bank of New York
Economic Surprise Index – Global	Citigroup	Refinitiv Eikon
Economic Surprise Index – U.S.	Citigroup	Refinitiv Eikon
Economic Surprise Index – AUS	Citigroup	Refinitiv Eikon
U.S. Investment Grade CDS Spread	Refinitiv	Refinitiv Eikon
AUS Investment Grade CDS Spread	Refinitiv	Refinitiv Eikon
RBA Overnight Index Swap Rate	Reserve Bank of Australia	Reserve Bank of Australia

Table 17: Data, Sources, & Vendors

Note. This table reports the data used in this study. Source refers to the original creator of the data, while vendor refers to the data provider. The data is sorted by order of appearance in the study. *Refers to 30, 60, and 90 day ATM Option Implied Volatilities.

Appendix B: U.S. Federal Reserve – QE Timeline[28]

- **25 November 2008:** The FOMC announces LSAP 1. The focus of the program will be directed towards purchasing $500 billion worth of MBS and $100 billion worth of GSE debt to provide relief for dysfunctional housing credit markets.
- **18 March 2009:** LSAP 1 is expanded in size. An additional $750 billion in MBS, $300 billion in longer-term government bonds, and $100 billion in GSE debt are earmarked for purchase by the end of 2009.
- **10 August 2010:** The FOMC announces that the Federal Reserve's balance sheet will be sustained at its current size by reinvesting maturing debt into government bonds. Proceeds from government bond maturities will be rolled over into other government securities. Concerns over lacklustre inflationary growth are emphasised in the FOMC's statement.
- **21 September 2010:** The FOMC signals that further stimulus may be implemented to meet broader economic objectives such as reaching the inflation target.
- **3 November 2010:** The FOMC announces LSAP 2. Purchases are expanded to $600 billion in longer-term government bonds, defining a pace of $75 billion per month. The program is set to finish by mid-2011.
- **21 September 2011:** The FOMC announces that it will reinvest maturing debts into MBS while rolling over maturing government bonds into other government securities.
- **13 September 2012:** The FOMC initiates LSAP 3. Purchases will include $40 billion each month in MBS without a specific target for the total quantity, equating to an increase in longer-term security holdings of $85 billion each month. Strong forward guidance is also provided that further stimulus will be used to reach economic objectives, primarily, price stability.
- **12 December 2012:** The FOMC signals that it will continue purchasing $45 billion worth of longer-term government bonds each month, sustaining longer-term security purchases at a monthly rate of $85 billion.
- **20 March 2013:** The FOMC revises its forward guidance and states that the dimensions of the LSAPs will be contingent on meeting economic objectives.
- **1 May 2013:** The FOMC again revises its forward guidance, stating that the dimensions of the LSAPs will be particularly contingent on the inflation outlook.
- **22 May 2013:** In testimony to the U.S. Joint Economic Committee, Federal Reserve Chairman Ben Bernanke states that a potential reduction in purchases may be justified, establishing the possibility of an end to QE and triggering what market participants entitled as the "taper tantrum".
- **18 December 2013:** The FOMC announces a reduction in the size of monthly purchases. MBS purchases will be reduced to a monthly pace of $35 billion while longer-term government bond purchases will be reduced to $40 billion each month. The FOMC also signals that purchases will be reduced in a structured manner in the months to follow until September 2014.
- **17 September 2014:** The FOMC announces a policy normalisation plan and states it will hold assets at a level that allows for an efficient implementation of monetary policy. It also signals that the composition of future holdings on the balance sheet will be skewed towards government bonds.
- **29 October 2014:** The FOMC announces that asset purchases will cease. The reinvestment of maturing debt is sustained to allow the size of the balance sheet to remain constant but reversing asset holdings is not discussed.
- **16 December 2015:** The FOMC signals that maturing debt will be reinvested until the policy rate reaches a level deemed normal.

[28] Details of each announcement are sourced from the Board of Governors of the Federal Reserve System (2020b) and are cross-checked against Fawley and Neely (2013).

- **5 April 2017:** The FOMC meeting minutes highlight that the reinvestment of maturing debt may be phased out entirely.
- **14 June 2017:** The FOMC signals that it expects to normalise its balance sheet later in the year.
- **26 July 2017:** The FOMC states that it will soon commence normalising its balance sheet, conditional on the state of economic conditions.
- **20 September 2017:** The FOMC announces that it will begin the normalisation of its balance sheet in October 2017.
- **30 January 2019:** The FOMC provides longer-term plans for the normalisation of the balance sheet by stating that an ample supply of bank reserves is necessary for the efficient implementation of monetary policy. They state that asset purchases can be used again in the future if required.
- **30 March 2019:** The FOMC revises its longer-term plans for the normalisation of the balance sheet. They state that they intend to slow the decline of bank reserves and that the reduction of government bond holdings will be slowed in half while maturing MBS will be reinvested into government bonds at a maximum pace of $20 billion each month.
- **11 October 2019:** Following tight financial conditions in short-term U.S. dollar funding markets, the FOMC states that to sustain an abundant supply of bank reserves within the economic system, and to maintain control over the effective Federal Funds Rate, a continuation of government bond purchases into mid-2020 will be required. The FOMC highlights the goal is to increase excess reserves back to September 2019 levels.

Appendix C: Rolling Window Spillover Indices – Empirical Results

	Full Sample: 2006–2019			*Crisis Period: 2007–2012*			*Normalisation Period: 2013–2019*		
H-Step-Ahead	1–day	3–day	12–day	1–day	3–day	12–day	1–day	3–day	12–day
QE_{SHDW}	0.432*	0.597**	0.526*	-0.393	-0.285	-0.417	-0.605	-0.269	-0.056
	(0.033)	(0.009)	(0.022)	(0.316)	(0.411)	(0.238)	(0.135)	(0.638)	(0.923)
D_{QE}	1.216	0.662	-0.206	0.245	-0.057	-1.071	0.655	-0.154	-0.811
	(0.323)	(0.575)	(0.854)	(0.914)	(0.976)	(0.542)	(0.565)	(0.911)	(0.527)
SUR_G	-0.001	-0.004	-0.027	-0.010	0.005	-0.024	-0.033	-0.072	-0.079*
	(0.976)	(0.909)	(0.385)	(0.802)	(0.905)	(0.588)	(0.348)	(0.077)	(0.029)
SUR_{US}	-0.035*	-0.025	-0.006	-0.030	-0.049*	-0.019	-0.009	0.061**	0.062**
	(0.022)	(0.156)	(0.742)	(0.148)	(0.029)	(0.402)	(0.664)	(0.007)	(0.004)
SUR_{AU}	-0.021*	-0.019	-0.019	-0.004	0.000	0.002	0.026*	0.030	0.027
	(0.040)	(0.122)	(0.128)	(0.800)	(0.982)	(0.904)	(0.033)	(0.061)	(0.064)
OIS_{AU}	-0.834*	-1.399***	-1.005**	1.357	0.798	1.495	-9.734***	-10.953***	-8.901***
	(0.016)	(0.000)	(0.009)	(0.167)	(0.350)	(0.072)	(0.000)	(0.000)	(0.001)
CDS_{US}	0.100**	0.152***	0.135***	0.026	0.056	0.047	-0.020	0.096	0.066
	(0.002)	(0.000)	(0.001)	(0.453)	(0.147)	(0.245)	(0.691)	(0.258)	(0.397)
CDS_{AU}	-0.054**	-0.074**	-0.065**	-0.018	-0.029	-0.022	0.067*	0.063	0.068
	(0.006)	(0.002)	(0.007)	(0.461)	(0.227)	(0.369)	(0.011)	(0.267)	(0.169)
Intercept	17.886***	28.981***	34.493***	10.459*	22.374***	25.744***	30.831***	37.356***	41.142***
	(0.000)	(0.000)	(0.000)	(0.043)	(0.000)	(0.000)	(0.000)	(0.000)	(0.000)
Adjusted R^2	0.136	0.156	0.101	0.143	0.186	0.122	0.445	0.417	0.326
Observations	3463	3463	3463	1510	1510	1510	1762	1762	1762

Table 18: Results of 60-day Rolling Aggregate Volatility Spillover Index

Note. This table displays the result of the following regression estimated using OLS: $S^g_{ij}(H)_t = \alpha_t + \beta_1 QE_{SHDW_t} + \beta_2 D_{QE_t} + \beta_3 SUR_{G_t} + \beta_4 SUR_{US_t} + \beta_5 SUR_{AU_t} + \beta_6 OIS_{AU_t} + \beta_7 CDS_{US_t} + \beta_8 CDS_{AU_t} + \varepsilon_t$. The 1, 3, and 12 days represent the H-step-ahead forecast horizon for the rolling window estimation. The p-values (in parentheses below the coefficients) are derived from Newey and West (1986) heteroskedasticity and autocorrelation consistent standard errors. The levels of significance are defined as follows: '***' implies significance at the 0.1% level, '**' implies significance at the 1% level, and '*' implies significance at the 5% level.

	Full Sample: 2006–2019			*Crisis Period: 2007–2012*			*Normalisation Period: 2013–2019*		
H-Step-Ahead	1–day	3–day	12–day	1–day	3–day	12–day	1–day	3–day	12–day
QE_{SHDW}	0.445*	0.603*	0.548*	-0.421	-0.408	-0.486	-0.731*	-0.371	-0.250
	(0.032)	(0.013)	(0.023)	(0.305)	(0.263)	(0.179)	(0.049)	(0.485)	(0.658)
D_{QE}	0.786	0.669	0.394	0.882	1.498	1.296	-0.364	-0.995	-1.153
	(0.501)	(0.583)	(0.741)	(0.648)	(0.380)	(0.442)	(0.746)	(0.453)	(0.398)
SUR_G	0.009	-0.001	-0.024	0.011	0.024	-0.018	-0.036	-0.095*	-0.085*
	(0.721)	(0.966)	(0.476)	(0.795)	(0.617)	(0.719)	(0.272)	(0.013)	(0.019)
SUR_{US}	-0.039*	-0.027	-0.008	-0.038	-0.055*	-0.024	-0.005	0.069**	0.063**
	(0.011)	(0.144)	(0.650)	(0.078)	(0.021)	(0.350)	(0.777)	(0.002)	(0.004)
SUR_{AU}	-0.024*	-0.023	-0.024*	-0.002	0.001	0.001	0.020	0.021	0.016
	(0.017)	(0.056)	(0.050)	(0.886)	(0.935)	(0.932)	(0.064)	(0.163)	(0.287)
OIS_{AU}	-0.885*	-1.460***	-1.103**	1.537	1.067	1.590	-10.518***	-12.021***	-10.224***
	(0.013)	(0.000)	(0.007)	(0.125)	(0.230)	(0.065)	(0.000)	(0.000)	(0.000)
CDS_{US}	0.098**	0.153***	0.138***	0.011	0.040	0.036	-0.031	0.080	0.061
	(0.002)	(0.000)	(0.001)	(0.750)	(0.307)	(0.379)	(0.514)	(0.323)	(0.444)
CDS_{AU}	-0.050*	-0.074**	-0.065**	-0.005	-0.016	-0.015	0.077**	0.075	0.071
	(0.011)	(0.003)	(0.010)	(0.847)	(0.512)	(0.565)	(0.002)	(0.169)	(0.161)
Intercept	15.813***	26.521***	31.328***	7.352	18.361***	22.123***	30.232***	36.837***	40.574***
	(0.000)	(0.000)	(0.000)	(0.154)	(0.001)	(0.000)	(0.000)	(0.000)	(0.000)
Adjusted R^2	0.154	0.172	0.115	0.163	0.206	0.132	0.516	0.483	0.378
Observations	3453	3453	3453	1510	1510	1510	1762	1762	1762

Table 19: Results of 70-day Rolling Aggregate Volatility Spillover Index

Note. This table displays the result of the following regression estimated using OLS: $S^g_{ij}(H)_t = \alpha_t + \beta_1 QE_{SHDW_t} + \beta_2 D_{QE_t} + \beta_3 SUR_{G_t} + \beta_4 SUR_{US_t} + \beta_5 SUR_{AU_t} + \beta_6 OIS_{AU_t} + \beta_7 CDS_{US_t} + \beta_8 CDS_{AU_t} + \varepsilon_t$. The 1, 3, and 12 days represent the H-step-ahead forecast horizon for the rolling window estimation. The p-values (in parentheses below the coefficients) are derived from Newey and West (1986) heteroskedasticity and autocorrelation consistent standard errors. The levels of significance are defined as follows: '***' implies significance at the 0.1% level, '**' implies significance at the 1% level, and '*' implies significance at the 5% level.

	Full Sample: 2006–2019			*Crisis Period: 2007–2012*			*Normalisation Period: 2013–2019*		
H-Step-Ahead	1–day	3–day	12–day	1–day	3–day	12–day	1–day	3–day	12–day
QE_{SHDW}	0.438*	0.606*	0.574*	-0.501	-0.503	-0.519	-0.792*	-0.298	-0.221
	(0.041)	(0.015)	(0.019)	(0.244)	(0.189)	(0.174)	(0.015)	(0.547)	(0.686)
D_{QE}	1.446	1.019	0.790	1.329	1.526	1.607	0.527	-0.311	-0.618
	(0.156)	(0.351)	(0.447)	(0.470)	(0.348)	(0.303)	(0.551)	(0.778)	(0.586)
SUR_G	0.018	-0.002	-0.024	0.021	0.028	-0.020	-0.033	-0.110**	-0.088*
	(0.497)	(0.947)	(0.507)	(0.623)	(0.574)	(0.710)	(0.285)	(0.002)	(0.011)
SUR_{US}	-0.041**	-0.025	-0.008	-0.042	-0.055*	-0.024	-0.001	0.074***	0.065**
	(0.009)	(0.185)	(0.666)	(0.056)	(0.025)	(0.380)	(0.937)	(0.001)	(0.003)
SUR_{AU}	-0.023*	-0.025*	-0.027*	0.003	0.005	0.000	0.014	0.012	0.009
	(0.016)	(0.040)	(0.029)	(0.824)	(0.781)	(0.996)	(0.165)	(0.399)	(0.559)
OIS_{AU}	-0.921*	-1.538***	-1.224**	1.669	1.093	1.456	-11.000***	-12.258***	-10.708***
	(0.011)	(0.000)	(0.003)	(0.100)	(0.237)	(0.115)	(0.000)	(0.000)	(0.000)
CDS_{US}	0.090**	0.153***	0.141***	-0.004	0.038	0.040	-0.046	0.046	0.037
	(0.004)	(0.000)	(0.001)	(0.910)	(0.327)	(0.327)	(0.304)	(0.531)	(0.625)
CDS_{AU}	-0.042*	-0.072**	-0.065*	0.006	-0.013	-0.017	0.091***	0.096	0.084
	(0.034)	(0.005)	(0.011)	(0.800)	(0.606)	(0.538)	(0.000)	(0.057)	(0.085)
Intercept	14.410***	24.755***	29.040***	5.334	15.990**	20.087***	29.583***	35.960***	39.589***
	(0.000)	(0.000)	(0.000)	(0.302)	(0.003)	(0.000)	(0.000)	(0.000)	(0.000)
Adjusted R^2	0.154	0.185	0.132	0.170	0.213	0.137	0.568	0.543	0.429
Observations	3443	3443	3443	1510	1510	1510	1762	1762	1762

Table 20: Results of 80-day Rolling Aggregate Volatility Spillover Index

Note. This table displays the result of the following regression estimated using OLS: $S^g_{ij}(H)_t = \alpha_t + \beta_1 QE_{SHDW_t} + \beta_2 D_{QE_t} + \beta_3 SUR_{G_t} + \beta_4 SUR_{US_t} + \beta_5 SUR_{AU_t} + \beta_6 OIS_{AU_t} + \beta_7 CDS_{US_t} + \beta_8 CDS_{AU_t} + \varepsilon_t$. The 1, 3, and 12 days represent the H-step-ahead forecast horizon for the rolling window estimation. The p-values (in parentheses below the coefficients) are derived from Newey and West (1986) heteroskedasticity and autocorrelation consistent standard errors. The levels of significance are defined as follows: '***' implies significance at the 0.1% level, '**' implies significance at the 1% level, and '*' implies significance at the 5% level.

	Full Sample: 2006–2019			*Crisis Period: 2007–2012*			*Normalisation Period: 2013–2019*		
H-Step-Ahead	1–day	3–day	12–day	1–day	3–day	12–day	1–day	3–day	12–day
QE_{SHDW}	0.426	0.605*	0.591*	-0.573	-0.636	-0.611	-0.831**	-0.236	-0.178
	(0.053)	(0.017)	(0.017)	(0.208)	(0.110)	(0.122)	(0.004)	(0.611)	(0.728)
D_{QE}	0.844	0.879	0.679	0.576	1.154	1.136	0.066	-0.204	-0.476
	(0.396)	(0.390)	(0.503)	(0.763)	(0.493)	(0.511)	(0.927)	(0.822)	(0.628)
SUR_G	0.025	-0.001	-0.021	0.024	0.027	-0.019	-0.024	-0.108***	-0.083*
	(0.355)	(0.982)	(0.582)	(0.567)	(0.601)	(0.732)	(0.401)	(0.001)	(0.012)
SUR_{US}	-0.040*	-0.022	-0.007	-0.041	-0.050*	-0.022	-0.001	0.076***	0.067**
	(0.011)	(0.244)	(0.718)	(0.059)	(0.042)	(0.424)	(0.973)	(0.000)	(0.002)
SUR_{AU}	-0.023*	-0.024	-0.026*	0.008	0.012	0.006	0.010	0.006	0.007
	(0.016)	(0.051)	(0.038)	(0.628)	(0.451)	(0.728)	(0.267)	(0.642)	(0.646)
OIS_{AU}	-0.943**	-1.568***	-1.283**	1.743	1.279	1.590	-11.218***	-12.257***	-10.910***
	(0.010)	(0.000)	(0.002)	(0.101)	(0.189)	(0.102)	(0.000)	(0.000)	(0.000)
CDS_{US}	0.081*	0.142***	0.131***	-0.012	0.028	0.029	-0.073	0.007	0.005
	(0.011)	(0.000)	(0.001)	(0.732)	(0.471)	(0.468)	(0.068)	(0.916)	(0.940)
CDS_{AU}	-0.034	-0.063*	-0.056*	0.012	-0.005	-0.008	0.105***	0.117*	0.102*
	(0.101)	(0.017)	(0.029)	(0.630)	(0.858)	(0.773)	(0.000)	(0.017)	(0.030)
Intercept	13.415***	23.427***	27.320***	3.978	13.547*	17.464**	29.659***	35.483***	38.782***
	(0.000)	(0.000)	(0.000)	(0.460)	(0.014)	(0.002)	(0.000)	(0.000)	(0.000)
Adjusted R^2	0.146	0.185	0.134	0.164	0.214	0.139	0.597	0.577	0.469
Observations	3433	3433	3433	1510	1510	1510	1762	1762	1762

Table 21: Results of 90-day Rolling Aggregate Volatility Spillover Index

Note. This table displays the result of the following regression estimated using OLS: $S^g_{ij}(H)_t = \alpha_t + \beta_1 QE_{SHDW_t} + \beta_2 D_{QE_t} + \beta_3 SUR_{G_t} + \beta_4 SUR_{US_t} + \beta_5 SUR_{AU_t} + \beta_6 OIS_{AU_t} + \beta_7 CDS_{US_t} + \beta_8 CDS_{AU_t} + \varepsilon_t$. The 1, 3, and 12 days represent the H-step-ahead forecast horizon for the rolling window estimation. The p-values (in parentheses below the coefficients) are derived from Newey and West (1986) heteroskedasticity and autocorrelation consistent standard errors. The levels of significance are defined as follows: '***' implies significance at the 0.1% level, '**' implies significance at the 1% level, and '*' implies significance at the 5% level.

	Full Sample: 2006–2019			*Crisis Period: 2007–2012*			*Normalisation Period: 2013–2019*		
H-Step-Ahead	1–day	3–day	12–day	1–day	3–day	12–day	1–day	3–day	12–day
QE_{SOMA}	-16.781	-22.567	-34.937	4.389	9.217	-4.673	35.059	24.849	-4.463
	(0.372)	(0.242)	(0.083)	(0.803)	(0.518)	(0.717)	(0.600)	(0.767)	(0.960)
D_{QE}	0.375	-0.163	-0.786	0.189	-0.582	-1.200	0.332	-0.184	-0.738
	(0.804)	(0.901)	(0.535)	(0.946)	(0.809)	(0.594)	(0.759)	(0.873)	(0.512)
SUR_G	-0.010	-0.020	-0.046	-0.009	0.001	-0.033	-0.033	-0.078	-0.087*
	(0.726)	(0.563)	(0.186)	(0.823)	(0.988)	(0.516)	(0.395)	(0.071)	(0.016)
SUR_{US}	-0.034*	-0.021	0.002	-0.034	-0.052*	-0.018	-0.008	0.063*	0.062**
	(0.037)	(0.288)	(0.915)	(0.083)	(0.025)	(0.482)	(0.738)	(0.013)	(0.005)
SUR_{AU}	-0.011	-0.005	-0.007	-0.009	-0.001	-0.002	0.026	0.026	0.022
	(0.372)	(0.705)	(0.619)	(0.516)	(0.955)	(0.905)	(0.072)	(0.131)	(0.137)
OIS_{AU}	-0.642	-1.184**	-0.771	0.789	0.355	0.869	-8.033***	-10.302***	-8.792***
	(0.081)	(0.005)	(0.067)	(0.242)	(0.624)	(0.245)	(0.000)	(0.000)	(0.000)
CDS_{US}	0.093*	0.148**	0.128**	0.018	0.051	0.039	-0.019	0.091	0.076
	(0.014)	(0.001)	(0.004)	(0.586)	(0.215)	(0.395)	(0.751)	(0.341)	(0.386)
CDS_{AU}	-0.060*	-0.086**	-0.072**	-0.014	-0.028	-0.018	0.074*	0.070	0.065
	(0.013)	(0.003)	(0.009)	(0.592)	(0.265)	(0.502)	(0.017)	(0.280)	(0.257)
Intercept	18.312***	29.627***	34.983***	13.706***	24.960***	29.444***	26.935***	35.875***	40.695***
	(0.000)	(0.000)	(0.000)	(0.001)	(0.000)	(0.000)	(0.000)	(0.000)	(0.000)
Adjusted R^2	0.099	0.113	0.064	0.110	0.168	0.083	0.438	0.415	0.324
Observations	714	714	714	313	313	313	362	362	362

Table 22: Results of 60-day Rolling Aggregate Volatility Spillover Index (SOMA Portfolio)

Note. This table displays the result of the following regression estimated using OLS: $S^g_{ij}(H)_t = \alpha_t + \beta_1 QE_{SOMA_t} + \beta_2 D_{QE_t} + \beta_3 SUR_{G_t} + \beta_4 SUR_{US_t} + \beta_5 SUR_{AU_t} + \beta_6 OIS_{AU_t} + \beta_7 CDS_{US_t} + \beta_8 CDS_{AU_t} + \varepsilon_t$. The 1, 3, and 12 days represent the H-step-ahead forecast horizon for the rolling window estimation. The p-values (in parentheses below the coefficients) are derived from Newey and West (1986) heteroskedasticity and autocorrelation consistent standard errors. The levels of significance are defined as follows: '***' implies significance at the 0.1% level, '**' implies significance at the 1% level, and '*' implies significance at the 5% level.

	Full Sample: 2006–2019			*Crisis Period: 2007–2012*			*Normalisation Period: 2013–2019*		
H-Step-Ahead	1–day	3–day	12–day	1–day	3–day	12–day	1–day	3–day	12–day
QE_{SOMA}	-19.162	-28.172	-35.292	1.107	-0.946	-9.725	111.594*	107.081	64.624
	(0.346)	(0.181)	(0.128)	(0.954)	(0.951)	(0.485)	(0.042)	(0.156)	(0.419)
D_{QE}	0.346	0.162	0.176	1.229	1.734	1.841	-0.273	-0.854	-0.729
	(0.796)	(0.898)	(0.884)	(0.602)	(0.416)	(0.366)	(0.820)	(0.521)	(0.592)
SUR_G	0.001	-0.015	-0.041	0.018	0.028	-0.022	-0.037	-0.101**	-0.092**
	(0.973)	(0.678)	(0.283)	(0.685)	(0.612)	(0.714)	(0.315)	(0.009)	(0.010)
SUR_{US}	-0.038*	-0.022	-0.002	-0.045*	-0.060*	-0.024	-0.004	0.069**	0.062**
	(0.019)	(0.274)	(0.924)	(0.032)	(0.015)	(0.389)	(0.843)	(0.006)	(0.009)
SUR_{AU}	-0.015	-0.010	-0.013	-0.012	-0.005	-0.008	0.019	0.017	0.010
	(0.194)	(0.440)	(0.338)	(0.359)	(0.750)	(0.691)	(0.164)	(0.301)	(0.500)
OIS_{AU}	-0.718	-1.277**	-0.913*	0.962	0.437	0.808	-8.757***	-11.422***	-9.823***
	(0.074)	(0.005)	(0.044)	(0.147)	(0.547)	(0.297)	(0.000)	(0.000)	(0.000)
CDS_{US}	0.092*	0.151**	0.138**	0.001	0.035	0.037	-0.027	0.083	0.073
	(0.019)	(0.002)	(0.003)	(0.979)	(0.387)	(0.398)	(0.637)	(0.371)	(0.422)
CDS_{AU}	-0.055*	-0.085**	-0.077*	0.004	-0.011	-0.014	0.083**	0.078	0.067
	(0.028)	(0.006)	(0.011)	(0.881)	(0.671)	(0.618)	(0.008)	(0.226)	(0.264)
Intercept	16.302***	27.116***	31.765***	10.327*	21.399***	25.978***	26.184***	35.304***	39.371***
	(0.000)	(0.000)	(0.000)	(0.011)	(0.011)	(0.000)	(0.000)	(0.000)	(0.000)
Adjusted R^2	0.117	0.129	0.083	0.131	0.179	0.096	0.513	0.496	0.388
Observations	712	712	712	313	313	313	362	362	362

Table 23: Results of 70-day Rolling Aggregate Volatility Spillover Index (SOMA Portfolio)

Note. This table displays the result of the following regression estimated using OLS: $S^g_{ij}(H)_t = \alpha_t + \beta_1 QE_{SOMA_t} + \beta_2 D_{QE_t} + \beta_3 SUR_{G_t} + \beta_4 SUR_{US_t} + \beta_5 SUR_{AU_t} + \beta_6 OIS_{AU_t} + \beta_7 CDS_{US_t} + \beta_8 CDS_{AU_t} + \varepsilon_t$. The 1, 3, and 12 days represent the H-step-ahead forecast horizon for the rolling window estimation. The p-values (in parentheses below the coefficients) are derived from Newey and West (1986) heteroskedasticity and autocorrelation consistent standard errors. The levels of significance are defined as follows: '***' implies significance at the 0.1% level, '**' implies significance at the 1% level, and '*' implies significance at the 5% level.

	Full Sample: 2006–2019			*Crisis Period: 2007–2012*			*Normalisation Period: 2013–2019*		
H-Step-Ahead	1–day	3–day	12–day	1–day	3–day	12–day	1–day	3–day	12–day
QE_{SOMA}	-26.109	-35.011	-36.284	-3.152	-6.766	-9.566	68.254	55.970	30.317
	(0.233)	(0.117)	(0.131)	(0.866)	(0.678)	(0.527)	(0.199)	(0.477)	(0.728)
D_{QE}	0.911	0.532	0.423	1.532	1.902	1.972	0.614	-0.179	-0.286
	(0.431)	(0.643)	(0.701)	(0.488)	(0.323)	(0.295)	(0.517)	(0.866)	(0.801)
SUR_G	0.011	-0.014	-0.036	0.028	0.033	-0.019	-0.034	-0.115***	-0.092**
	(0.718)	(0.722)	(0.382)	(0.529)	(0.557)	(0.770)	(0.351)	(0.001)	(0.006)
SUR_{US}	-0.039*	-0.021	-0.003	-0.049*	-0.060*	-0.026	0.001	0.075**	0.065**
	(0.020)	(0.322)	(0.896)	(0.021)	(0.018)	(0.387)	(0.976)	(0.003)	(0.010)
SUR_{AU}	-0.014	-0.011	-0.015	-0.009	-0.006	-0.011	0.012	0.009	0.005
	(0.207)	(0.403)	(0.278)	(0.518)	(0.741)	(0.564)	(0.381)	(0.555)	(0.754)
OIS_{AU}	-0.759	-1.340**	-1.023*	0.923	0.281	0.615	-8.934***	-11.705***	-10.292***
	(0.073)	(0.004)	(0.028)	(0.158)	(0.689)	(0.424)	(0.000)	(0.000)	(0.000)
CDS_{US}	0.082*	0.147**	0.139**	-0.010	0.034	0.041	-0.053	0.041	0.038
	(0.036)	(0.002)	(0.004)	(0.765)	(0.384)	(0.327)	(0.348)	(0.632)	(0.672)
CDS_{AU}	-0.046	-0.080*	-0.075*	0.013	-0.007	-0.014	0.103***	0.104	0.088
	(0.070)	(0.011)	(0.016)	(0.631)	(0.789)	(0.621)	(0.001)	(0.086)	(0.145)
Intercept	14.830***	25.253***	29.408***	9.022*	19.897***	24.138***	25.179***	34.532***	38.440***
	(0.000)	(0.000)	(0.000)	(0.022)	(0.000)	(0.000)	(0.000)	(0.000)	(0.000)
Adjusted R^2	0.117	0.141	0.093	0.135	0.183	0.097	0.550	0.549	0.434
Observations	710	710	710	313	313	313	362	362	362

Table 24: Results of 80-day Rolling Aggregate Volatility Spillover Index (SOMA Portfolio)

Note. This table displays the result of the following regression estimated using OLS: $S^g_{ij}(H)_t = \alpha_t + \beta_1 QE_{SOMA_t} + \beta_2 D_{QE_t} + \beta_3 SUR_{G_t} + \beta_4 SUR_{US_t} + \beta_5 SUR_{AU_t} + \beta_6 OIS_{AU_t} + \beta_7 CDS_{US_t} + \beta_8 CDS_{AU_t} + \varepsilon_t$. The 1, 3, and 12 days represent the H-step-ahead forecast horizon for the rolling window estimation. The p-values (in parentheses below the coefficients) are derived from Newey and West (1986) heteroskedasticity and autocorrelation consistent standard errors. The levels of significance are defined as follows: '***' implies significance at the 0.1% level, '**' implies significance at the 1% level, and '*' implies significance at the 5% level.

	Full Sample: 2006–2019			*Crisis Period: 2007–2012*			*Normalisation Period: 2013–2019*		
H-Step-Ahead	1–day	3–day	12–day	1–day	3–day	12–day	1–day	3–day	12–day
QE_{SOMA}	-33.750	-40.358	-37.633	-13.549	-13.816	-10.261	121.791**	85.885	53.324
	(0.150)	(0.089)	(0.132)	(0.497)	(0.455)	(0.551)	(0.010)	(0.252)	(0.512)
D_{QE}	0.543	0.351	0.100	1.242	1.657	1.301	0.288	-0.167	-0.332
	(0.635)	(0.763)	(0.935)	(0.593)	(0.423)	(0.550)	(0.699)	(0.851)	(0.725)
SUR_G	0.018	-0.012	-0.034	0.030	0.033	-0.016	-0.023	-0.114***	-0.087**
	(0.558)	(0.770)	(0.444)	(0.515)	(0.574)	(0.813)	(0.514)	(0.001)	(0.007)
SUR_{US}	-0.037*	-0.019	-0.002	-0.045*	-0.057*	-0.026	0.000	0.075**	0.067**
	(0.033)	(0.403)	(0.940)	(0.035)	(0.034)	(0.422)	(0.995)	(0.002)	(0.007)
SUR_{AU}	-0.014	-0.011	-0.014	-0.005	-0.002	-0.008	0.007	0.003	0.003
	(0.227)	(0.455)	(0.355)	(0.702)	(0.926)	(0.713)	(0.549)	(0.819)	(0.844)
OIS_{AU}	-0.783	-1.355**	-1.050*	0.841	0.238	0.656	-9.134***	-11.949***	-10.612***
	(0.080)	(0.004)	(0.030)	(0.208)	(0.736)	(0.408)	(0.000)	(0.000)	(0.000)
CDS_{US}	0.072	0.131**	0.123*	-0.017	0.023	0.025	-0.087	-0.011	-0.006
	(0.080)	(0.007)	(0.011)	(0.659)	(0.557)	(0.539)	(0.071)	(0.887)	(0.939)
CDS_{AU}	-0.036	-0.067*	-0.062	0.019	0.003	-0.001	0.119***	0.129*	0.110
	(0.186)	(0.039)	(0.052)	(0.542)	(0.924)	(0.966)	(0.000)	(0.026)	(0.055)
Intercept	13.742***	23.893***	27.727***	8.313*	18.488***	21.990***	25.550***	34.985***	38.381***
	(0.000)	(0.000)	(0.000)	(0.040)	(0.000)	(0.000)	(0.000)	(0.000)	(0.000)
Adjusted R^2	0.109	0.139	0.089	0.117	0.173	0.093	0.571	0.579	0.467
Observations	708	708	708	313	313	313	362	362	362

Table 25: Results of 90-day Rolling Aggregate Volatility Spillover Index (SOMA Portfolio)

Note. This table displays the result of the following regression estimated using OLS: $S^g_{ij}(H)_t = \alpha_t + \beta_1 QE_{SOMA_t} + \beta_2 D_{QE_t} + \beta_3 SUR_{G_t} + \beta_4 SUR_{US_t} + \beta_5 SUR_{AU_t} + \beta_6 OIS_{AU_t} + \beta_7 CDS_{US_t} + \beta_8 CDS_{AU_t} + \varepsilon_t$. The 1, 3, and 12 days represent the H-step-ahead forecast horizon for the rolling window estimation. The p-values (in parentheses below the coefficients) are derived from Newey and West (1986) heteroskedasticity and autocorrelation consistent standard errors. The levels of significance are defined as follows: '***' implies significance at the 0.1% level, '**' implies significance at the 1% level, and '*' implies significance at the 5% level.

Full Sample: 2006–2019

	VIX/MOVE	VIX/AVIX	VIX/AGSVIX	MOVE/AVIX	MOVE/AGSVIX	AVIX/AGSVIX
QE_{SHDW}	0.076	0.038	0.045	0.086	-0.021	0.097
	(0.194)	(0.735)	(0.500)	(0.156)	(0.729)	(0.085)
D_{QE}	-0.143	0.374	-0.156	-0.129	0.430	0.371
	(0.591)	(0.451)	(0.651)	(0.694)	(0.266)	(0.170)
SUR_G	-0.010	0.008	0.009	0.000	-0.006	0.022***
	(0.302)	(0.541)	(0.324)	(0.980)	(0.535)	(0.001)
SUR_{US}	0.011*	-0.005	0.004	-0.003	0.003	-0.010*
	(0.028)	(0.581)	(0.386)	(0.639)	(0.469)	(0.021)
SUR_{AU}	-0.003	0.008	-0.001	0.005	0.002	0.002
	(0.354)	(0.231)	(0.790)	(0.291)	(0.542)	(0.447)
OIS_{AU}	-0.216*	-0.653***	-0.259**	-0.329**	0.112	0.021
	(0.037)	(0.001)	(0.010)	(0.005)	(0.389)	(0.801)
CDS_{US}	0.024*	0.053**	0.020*	0.001	-0.013	-0.009
	(0.027)	(0.005)	(0.043)	(0.929)	(0.353)	(0.313)
CDS_{AU}	-0.011	-0.015	-0.008	0.006	0.003	0.015*
	(0.079)	(0.221)	(0.229)	(0.460)	(0.730)	(0.017)
Intercept	0.390	2.761***	0.452	0.995*	0.744	-0.812*
	(0.384)	(0.001)	(0.243)	(0.037)	(0.133)	(0.020)
Adjusted R^2	0.061	0.137	0.045	0.096	0.019	0.068
Observations	3463	3463	3463	3463	3463	3463

Table 26: Results of 60-day Rolling Pairwise Volatility Spillover Indices (Full Sample)

Note. This table displays the result of the following regression estimated using OLS: $S^g_{ij}(H)_t = \alpha_t + \beta_1 QE_{SHDW_t} + \beta_2 D_{QE_t} + \beta_3 SUR_{G_t} + \beta_4 SUR_{US_t} + \beta_5 SUR_{AU_t} + \beta_6 OIS_{AU_t} + \beta_7 CDS_{US_t} + \beta_8 CDS_{AU_t} + \varepsilon_t$. The p-values (in parentheses below the coefficients) are derived from Newey and West (1986) heteroskedasticity and autocorrelation consistent standard errors. The levels of significance are defined as follows: '***' implies significance at the 0.1% level, '**' implies significance at the 1% level, and '*' implies significance at the 5% level.

Crisis Period: 2007–2012

	VIX/MOVE	VIX/AVIX	VIX/AGSVIX	MOVE/AVIX	MOVE/AGSVIX	AVIX/AGSVIX
QE_{SHDW}	-0.043	-0.386*	-0.001	-0.165	0.129	-0.021
	(0.523)	(0.011)	(0.995)	(0.080)	(0.232)	(0.786)
D_{QE}	0.465	1.024	-0.496	-0.014	-0.497	0.463
	(0.281)	(0.240)	(0.488)	(0.979)	(0.231)	(0.203)
SUR_G	-0.024*	0.009	0.007	0.013	0.006	0.025**
	(0.033)	(0.604)	(0.462)	(0.404)	(0.565)	(0.005)
SUR_{US}	0.013**	-0.016	0.004	-0.006	-0.004	-0.014**
	(0.006)	(0.117)	(0.378)	(0.431)	(0.338)	(0.005)
SUR_{AU}	0.010**	0.028**	0.002	0.011	-0.007	0.002
	(0.002)	(0.005)	(0.697)	(0.083)	(0.094)	(0.632)
OIS_{AU}	0.181	-0.004	-0.033	0.494*	0.047	0.300*
	(0.332)	(0.991)	(0.893)	(0.014)	(0.783)	(0.037)
CDS_{US}	0.010	0.013	0.011	-0.009	-0.007	-0.013
	(0.163)	(0.441)	(0.361)	(0.496)	(0.674)	(0.210)
CDS_{AU}	-0.008	0.001	-0.002	0.016*	0.005	0.019*
	(0.122)	(0.947)	(0.794)	(0.029)	(0.622)	(0.018)
Intercept	-0.619	1.446	-0.459	-3.588**	0.186	-2.408*
	(0.562)	(0.538)	(0.734)	(0.002)	(0.872)	(0.014)
Adjusted R^2	0.137	0.282	0.025	0.121	0.048	0.098
Observations	1510	1510	1510	1510	1510	1510

Table 27: Results of 60-day Rolling Pairwise Volatility Spillover Indices (Crisis Period)

Note. This table displays the result of the following regression estimated using OLS: $S^g_{ij}(H)_t = \alpha_t + \beta_1 QE_{SHDW_t} + \beta_2 D_{QE_t} + \beta_3 SUR_{G_t} + \beta_4 SUR_{US_t} + \beta_5 SUR_{AU_t} + \beta_6 OIS_{AU_t} + \beta_7 CDS_{US_t} + \beta_8 CDS_{AU_t} + \varepsilon_t$. The p-values (in parentheses below the coefficients) are derived from Newey and West (1986) heteroskedasticity and autocorrelation consistent standard errors. The levels of significance are defined as follows: '***' implies significance at the 0.1% level, '**' implies significance at the 1% level, and '*' implies significance at the 5% level.

Normalisation Period: 2013–2019

	VIX/MOVE	VIX/AVIX	VIX/AGSVIX	MOVE/AVIX	MOVE/AGSVIX	AVIX/AGSVIX
QE_{SHDW}	0.163	0.073	-0.417**	-0.306	-0.509	0.177
	(0.225)	(0.803)	(0.009)	(0.105)	(0.055)	(0.170)
D_{QE}	-0.437	0.250	-0.134	-0.350	0.544	0.163
	(0.146)	(0.705)	(0.720)	(0.315)	(0.209)	(0.608)
SUR_G	0.032**	-0.004	0.019	-0.036**	-0.027	0.028**
	(0.004)	(0.868)	(0.229)	(0.007)	(0.062)	(0.006)
SUR_{US}	0.003	0.018	0.001	0.016*	0.016	-0.003
	(0.631)	(0.113)	(0.861)	(0.030)	(0.085)	(0.688)
SUR_{AU}	-0.006	-0.006	0.001	0.007	0.011	0.006
	(0.258)	(0.565)	(0.802)	(0.146)	(0.168)	(0.188)
OIS_{AU}	0.727	-2.071	-1.823**	-3.322***	-1.573	0.251
	(0.273)	(0.065)	(0.005)	(0.000)	(0.235)	(0.614)
CDS_{US}	0.057*	0.122*	0.039	-0.055	-0.082***	-0.027
	(0.039)	(0.020)	(0.165)	(0.081)	(0.000)	(0.337)
CDS_{AU}	-0.048**	-0.027	-0.030	0.075**	0.036**	0.013
	(0.006)	(0.450)	(0.106)	(0.002)	(0.007)	(0.420)
Intercept	-0.080	1.914	3.975**	4.094*	5.515*	0.165
	(0.943)	(0.470)	(0.003)	(0.018)	(0.026)	(0.883)
Adjusted R^2	0.156	0.163	0.106	0.266	0.148	0.090
Observations	1762	1762	1762	1762	1762	1762

Table 28: Results of 60-day Rolling Pairwise Volatility Spillover Indices (Normalisation Period)

Note. This table displays the result of the following regression estimated using OLS: $S^g_{ij}(H)_t = \alpha_t + \beta_1 QE_{SHDW_t} + \beta_2 D_{QE_t} + \beta_3 SUR_{G_t} + \beta_4 SUR_{US_t} + \beta_5 SUR_{AU_t} + \beta_6 OIS_{AU_t} + \beta_7 CDS_{US_t} + \beta_8 CDS_{AU_t} + \varepsilon_t$. The p-values (in parentheses below the coefficients) are derived from Newey and West (1986) heteroskedasticity and autocorrelation consistent standard errors. The levels of significance are defined as follows: '***' implies significance at the 0.1% level, '**' implies significance at the 1% level, and '*' implies significance at the 5% level.

Full Sample: 2006–2019

	VIX/MOVE	VIX/AVIX	VIX/AGSVIX	MOVE/AVIX	MOVE/AGSVIX	AVIX/AGSVIX
QE_{SHDW}	0.064	0.036	0.027	0.109*	0.027	0.069*
	(0.142)	(0.744)	(0.508)	(0.050)	(0.609)	(0.039)
D_{QE}	-0.107	0.313	0.054	0.048	0.398	0.159
	(0.547)	(0.576)	(0.813)	(0.871)	(0.281)	(0.405)
SUR_G	-0.011	0.001	0.008	0.003	-0.007	0.012**
	(0.118)	(0.949)	(0.228)	(0.775)	(0.360)	(0.005)
SUR_{US}	0.011**	-0.001	0.002	-0.003	0.005	-0.006*
	(0.006)	(0.889)	(0.628)	(0.539)	(0.256)	(0.021)
SUR_{AU}	0.000	0.008	-0.003	0.002	0.002	-0.001
	(0.861)	(0.234)	(0.301)	(0.617)	(0.557)	(0.700)
OIS_{AU}	-0.195*	-0.579**	-0.108	-0.323***	0.101	0.017
	(0.021)	(0.003)	(0.159)	(0.001)	(0.374)	(0.782)
CDS_{US}	0.011	0.052**	0.007	0.009	-0.007	-0.007
	(0.168)	(0.009)	(0.378)	(0.459)	(0.561)	(0.344)
CDS_{AU}	-0.005	-0.012	-0.001	0.001	-0.002	0.006
	(0.320)	(0.353)	(0.781)	(0.917)	(0.826)	(0.121)
Intercept	0.490	2.838***	0.278	0.879*	0.703	-0.188
	(0.162)	(0.001)	(0.405)	(0.043)	(0.117)	(0.436)
Adjusted R^2	0.098	0.169	0.034	0.103	0.055	0.044
Observations	3453	3453	3453	3453	3453	3453

Table 29: Results of 70-day Rolling Pairwise Volatility Spillover Indices (Full Sample)

Note. This table displays the result of the following regression estimated using OLS: $S^g_{ij}(H)_t = \alpha_t + \beta_1 QE_{SHDW_t} + \beta_2 D_{QE_t} + \beta_3 SUR_{G_t} + \beta_4 SUR_{US_t} + \beta_5 SUR_{AU_t} + \beta_6 OIS_{AU_t} + \beta_7 CDS_{US_t} + \beta_8 CDS_{AU_t} + \varepsilon_t$. The p-values (in parentheses below the coefficients) are derived from Newey and West (1986) heteroskedasticity and autocorrelation consistent standard errors. The levels of significance are defined as follows: '***' implies significance at the 0.1% level, '**' implies significance at the 1% level, and '*' implies significance at the 5% level.

Crisis Period: 2007–2012

	VIX/MOVE	VIX/AVIX	VIX/AGSVIX	MOVE/AVIX	MOVE/AGSVIX	AVIX/AGSVIX
QE_{SHDW}	0.033	-0.382*	-0.042	-0.039	0.196*	0.003
	(0.547)	(0.011)	(0.470)	(0.658)	(0.022)	(0.958)
D_{QE}	0.270	1.331	0.220	0.222	-0.200	0.125
	(0.485)	(0.153)	(0.549)	(0.565)	(0.683)	(0.659)
SUR_G	-0.020*	0.008	0.013	0.009	0.012	0.014**
	(0.024)	(0.636)	(0.066)	(0.535)	(0.170)	(0.010)
SUR_{US}	0.011**	-0.012	-0.001	-0.002	-0.005	-0.009**
	(0.010)	(0.200)	(0.848)	(0.716)	(0.163)	(0.004)
SUR_{AU}	0.007*	0.029**	-0.001	0.009	-0.007	-0.001
	(0.015)	(0.004)	(0.682)	(0.103)	(0.060)	(0.738)
OIS_{AU}	-0.105	0.008	0.124	0.248	0.011	0.238
	(0.353)	(0.982)	(0.490)	(0.189)	(0.928)	(0.097)
CDS_{US}	0.004	0.014	-0.004	0.004	-0.003	-0.010
	(0.438)	(0.308)	(0.615)	(0.760)	(0.787)	(0.143)
CDS_{AU}	-0.004	0.004	0.007	0.006	0.003	0.010*
	(0.235)	(0.655)	(0.173)	(0.308)	(0.708)	(0.032)
Intercept	0.685	1.479	-0.874	-2.222*	0.286	-1.428
	(0.348)	(0.496)	(0.398)	(0.042)	(0.752)	(0.081)
Adjusted R^2	0.158	0.391	0.048	0.103	0.176	0.085
Observations	1510	1510	1510	1510	1510	1510

Table 30: Results of 70-day Rolling Pairwise Volatility Spillover Indices (Crisis Period)

Note. This table displays the result of the following regression estimated using OLS: $S^g_{ij}(H)_t = \alpha_t + \beta_1 QE_{SHDW_t} + \beta_2 D_{QE_t} + \beta_3 SUR_{G_t} + \beta_4 SUR_{US_t} + \beta_5 SUR_{AU_t} + \beta_6 OIS_{AU_t} + \beta_7 CDS_{US_t} + \beta_8 CDS_{AU_t} + \varepsilon_t$. The p-values (in parentheses below the coefficients) are derived from Newey and West (1986) heteroskedasticity and autocorrelation consistent standard errors. The levels of significance are defined as follows: '***' implies significance at the 0.1% level, '**' implies significance at the 1% level, and '*' implies significance at the 5% level.

Normalisation Period: 2013–2019

	VIX/MOVE	VIX/AVIX	VIX/AGSVIX	MOVE/AVIX	MOVE/AGSVIX	AVIX/AGSVIX
QE_{SHDW}	0.297**	0.020	-0.211	-0.330	-0.367	-0.033
	(0.009)	(0.944)	(0.171)	(0.052)	(0.143)	(0.716)
D_{QE}	-0.249	0.126	-0.209	-0.121	0.339	-0.030
	(0.247)	(0.849)	(0.445)	(0.713)	(0.342)	(0.897)
SUR_G	0.020*	-0.025	0.015	-0.025*	-0.036**	0.018**
	(0.012)	(0.308)	(0.223)	(0.021)	(0.009)	(0.006)
SUR_{US}	0.006	0.023	0.000	0.007	0.021**	0.000
	(0.204)	(0.057)	(0.958)	(0.210)	(0.010)	(0.951)
SUR_{AU}	-0.002	-0.012	-0.002	0.002	0.011	0.005
	(0.658)	(0.200)	(0.733)	(0.614)	(0.080)	(0.094)
OIS_{AU}	1.351**	-2.327*	-0.686	-3.165***	-1.322	-0.374
	(0.007)	(0.027)	(0.298)	(0.000)	(0.280)	(0.342)
CDS_{US}	0.049*	0.126*	0.013	-0.041	-0.084***	0.000
	(0.028)	(0.013)	(0.542)	(0.101)	(0.000)	(0.986)
CDS_{AU}	-0.042**	-0.018	-0.028	0.063***	0.035**	0.000
	(0.007)	(0.624)	(0.060)	(0.001)	(0.002)	(0.968)
Intercept	-1.401	1.682	3.322*	3.962*	5.211*	0.712
	(0.135)	(0.475)	(0.013)	(0.020)	(0.020)	(0.312)
Adjusted R^2	0.214	0.194	0.130	0.314	0.201	0.099
Observations	1762	1762	1762	1762	1762	1762

Table 31: Results of 70-day Rolling Pairwise Volatility Spillover Indices (Normalisation Period)

Note. This table displays the result of the following regression estimated using OLS: $S^g_{ij}(H)_t = \alpha_t + \beta_1 QE_{SHDW_t} + \beta_2 D_{QE_t} + \beta_3 SUR_{G_t} + \beta_4 SUR_{US_t} + \beta_5 SUR_{AU_t} + \beta_6 OIS_{AU_t} + \beta_7 CDS_{US_t} + \beta_8 CDS_{AU_t} + \varepsilon_t$. The p-values (in parentheses below the coefficients) are derived from Newey and West (1986) heteroskedasticity and autocorrelation consistent standard errors. The levels of significance are defined as follows: '***' implies significance at the 0.1% level, '**' implies significance at the 1% level, and '*' implies significance at the 5% level.

Full Sample: 2006–2019

	VIX/MOVE	VIX/AVIX	VIX/AGSVIX	MOVE/AVIX	MOVE/AGSVIX	AVIX/AGSVIX
QE_{SHDW}	0.058	0.092	0.048	0.112	-0.005	0.036
	(0.255)	(0.428)	(0.424)	(0.053)	(0.923)	(0.382)
D_{QE}	-0.261	0.025	-0.123	0.175	-0.018	0.317
	(0.209)	(0.965)	(0.702)	(0.502)	(0.957)	(0.105)
SUR_G	-0.011	-0.003	0.004	0.005	-0.009	0.015**
	(0.175)	(0.819)	(0.602)	(0.635)	(0.233)	(0.004)
SUR_{US}	0.011*	0.004	0.006	-0.003	0.004	-0.007*
	(0.013)	(0.680)	(0.129)	(0.669)	(0.299)	(0.029)
SUR_{AU}	-0.003	0.006	-0.001	0.001	0.000	0.005*
	(0.417)	(0.346)	(0.653)	(0.808)	(0.974)	(0.035)
OIS_{AU}	-0.221*	-0.677***	-0.253**	-0.345***	0.091	0.063
	(0.020)	(0.000)	(0.005)	(0.001)	(0.424)	(0.382)
CDS_{US}	0.023*	0.055**	0.020*	-0.005	-0.009	-0.011
	(0.015)	(0.004)	(0.012)	(0.696)	(0.446)	(0.092)
CDS_{AU}	-0.013*	-0.013	-0.009	0.012	0.001	0.012**
	(0.040)	(0.314)	(0.110)	(0.180)	(0.859)	(0.005)
Intercept	0.606	2.967***	0.589	1.113*	0.602	-0.556
	(0.142)	(0.000)	(0.087)	(0.013)	(0.175)	(0.055)
Adjusted R^2	0.090	0.179	0.069	0.130	0.023	0.073
Observations	3443	3443	3443	3443	3443	3443

Table 32: Results of 80-day Rolling Pairwise Volatility Spillover Indices (Full Sample)

Note. This table displays the result of the following regression estimated using OLS: $S^g_{ij}(H)_t = \alpha_t + \beta_1 QE_{SHDW_t} + \beta_2 D_{QE_t} + \beta_3 SUR_{G_t} + \beta_4 SUR_{US_t} + \beta_5 SUR_{AU_t} + \beta_6 OIS_{AU_t} + \beta_7 CDS_{US_t} + \beta_8 CDS_{AU_t} + \varepsilon_t$. The p-values (in parentheses below the coefficients) are derived from Newey and West (1986) heteroskedasticity and autocorrelation consistent standard errors. The levels of significance are defined as follows: '***' implies significance at the 0.1% level, '**' implies significance at the 1% level, and '*' implies significance at the 5% level.

Crisis Period: 2007–2012

	VIX/MOVE	VIX/AVIX	VIX/AGSVIX	MOVE/AVIX	MOVE/AGSVIX	AVIX/AGSVIX
QE_{SHDW}	-0.015	-0.401**	0.087	-0.153	0.125	-0.076
	(0.801)	(0.007)	(0.341)	(0.075)	(0.157)	(0.179)
D_{QE}	-0.039	1.289	0.168	0.673	-0.665	0.489*
	(0.931)	(0.124)	(0.780)	(0.059)	(0.146)	(0.035)
SUR_G	-0.031***	0.009	0.006	0.020	0.008	0.018***
	(0.001)	(0.587)	(0.403)	(0.168)	(0.342)	(0.001)
SUR_{US}	0.015***	-0.008	0.003	-0.004	-0.004	-0.010**
	(0.001)	(0.353)	(0.427)	(0.603)	(0.288)	(0.005)
SUR_{AU}	0.006*	0.027**	-0.002	0.010	-0.007*	0.007
	(0.026)	(0.009)	(0.474)	(0.068)	(0.035)	(0.062)
OIS_{AU}	0.002	0.058	-0.274	0.474**	0.052	0.331**
	(0.990)	(0.859)	(0.187)	(0.007)	(0.684)	(0.004)
CDS_{US}	0.014*	0.019	0.014	-0.011	-0.007	-0.018**
	(0.017)	(0.165)	(0.139)	(0.368)	(0.581)	(0.004)
CDS_{AU}	-0.013**	0.004	-0.004	0.020**	0.006	0.018***
	(0.003)	(0.660)	(0.507)	(0.003)	(0.432)	(0.000)
Intercept	0.639	0.478	0.792	-3.812***	0.005	-1.998**
	(0.461)	(0.807)	(0.473)	(0.001)	(0.996)	(0.002)
Adjusted R^2	0.188	0.383	0.058	0.163	0.078	0.111
Observations	1510	1510	1510	1510	1510	1510

Table 33: Results of 80-day Rolling Pairwise Volatility Spillover Indices (Crisis Period)

Note. This table displays the result of the following regression estimated using OLS: $S^g_{ij}(H)_t = \alpha_t + \beta_1 QE_{SHDW_t} + \beta_2 D_{QE_t} + \beta_3 SUR_{G_t} + \beta_4 SUR_{US_t} + \beta_5 SUR_{AU_t} + \beta_6 OIS_{AU_t} + \beta_7 CDS_{US_t} + \beta_8 CDS_{AU_t} + \varepsilon_t$. The p-values (in parentheses below the coefficients) are derived from Newey and West (1986) heteroskedasticity and autocorrelation consistent standard errors. The levels of significance are defined as follows: '***' implies significance at the 0.1% level, '**' implies significance at the 1% level, and '*' implies significance at the 5% level.

Normalisation Period: 2013–2019

	VIX/MOVE	VIX/AVIX	VIX/AGSVIX	MOVE/AVIX	MOVE/AGSVIX	AVIX/AGSVIX
QE_{SHDW}	0.191	0.445	-0.309	-0.235	-0.575*	0.057
	(0.154)	(0.136)	(0.055)	(0.158)	(0.013)	(0.609)
D_{QE}	-0.417*	-0.347	-0.441	-0.099	0.005	0.132
	(0.043)	(0.578)	(0.167)	(0.707)	(0.987)	(0.611)
SUR_G	0.026*	-0.027	0.012	-0.031**	-0.037**	0.025**
	(0.012)	(0.238)	(0.469)	(0.006)	(0.004)	(0.005)
SUR_{US}	0.006	0.031**	0.005	0.012	0.017*	-0.004
	(0.347)	(0.009)	(0.452)	(0.068)	(0.015)	(0.489)
SUR_{AU}	0.001	-0.011	0.000	-0.005	0.006	0.006
	(0.857)	(0.197)	(0.990)	(0.289)	(0.244)	(0.131)
OIS_{AU}	0.589	-0.954	-1.185*	-2.938***	-2.138*	0.259
	(0.364)	(0.372)	(0.047)	(0.000)	(0.047)	(0.572)
CDS_{US}	0.055*	0.103*	0.036	-0.067**	-0.082***	0.005
	(0.036)	(0.034)	(0.149)	(0.008)	(0.000)	(0.809)
CDS_{AU}	-0.037*	-0.017	-0.035*	0.078***	0.035***	-0.008
	(0.029)	(0.633)	(0.032)	(0.000)	(0.000)	(0.610)
Intercept	-0.704	0.602	3.546**	4.206*	6.541**	-0.198
	(0.501)	(0.805)	(0.004)	(0.018)	(0.002)	(0.822)
Adjusted R^2	0.153	0.212	0.123	0.347	0.252	0.084
Observations	1762	1762	1762	1762	1762	1762

Table 34: Results of 80-day Rolling Pairwise Volatility Spillover Indices (Normalisation Period)

Note. This table displays the result of the following regression estimated using OLS: $S^g_{ij}(H)_t = \alpha_t + \beta_1 QE_{SHDW_t} + \beta_2 D_{QE_t} + \beta_3 SUR_{G_t} + \beta_4 SUR_{US_t} + \beta_5 SUR_{AU_t} + \beta_6 OIS_{AU_t} + \beta_7 CDS_{US_t} + \beta_8 CDS_{AU_t} + \varepsilon_t$. The p-values (in parentheses below the coefficients) are derived from Newey and West (1986) heteroskedasticity and autocorrelation consistent standard errors. The levels of significance are defined as follows: '***' implies significance at the 0.1% level, '**' implies significance at the 1% level, and '*' implies significance at the 5% level.

Full Sample: 2006–2019

	VIX/MOVE	VIX/AVIX	VIX/AGSVIX	MOVE/AVIX	MOVE/AGSVIX	AVIX/AGSVIX
QE_{SHDW}	0.056	0.122	0.043	0.114*	-0.002	0.034
	(0.253)	(0.292)	(0.454)	(0.048)	(0.967)	(0.345)
D_{QE}	-0.369	0.114	0.010	0.101	0.264	0.285
	(0.053)	(0.829)	(0.970)	(0.662)	(0.407)	(0.146)
SUR_G	-0.012	-0.007	0.002	0.007	-0.009	0.011*
	(0.115)	(0.633)	(0.799)	(0.517)	(0.211)	(0.019)
SUR_{US}	0.010*	0.009	0.007	-0.002	0.004	-0.005
	(0.011)	(0.375)	(0.064)	(0.729)	(0.274)	(0.081)
SUR_{AU}	-0.002	0.007	0.000	0.001	0.000	0.004*
	(0.467)	(0.333)	(0.882)	(0.899)	(0.929)	(0.035)
OIS_{AU}	-0.226*	-0.677***	-0.246**	-0.346***	0.079	0.084
	(0.014)	(0.000)	(0.004)	(0.001)	(0.455)	(0.200)
CDS_{US}	0.023*	0.054**	0.021**	-0.007	-0.009	-0.009
	(0.012)	(0.004)	(0.002)	(0.581)	(0.375)	(0.146)
CDS_{AU}	-0.013*	-0.012	-0.010*	0.013	0.002	0.011*
	(0.028)	(0.370)	(0.037)	(0.123)	(0.744)	(0.013)
Intercept	0.674	2.995***	0.584	1.094*	0.549	-0.585*
	(0.086)	(0.000)	(0.071)	(0.012)	(0.189)	(0.029)
Adjusted R^2	0.099	0.199	0.084	0.149	0.024	0.069
Observations	3433	3433	3433	3433	3433	3433

Table 35: Results of 90-day Rolling Pairwise Volatility Spillover Indices (Full Sample)

Note. This table displays the result of the following regression estimated using OLS: $S^g_{ij}(H)_t = \alpha_t + \beta_1 QE_{SHDW_t} + \beta_2 D_{QE_t} + \beta_3 SUR_{G_t} + \beta_4 SUR_{US_t} + \beta_5 SUR_{AU_t} + \beta_6 OIS_{AU_t} + \beta_7 CDS_{US_t} + \beta_8 CDS_{AU_t} + \varepsilon_t$. The p-values (in parentheses below the coefficients) are derived from Newey and West (1986) heteroskedasticity and autocorrelation consistent standard errors. The levels of significance are defined as follows: '***' implies significance at the 0.1% level, '**' implies significance at the 1% level, and '*' implies significance at the 5% level.

Crisis Period: 2007–2012

	VIX/MOVE	VIX/AVIX	VIX/AGSVIX	MOVE/AVIX	MOVE/AGSVIX	AVIX/AGSVIX
QE_{SHDW}	-0.005	-0.418**	0.113	-0.163*	0.143	-0.090
	(0.928)	(0.004)	(0.175)	(0.046)	(0.068)	(0.059)
D_{QE}	-0.037	1.134	0.053	0.248	-0.215	0.312
	(0.917)	(0.082)	(0.908)	(0.582)	(0.626)	(0.251)
SUR_G	-0.034***	0.011	0.006	0.024	0.008	0.014**
	(0.000)	(0.484)	(0.314)	(0.080)	(0.277)	(0.003)
SUR_{US}	0.015***	-0.003	0.003	-0.003	-0.005	-0.007*
	(0.000)	(0.667)	(0.422)	(0.599)	(0.161)	(0.026)
SUR_{AU}	0.005	0.028**	-0.003	0.010*	-0.009**	0.008**
	(0.073)	(0.005)	(0.357)	(0.046)	(0.009)	(0.007)
OIS_{AU}	-0.042	0.180	-0.326	0.483**	-0.015	0.361***
	(0.785)	(0.580)	(0.094)	(0.004)	(0.891)	(0.001)
CDS_{US}	0.015**	0.019	0.016*	-0.013	-0.007	-0.016**
	(0.007)	(0.167)	(0.034)	(0.282)	(0.539)	(0.005)
CDS_{AU}	-0.015***	0.008	-0.006	0.022***	0.006	0.016***
	(0.000)	(0.407)	(0.293)	(0.001)	(0.366)	(0.000)
Intercept	0.950	-0.481	0.964	-3.994***	0.287	-2.076***
	(0.239)	(0.801)	(0.348)	(0.000)	(0.703)	(0.000)
Adjusted R^2	0.251	0.428	0.094	0.199	0.098	0.108
Observations	1510	1510	1510	1510	1510	1510

Table 36: Results of 90-day Rolling Pairwise Volatility Spillover Indices (Crisis Period)

Note. This table displays the result of the following regression estimated using OLS: $S^g_{ij}(H)_t = \alpha_t + \beta_1 QE_{SHDW_t} + \beta_2 D_{QE_t} + \beta_3 SUR_{G_t} + \beta_4 SUR_{US_t} + \beta_5 SUR_{AU_t} + \beta_6 OIS_{AU_t} + \beta_7 CDS_{US_t} + \beta_8 CDS_{AU_t} + \varepsilon_t$. The p-values (in parentheses below the coefficients) are derived from Newey and West (1986) heteroskedasticity and autocorrelation consistent standard errors. The levels of significance are defined as follows: '***' implies significance at the 0.1% level, '**' implies significance at the 1% level, and '*' implies significance at the 5% level.

Normalisation Period: 2013–2019

	VIX/MOVE	VIX/AVIX	VIX/AGSVIX	MOVE/AVIX	MOVE/AGSVIX	AVIX/AGSVIX
QE_{SHDW}	0.190	0.548	-0.286	-0.178	-0.540*	0.029
	(0.169)	(0.062)	(0.064)	(0.267)	(0.011)	(0.778)
D_{QE}	-0.600**	-0.110	-0.157	0.050	0.175	0.249
	(0.007)	(0.882)	(0.573)	(0.833)	(0.589)	(0.351)
SUR_G	0.026*	-0.035	0.007	-0.030**	-0.038***	0.021**
	(0.011)	(0.104)	(0.682)	(0.005)	(0.001)	(0.010)
SUR_{US}	0.004	0.036***	0.007	0.012*	0.019**	-0.005
	(0.547)	(0.001)	(0.286)	(0.034)	(0.002)	(0.339)
SUR_{AU}	0.003	-0.012	0.000	-0.006	0.007	0.002
	(0.609)	(0.137)	(0.967)	(0.117)	(0.076)	(0.589)
OIS_{AU}	0.585	-0.655	-0.981	-2.707***	-2.128*	0.277
	(0.369)	(0.528)	(0.074)	(0.000)	(0.024)	(0.519)
CDS_{US}	0.062*	0.104*	0.035	-0.078***	-0.085***	0.017
	(0.019)	(0.029)	(0.168)	(0.001)	(0.000)	(0.411)
CDS_{AU}	-0.040*	-0.017	-0.036*	0.081***	0.040***	-0.016
	(0.019)	(0.627)	(0.031)	(0.000)	(0.000)	(0.258)
Intercept	-0.936	0.181	3.324	4.238	6.246***	-0.265
	(0.387)	(0.938)	(0.003)**	(0.013)*	(0.001)	(0.758)
Adjusted R^2	0.159	0.246	0.131	0.379	0.292	0.064
Observations	1762	1762	1762	1762	1762	1762

Table 37: Results of 90-day Rolling Pairwise Volatility Spillover Indices (Normalisation Period)

Note. This table displays the result of the following regression estimated using OLS: $S^g_{ij}(H)_t = \alpha_t + \beta_1 QE_{SHDW_t} + \beta_2 D_{QE_t} + \beta_3 SUR_{G_t} + \beta_4 SUR_{US_t} + \beta_5 SUR_{AU_t} + \beta_6 OIS_{AU_t} + \beta_7 CDS_{US_t} + \beta_8 CDS_{AU_t} + \varepsilon_t$. The p-values (in parentheses below the coefficients) are derived from Newey and West (1986) heteroskedasticity and autocorrelation consistent standard errors. The levels of significance are defined as follows: '***' implies significance at the 0.1% level, '**' implies significance at the 1% level, and '*' implies significance at the 5% level.

Full Sample: 2006–2019

	VIX/MOVE	VIX/AVIX	VIX/AGSVIX	MOVE/AVIX	MOVE/AGSVIX	AVIX/AGSVIX
QE_{SOMA}	-8.602	-19.416*	-4.657	-12.683	-7.231	-5.355
	(0.062)	(0.025)	(0.438)	(0.133)	(0.057)	(0.222)
D_{QE}	-0.271	0.839	-0.366	0.013	0.542	0.291
	(0.435)	(0.178)	(0.328)	(0.975)	(0.216)	(0.436)
SUR_G	-0.015	0.008	0.007	-0.002	-0.007	0.022**
	(0.168)	(0.614)	(0.435)	(0.844)	(0.503)	(0.003)
SUR_{US}	0.013*	-0.005	0.005	-0.002	0.005	-0.010*
	(0.022)	(0.623)	(0.235)	(0.774)	(0.370)	(0.036)
SUR_{AU}	-0.002	0.008	0.000	0.007	0.001	0.004
	(0.602)	(0.230)	(0.947)	(0.186)	(0.819)	(0.305)
OIS_{AU}	-0.201	-0.637***	-0.263**	-0.285*	0.087	0.059
	(0.092)	(0.001)	(0.009)	(0.025)	(0.551)	(0.545)
CDS_{US}	0.026*	0.052*	0.024*	-0.001	-0.012	-0.012
	(0.038)	(0.015)	(0.019)	(0.954)	(0.457)	(0.302)
CDS_{AU}	-0.014	-0.014	-0.011	0.006	0.003	0.016
	(0.051)	(0.371)	(0.116)	(0.499)	(0.787)	(0.061)
Intercept	0.527	2.586*	0.444	0.999	0.812	-0.752
	(0.331)	(0.011)	(0.306)	(0.065)	(0.126)	(0.061)
Adjusted R^2	0.056	0.137	0.044	0.083	0.016	0.053
Observations	714	714	714	714	714	714

Table 38: Results of 60-day Rolling Pairwise Volatility Spillover Indices (Full Sample – SOMA Portfolio)

Note. This table displays the result of the following regression estimated using OLS: $S^g_{ij}(H)_t = \alpha_t + \beta_1 QE_{SOMA_t} + \beta_2 D_{QE_t} + \beta_3 SUR_{G_t} + \beta_4 SUR_{US_t} + \beta_5 SUR_{AU_t} + \beta_6 OIS_{AU_t} + \beta_7 CDS_{US_t} + \beta_8 CDS_{AU_t} + \varepsilon_t$. The p-values (in parentheses below the coefficients) are derived from Newey and West (1986) heteroskedasticity and autocorrelation consistent standard errors. The levels of significance are defined as follows: '***' implies significance at the 0.1% level, '**' implies significance at the 1% level, and '*' implies significance at the 5% level.

Crisis Period: 2007–2012

	VIX/MOVE	VIX/AVIX	VIX/AGSVIX	MOVE/AVIX	MOVE/AGSVIX	AVIX/AGSVIX
QE_{SOMA}	-8.991*	-20.312*	-4.661	-5.750	-3.130	-3.001
	(0.012)	(0.019)	(0.455)	(0.297)	(0.523)	(0.477)
D_{QE}	0.864	2.302*	-0.315	0.425	-0.531	0.515
	(0.056)	(0.040)	(0.716)	(0.499)	(0.321)	(0.318)
SUR_G	-0.028*	0.005	0.006	0.014	0.005	0.027*
	(0.032)	(0.797)	(0.538)	(0.444)	(0.694)	(0.015)
SUR_{US}	0.015**	-0.018	0.005	-0.008	-0.003	-0.015**
	(0.007)	(0.091)	(0.272)	(0.355)	(0.582)	(0.008)
SUR_{AU}	0.010**	0.018	0.003	0.007	-0.005	0.002
	(0.004)	(0.063)	(0.509)	(0.395)	(0.415)	(0.696)
OIS_{AU}	0.076	-0.777**	-0.029	0.213	0.265	0.233
	(0.571)	(0.003)	(0.876)	(0.180)	(0.241)	(0.205)
CDS_{US}	0.013	0.025	0.012	-0.008	-0.009	-0.017
	(0.135)	(0.137)	(0.302)	(0.570)	(0.692)	(0.221)
CDS_{AU}	-0.010	-0.005	-0.002	0.017*	0.005	0.022*
	(0.100)	(0.709)	(0.776)	(0.048)	(0.686)	(0.042)
Intercept	-0.094	4.954*	-0.579	-2.252**	-0.823	-2.058
	(0.915)	(0.013)	(0.640)	(0.008)	(0.362)	(0.089)
Adjusted R^2	0.133	0.253	0.015	0.084	0.022	0.079
Observations	313	313	313	313	313	313

Table 39: Results of 60-day Rolling Pairwise Volatility Spillover Indices (Crisis Period – SOMA Portfolio)

Note. This table displays the result of the following regression estimated using OLS: $S^g_{ij}(H)_t = \alpha_t + \beta_1 QE_{SOMA_t} + \beta_2 D_{QE_t} + \beta_3 SUR_{G_t} + \beta_4 SUR_{US_t} + \beta_5 SUR_{AU_t} + \beta_6 OIS_{AU_t} + \beta_7 CDS_{US_t} + \beta_8 CDS_{AU_t} + \varepsilon_t$. The p-values (in parentheses below the coefficients) are derived from Newey and West (1986) heteroskedasticity and autocorrelation consistent standard errors. The levels of significance are defined as follows: '***' implies significance at the 0.1% level, '**' implies significance at the 1% level, and '*' implies significance at the 5% level.

Normalisation Period: 2013–2019

	VIX/MOVE	VIX/AVIX	VIX/AGSVIX	MOVE/AVIX	MOVE/AGSVIX	AVIX/AGSVIX
QE_{SOMA}	-0.935	-24.905	46.694	48.745	64.193	-17.324
	(0.973)	(0.603)	(0.131)	(0.235)	(0.120)	(0.408)
D_{QE}	-0.722*	0.533	-0.321	-0.186	0.696	0.179
	(0.044)	(0.451)	(0.324)	(0.672)	(0.139)	(0.683)
SUR_G	0.028*	0.000	0.021	-0.038*	-0.028	0.029*
	(0.032)	(0.995)	(0.252)	(0.012)	(0.087)	(0.012)
SUR_{US}	0.004	0.017	0.003	0.018	0.018	-0.003
	(0.579)	(0.207)	(0.739)	(0.052)	(0.133)	(0.732)
SUR_{AU}	-0.008	-0.008	-0.001	0.007	0.010	0.004
	(0.145)	(0.416)	(0.876)	(0.130)	(0.313)	(0.439)
OIS_{AU}	0.300	-2.149***	-0.714	-2.626***	-0.307	-0.288
	(0.564)	(0.001)	(0.089)	(0.000)	(0.719)	(0.411)
CDS_{US}	0.066*	0.125*	0.042	-0.061*	-0.081**	-0.017
	(0.050)	(0.038)	(0.177)	(0.032)	(0.003)	(0.613)
CDS_{AU}	-0.056*	-0.028	-0.028	0.083***	0.039*	0.010
	(0.015)	(0.522)	(0.154)	(0.000)	(0.020)	(0.621)
Intercept	0.857	1.850	1.630	2.522*	2.765	0.782
	(0.343)	(0.363)	(0.135)	(0.029)	(0.065)	(0.444)
Adjusted R^2	0.157	0.149	0.082	0.263	0.095	0.067
Observations	362	362	362	362	362	362

Table 40: Results of 60-day Rolling Pairwise Volatility Spillover Indices (Normalisation Period – SOMA Portfolio)

Note. This table displays the result of the following regression estimated using OLS: $S^g_{ij}(H)_t = \alpha_t + \beta_1 QE_{SOMA_t} + \beta_2 D_{QE_t} + \beta_3 SUR_{G_t} + \beta_4 SUR_{US_t} + \beta_5 SUR_{AU_t} + \beta_6 OIS_{AU_t} + \beta_7 CDS_{US_t} + \beta_8 CDS_{AU_t} + \varepsilon_t$. The p-values (in parentheses below the coefficients) are derived from Newey and West (1986) heteroskedasticity and autocorrelation consistent standard errors. The levels of significance are defined as follows: '***' implies significance at the 0.1% level, '**' implies significance at the 1% level, and '*' implies significance at the 5% level.

Full Sample: 2006–2019

	VIX/MOVE	VIX/AVIX	VIX/AGSVIX	MOVE/AVIX	MOVE/AGSVIX	AVIX/AGSVIX
QE_{SOMA}	-1.837	-16.304*	-4.196	-10.567*	-1.860	-3.862
	(0.473)	(0.045)	(0.397)	(0.039)	(0.626)	(0.240)
D_{QE}	-0.183	0.513	0.068	-0.041	0.490	-0.077
	(0.337)	(0.419)	(0.766)	(0.899)	(0.217)	(0.768)
SUR_G	-0.014	-0.001	0.007	-0.001	-0.010	0.011*
	(0.094)	(0.967)	(0.274)	(0.950)	(0.327)	(0.028)
SUR_{US}	0.012**	0.000	0.003	-0.001	0.006	-0.005
	(0.010)	(0.990)	(0.428)	(0.802)	(0.246)	(0.081)
SUR_{AU}	0.002	0.009	-0.002	0.004	0.001	0.000
	(0.472)	(0.215)	(0.330)	(0.320)	(0.657)	(0.801)
OIS_{AU}	-0.188*	-0.575**	-0.128	-0.264*	0.108	0.037
	(0.039)	(0.004)	(0.099)	(0.017)	(0.385)	(0.581)
CDS_{US}	0.014	0.053*	0.010	0.008	-0.005	-0.005
	(0.120)	(0.022)	(0.220)	(0.553)	(0.726)	(0.560)
CDS_{AU}	-0.008	-0.012	-0.003	0.000	-0.004	0.004
	(0.161)	(0.449)	(0.544)	(0.971)	(0.654)	(0.457)
Intercept	0.559	2.770**	0.296	0.914	0.727	-0.115
	(0.190)	(0.009)	(0.427)	(0.069)	(0.150)	(0.683)
Adjusted R^2	0.094	0.172	0.035	0.081	0.050	0.023
Observations	712	712	712	712	712	712

Table 41: Results of 70-day Rolling Pairwise Volatility Spillover Indices (Full Sample – SOMA Portfolio)

Note. This table displays the result of the following regression estimated using OLS: $S^g_{ij}(H)_t = \alpha_t + \beta_1 QE_{SOMA_t} + \beta_2 D_{QE_t} + \beta_3 SUR_{G_t} + \beta_4 SUR_{US_t} + \beta_5 SUR_{AU_t} + \beta_6 OIS_{AU_t} + \beta_7 CDS_{US_t} + \beta_8 CDS_{AU_t} + \varepsilon_t$. The p-values (in parentheses below the coefficients) are derived from Newey and West (1986) heteroskedasticity and autocorrelation consistent standard errors. The levels of significance are defined as follows: '***' implies significance at the 0.1% level, '**' implies significance at the 1% level, and '*' implies significance at the 5% level.

Crisis Period: 2007–2012

	VIX/MOVE	VIX/AVIX	VIX/AGSVIX	MOVE/AVIX	MOVE/AGSVIX	AVIX/AGSVIX
QE_{SOMA}	-1.624	-18.608*	-5.006	-6.568	2.857	-1.887
	(0.502)	(0.028)	(0.172)	(0.070)	(0.521)	(0.492)
D_{QE}	0.384	2.067	0.423	0.338	-0.511	-0.043
	(0.193)	(0.057)	(0.325)	(0.492)	(0.401)	(0.919)
SUR_G	-0.021*	0.003	0.013	0.007	0.011	0.013*
	(0.044)	(0.856)	(0.052)	(0.682)	(0.278)	(0.038)
SUR_{US}	0.012*	-0.012	-0.001	-0.001	-0.004	-0.008*
	(0.019)	(0.267)	(0.845)	(0.853)	(0.333)	(0.012)
SUR_{AU}	0.008**	0.019*	-0.003	0.007	-0.003	-0.001
	(0.002)	(0.046)	(0.366)	(0.181)	(0.599)	(0.836)
OIS_{AU}	-0.065	-0.741**	0.017	0.191	0.349	0.223
	(0.463)	(0.002)	(0.895)	(0.182)	(0.055)	(0.078)
CDS_{US}	0.005	0.026	-0.002	0.002	-0.006	-0.009
	(0.405)	(0.090)	(0.785)	(0.864)	(0.698)	(0.219)
CDS_{AU}	-0.005	-0.001	0.007	0.007	0.003	0.009
	(0.218)	(0.905)	(0.206)	(0.202)	(0.669)	(0.073)
Intercept	0.422	4.961**	-0.431	-1.850*	-1.291	-1.299
	(0.510)	(0.007)	(0.603)	(0.047)	(0.194)	(0.121)
Adjusted R^2	0.141	0.361	0.043	0.100	0.101	0.064
Observations	313	313	313	313	313	313

Table 42: Results of 70-day Rolling Pairwise Volatility Spillover Indices (Crisis Period – SOMA Portfolio)

Note. This table displays the result of the following regression estimated using OLS: $S^g_{ij}(H)_t = \alpha_t + \beta_1 QE_{SOMA_t} + \beta_2 D_{QE_t} + \beta_3 SUR_{G_t} + \beta_4 SUR_{US_t} + \beta_5 SUR_{AU_t} + \beta_6 OIS_{AU_t} + \beta_7 CDS_{US_t} + \beta_8 CDS_{AU_t} + \varepsilon_t$. The p-values (in parentheses below the coefficients) are derived from Newey and West (1986) heteroskedasticity and autocorrelation consistent standard errors. The levels of significance are defined as follows: '***' implies significance at the 0.1% level, '**' implies significance at the 1% level, and '*' implies significance at the 5% level.

Normalisation Period: 2013–2019

	VIX/MOVE	VIX/AVIX	VIX/AGSVIX	MOVE/AVIX	MOVE/AGSVIX	AVIX/AGSVIX
QE_{SOMA}	-32.044	-11.233	21.046	79.561*	62.567	13.529
	(0.124)	(0.816)	(0.437)	(0.021)	(0.134)	(0.359)
D_{QE}	-0.405	0.309	-0.140	-0.128	0.652	-0.167
	(0.060)	(0.698)	(0.609)	(0.706)	(0.098)	(0.556)
SUR_G	0.017*	-0.026	0.015	-0.026*	-0.036*	0.019**
	(0.040)	(0.351)	(0.241)	(0.026)	(0.024)	(0.002)
SUR_{US}	0.006	0.023	0.002	0.008	0.021*	0.000
	(0.274)	(0.104)	(0.799)	(0.221)	(0.040)	(0.940)
SUR_{AU}	-0.002	-0.013	-0.002	0.002	0.009	0.004
	(0.706)	(0.199)	(0.651)	(0.630)	(0.247)	(0.288)
OIS_{AU}	0.581	-2.460***	-0.143	-2.456***	-0.383	-0.348
	(0.115)	(0.000)	(0.705)	(0.000)	(0.620)	(0.128)
CDS_{US}	0.057*	0.120*	0.024	-0.044	-0.072***	0.003
	(0.035)	(0.046)	(0.321)	(0.054)	(0.000)	(0.857)
CDS_{AU}	-0.050*	-0.014	-0.032	0.067***	0.032*	-0.001
	(0.012)	(0.753)	(0.075)	(0.000)	(0.021)	(0.917)
Intercept	0.116	1.969	1.913*	2.378*	2.902*	0.530
	(0.880)	(0.273)	(0.019)	(0.030)	(0.025)	(0.335)
Adjusted R^2	0.199	0.184	0.109	0.310	0.156	0.095
Observations	362	362	362	362	362	362

Table 43: Results of 70-day Rolling Pairwise Volatility Spillover Indices (Normalisation Period – SOMA Portfolio)

Note. This table displays the result of the following regression estimated using OLS: $S^g_{ij}(H)_t = \alpha_t + \beta_1 QE_{SOMA_t} + \beta_2 D_{QE_t} + \beta_3 SUR_{G_t} + \beta_4 SUR_{US_t} + \beta_5 SUR_{AU_t} + \beta_6 OIS_{AU_t} + \beta_7 CDS_{US_t} + \beta_8 CDS_{AU_t} + \varepsilon_t$. The p-values (in parentheses below the coefficients) are derived from Newey and West (1986) heteroskedasticity and autocorrelation consistent standard errors. The levels of significance are defined as follows: '***' implies significance at the 0.1% level, '**' implies significance at the 1% level, and '*' implies significance at the 5% level.

Full Sample: 2006–2019

	VIX/MOVE	VIX/AVIX	VIX/AGSVIX	MOVE/AVIX	MOVE/AGSVIX	AVIX/AGSVIX
QE_{SOMA}	-9.637**	-22.459*	1.080	-11.857	-2.651	-3.680
	(0.007)	(0.016)	(0.839)	(0.083)	(0.453)	(0.231)
D_{QE}	-0.259	0.321	-0.225	0.190	0.096	0.260
	(0.265)	(0.614)	(0.520)	(0.514)	(0.792)	(0.276)
SUR_G	-0.014	-0.006	0.003	0.002	-0.010	0.015*
	(0.146)	(0.755)	(0.741)	(0.852)	(0.295)	(0.016)
SUR_{US}	0.013*	0.006	0.007	-0.002	0.005	-0.007
	(0.011)	(0.581)	(0.104)	(0.783)	(0.288)	(0.061)
SUR_{AU}	-0.001	0.008	-0.001	0.003	0.000	0.006*
	(0.749)	(0.271)	(0.824)	(0.524)	(0.921)	(0.030)
OIS_{AU}	-0.225*	-0.654***	-0.250**	-0.303*	0.084	0.063
	(0.042)	(0.001)	(0.005)	(0.011)	(0.512)	(0.450)
CDS_{US}	0.026*	0.053*	0.024**	-0.006	-0.008	-0.011
	(0.024)	(0.018)	(0.004)	(0.704)	(0.561)	(0.162)
CDS_{AU}	-0.015*	-0.012	-0.013*	0.010	0.001	0.012*
	(0.035)	(0.442)	(0.039)	(0.297)	(0.911)	(0.031)
Intercept	0.648	2.934**	0.585	1.162*	0.571	-0.490
	(0.202)	(0.005)	(0.142)	(0.032)	(0.264)	(0.167)
Adjusted R^2	0.103	0.184	0.067	0.111	0.016	0.064
Observations	710	710	710	710	710	710

Table 44: Results of 80-day Rolling Pairwise Volatility Spillover Indices (Full Sample – SOMA Portfolio)

Note. This table displays the result of the following regression estimated using OLS: $S^g_{ij}(H)_t = \alpha_t + \beta_1 QE_{SOMA_t} + \beta_2 D_{QE_t} + \beta_3 SUR_{G_t} + \beta_4 SUR_{US_t} + \beta_5 SUR_{AU_t} + \beta_6 OIS_{AU_t} + \beta_7 CDS_{US_t} + \beta_8 CDS_{AU_t} + \varepsilon_t$. The p-values (in parentheses below the coefficients) are derived from Newey and West (1986) heteroskedasticity and autocorrelation consistent standard errors. The levels of significance are defined as follows: '***' implies significance at the 0.1% level, '**' implies significance at the 1% level, and '*' implies significance at the 5% level.

Crisis Period: 2007–2012

	VIX/MOVE	VIX/AVIX	VIX/AGSVIX	MOVE/AVIX	MOVE/AGSVIX	AVIX/AGSVIX
QE_{SOMA}	-9.183*	-24.265**	0.578	-7.556	-0.555	-4.041
	(0.012)	(0.005)	(0.913)	(0.064)	(0.892)	(0.174)
D_{QE}	0.294	2.474**	0.044	1.006**	-0.791	0.633
	(0.439)	(0.008)	(0.951)	(0.002)	(0.172)	(0.064)
SUR_G	-0.033**	0.005	0.007	0.019	0.009	0.017**
	(0.002)	(0.763)	(0.377)	(0.293)	(0.369)	(0.008)
SUR_{US}	0.017***	-0.008	0.004	-0.005	-0.003	-0.010**
	(0.000)	(0.431)	(0.328)	(0.546)	(0.412)	(0.008)
SUR_{AU}	0.006**	0.016	0.000	0.006	-0.004	0.005
	(0.004)	(0.104)	(0.986)	(0.390)	(0.397)	(0.241)
OIS_{AU}	-0.082	-0.735***	-0.108	0.172	0.259	0.164
	(0.539)	(0.000)	(0.446)	(0.293)	(0.113)	(0.203)
CDS_{US}	0.017**	0.029	0.015	-0.009	-0.010	-0.016*
	(0.005)	(0.051)	(0.072)	(0.525)	(0.541)	(0.013)
CDS_{AU}	-0.015***	0.001	-0.005	0.020*	0.008	0.017***
	(0.001)	(0.954)	(0.440)	(0.015)	(0.367)	(0.000)
Intercept	0.943	4.149**	-0.151	-2.355*	-0.984	-1.209
	(0.259)	(0.009)	(0.877)	(0.021)	(0.167)	(0.115)
Adjusted R^2	0.206	0.357	0.040	0.124	0.042	0.089
Observations	313	313	313	313	313	313

Table 45: Results of 80-day Rolling Pairwise Volatility Spillover Indices (Crisis Period – SOMA Portfolio)

Note. This table displays the result of the following regression estimated using OLS: $S^g_{ij}(H)_t = \alpha_t + \beta_1 QE_{SOMA_t} + \beta_2 D_{QE_t} + \beta_3 SUR_{G_t} + \beta_4 SUR_{US_t} + \beta_5 SUR_{AU_t} + \beta_6 OIS_{AU_t} + \beta_7 CDS_{US_t} + \beta_8 CDS_{AU_t} + \varepsilon_t$. The p-values (in parentheses below the coefficients) are derived from Newey and West (1986) heteroskedasticity and autocorrelation consistent standard errors. The levels of significance are defined as follows: '***' implies significance at the 0.1% level, '**' implies significance at the 1% level, and '*' implies significance at the 5% level.

Normalisation Period: 2013–2019

	VIX/MOVE	VIX/AVIX	VIX/AGSVIX	MOVE/AVIX	MOVE/AGSVIX	AVIX/AGSVIX
QE_{SOMA}	-9.460	-49.532	28.978	50.587	96.464*	15.853
	(0.704)	(0.253)	(0.315)	(0.140)	(0.039)	(0.322)
D_{QE}	-0.563*	-0.274	-0.344	-0.010	0.303	0.037
	(0.013)	(0.651)	(0.326)	(0.971)	(0.399)	(0.903)
SUR_G	0.023*	-0.030	0.012	-0.031*	-0.037*	0.026**
	(0.035)	(0.232)	(0.525)	(0.016)	(0.016)	(0.008)
SUR_{US}	0.007	0.031*	0.006	0.012	0.017	-0.004
	(0.341)	(0.023)	(0.396)	(0.119)	(0.065)	(0.520)
SUR_{AU}	0.001	-0.011	-0.002	-0.004	0.004	0.007
	(0.895)	(0.265)	(0.693)	(0.374)	(0.530)	(0.166)
OIS_{AU}	0.032	-2.324***	-0.343	-2.419***	-0.684	-0.001
	(0.947)	(0.000)	(0.400)	(0.000)	(0.378)	(0.997)
CDS_{US}	0.060	0.096	0.038	-0.068**	-0.075**	0.010
	(0.068)	(0.122)	(0.168)	(0.004)	(0.002)	(0.715)
CDS_{AU}	-0.041	-0.014	-0.034	0.081***	0.035*	-0.009
	(0.066)	(0.766)	(0.068)	(0.000)	(0.020)	(0.614)
Intercept	0.344	3.361	1.767	2.988*	3.307*	0.147
	(0.694)	(0.099)	(0.059)	(0.011)	(0.023)	(0.846)
Adjusted R^2	0.149	0.190	0.101	0.345	0.174	0.079
Observations	362	362	362	362	362	362

Table 46: Results of 80-day Rolling Pairwise Volatility Spillover Indices (Normalisation Period – SOMA Portfolio)

Note. This table displays the result of the following regression estimated using OLS: $S^g_{ij}(H)_t = \alpha_t + \beta_1 QE_{SOMA_t} + \beta_2 D_{QE_t} + \beta_3 SUR_{G_t} + \beta_4 SUR_{US_t} + \beta_5 SUR_{AU_t} + \beta_6 OIS_{AU_t} + \beta_7 CDS_{US_t} + \beta_8 CDS_{AU_t} + \varepsilon_t$. The p-values (in parentheses below the coefficients) are derived from Newey and West (1986) heteroskedasticity and autocorrelation consistent standard errors. The levels of significance are defined as follows: '***' implies significance at the 0.1% level, '**' implies significance at the 1% level, and '*' implies significance at the 5% level.

Full Sample: 2006–2019

	VIX/MOVE	VIX/AVIX	VIX/AGSVIX	MOVE/AVIX	MOVE/AGSVIX	AVIX/AGSVIX
QE_{SOMA}	-6.269*	-20.394	0.544	-10.868	0.709	-1.013
	(0.047)	(0.058)	(0.893)	(0.096)	(0.835)	(0.728)
D_{QE}	-0.477*	0.163	-0.078	0.094	0.311	0.189
	(0.034)	(0.798)	(0.806)	(0.714)	(0.383)	(0.396)
SUR_G	-0.016	-0.011	0.000	0.005	-0.010	0.010
	(0.098)	(0.594)	(0.961)	(0.714)	(0.287)	(0.097)
SUR_{US}	0.012*	0.011	0.008	-0.001	0.004	-0.006
	(0.017)	(0.363)	(0.061)	(0.866)	(0.336)	(0.142)
SUR_{AU}	-0.001	0.009	0.000	0.003	-0.001	0.005*
	(0.790)	(0.242)	(0.965)	(0.582)	(0.775)	(0.031)
OIS_{AU}	-0.223*	-0.654**	-0.248**	-0.311**	0.068	0.081
	(0.038)	(0.002)	(0.004)	(0.007)	(0.566)	(0.315)
CDS_{US}	0.026*	0.053*	0.024**	-0.008	-0.008	-0.007
	(0.023)	(0.023)	(0.003)	(0.593)	(0.526)	(0.342)
CDS_{AU}	-0.016*	-0.012	-0.013*	0.012	0.001	0.009
	(0.027)	(0.486)	(0.027)	(0.222)	(0.881)	(0.104)
Intercept	0.735	3.036**	0.635	1.186*	0.558	-0.526
	(0.135)	(0.004)	(0.097)	(0.027)	(0.252)	(0.122)
Adjusted R^2	0.110	0.200	0.077	0.132	0.016	0.056
Observations	708	708	708	708	708	708

Table 47: Results of 90-day Rolling Pairwise Volatility Spillover Indices (Full Sample – SOMA Portfolio)

Note. This table displays the result of the following regression estimated using OLS: $S^g_{ij}(H)_t = \alpha_t + \beta_1 QE_{SOMA_t} + \beta_2 D_{QE_t} + \beta_3 SUR_{G_t} + \beta_4 SUR_{US_t} + \beta_5 SUR_{AU_t} + \beta_6 OIS_{AU_t} + \beta_7 CDS_{US_t} + \beta_8 CDS_{AU_t} + \varepsilon_t$. The p-values (in parentheses below the coefficients) are derived from Newey and West (1986) heteroskedasticity and autocorrelation consistent standard errors. The levels of significance are defined as follows: '***' implies significance at the 0.1% level, '**' implies significance at the 1% level, and '*' implies significance at the 5% level.

Crisis Period: 2007–2012

	VIX/MOVE	VIX/AVIX	VIX/AGSVIX	MOVE/AVIX	MOVE/AGSVIX	AVIX/AGSVIX
QE_{SOMA}	-5.477*	-20.861*	0.034	-6.528	2.658	-1.398
	(0.050)	(0.025)	(0.993)	(0.119)	(0.503)	(0.615)
D_{QE}	0.052	2.176*	-0.056	0.650	-0.435	0.344
	(0.895)	(0.019)	(0.927)	(0.104)	(0.427)	(0.368)
SUR_G	-0.038***	0.009	0.006	0.025	0.008	0.013*
	(0.000)	(0.586)	(0.414)	(0.160)	(0.340)	(0.027)
SUR_{US}	0.017***	-0.004	0.004	-0.005	-0.004	-0.008*
	(0.000)	(0.692)	(0.265)	(0.551)	(0.200)	(0.024)
SUR_{AU}	0.005*	0.017	0.000	0.006	-0.006	0.006
	(0.024)	(0.103)	(0.999)	(0.353)	(0.249)	(0.098)
OIS_{AU}	-0.093	-0.635***	-0.143	0.176	0.218	0.185
	(0.493)	(0.001)	(0.314)	(0.269)	(0.143)	(0.118)
CDS_{US}	0.018**	0.028	0.016*	-0.011	-0.009	-0.013*
	(0.004)	(0.052)	(0.035)	(0.426)	(0.529)	(0.020)
CDS_{AU}	-0.017***	0.006	-0.006	0.022**	0.007	0.015***
	(0.000)	(0.647)	(0.297)	(0.006)	(0.372)	(0.000)
Intercept	1.150	3.239*	0.026	-2.572*	-0.795	-1.284
	(0.169)	(0.036)	(0.978)	(0.014)	(0.245)	(0.071)
Adjusted R^2	0.267	0.384	0.055	0.157	0.042	0.084
Observations	313	313	313	313	313	313

Table 48: Results of 90-day Rolling Pairwise Volatility Spillover Indices (Crisis Period – SOMA Portfolio)

Note. This table displays the result of the following regression estimated using OLS: $S^g_{ij}(H)_t = \alpha_t + \beta_1 QE_{SOMA_t} + \beta_2 D_{QE_t} + \beta_3 SUR_{G_t} + \beta_4 SUR_{US_t} + \beta_5 SUR_{AU_t} + \beta_6 OIS_{AU_t} + \beta_7 CDS_{US_t} + \beta_8 CDS_{AU_t} + \varepsilon_t$. The p-values (in parentheses below the coefficients) are derived from Newey and West (1986) heteroskedasticity and autocorrelation consistent standard errors. The levels of significance are defined as follows: '***' implies significance at the 0.1% level, '**' implies significance at the 1% level, and '*' implies significance at the 5% level.

Normalisation Period: 2013–2019

	VIX/MOVE	VIX/AVIX	VIX/AGSVIX	MOVE/AVIX	MOVE/AGSVIX	AVIX/AGSVIX
QE_{SOMA}	-21.746	-75.699	34.220	55.480	102.373*	11.782
	(0.347)	(0.082)	(0.166)	(0.080)	(0.023)	(0.400)
D_{QE}	-0.782***	-0.299	-0.104	0.058	0.396	0.197
	(0.001)	(0.688)	(0.742)	(0.797)	(0.228)	(0.499)
SUR_G	0.022*	-0.040	0.006	-0.030**	-0.037**	0.021*
	(0.043)	(0.105)	(0.738)	(0.010)	(0.010)	(0.023)
SUR_{US}	0.005	0.037**	0.008	0.012	0.018*	-0.005
	(0.536)	(0.010)	(0.290)	(0.062)	(0.024)	(0.408)
SUR_{AU}	0.003	-0.012	-0.001	-0.006	0.005	0.002
	(0.650)	(0.225)	(0.863)	(0.162)	(0.280)	(0.688)
OIS_{AU}	0.053	-2.225**	-0.231	-2.359***	-0.780	0.124
	(0.909)	(0.002)	(0.548)	(0.000)	(0.252)	(0.666)
CDS_{US}	0.066	0.094	0.035	-0.081***	-0.077***	0.024
	(0.053)	(0.134)	(0.214)	(0.000)	(0.001)	(0.300)
CDS_{AU}	-0.043	-0.016	-0.034	0.084***	0.039**	-0.019
	(0.061)	(0.740)	(0.073)	(0.000)	(0.004)	(0.256)
Intercept	0.069	3.700	1.703*	3.501**	3.206*	-0.170
	(0.937)	(0.066)	(0.044)	(0.002)	(0.019)	(0.814)
Adjusted R^2	0.152	0.217	0.097	0.396	0.222	0.057
Observations	362	362	362	362	362	362

Table 49: Results of 90-day Rolling Pairwise Volatility Spillover Indices (Normalisation Period – SOMA Portfolio)

Note. This table displays the result of the following regression estimated using OLS: $S^g_{ij}(H)_t = \alpha_t + \beta_1 QE_{SOMA_t} + \beta_2 D_{QE_t} + \beta_3 SUR_{G_t} + \beta_4 SUR_{US_t} + \beta_5 SUR_{AU_t} + \beta_6 OIS_{AU_t} + \beta_7 CDS_{US_t} + \beta_8 CDS_{AU_t} + \varepsilon_t$. The p-values (in parentheses below the coefficients) are derived from Newey and West (1986) heteroskedasticity and autocorrelation consistent standard errors. The levels of significance are defined as follows: '***' implies significance at the 0.1% level, '**' implies significance at the 1% level, and '*' implies significance at the 5% level.

Appendix D: Descriptive Statistics of Control Variables

	Levels					
	SUR_G	SUR_{US}	SUR_{AU}	OIS_{AU}	CDS_{US}	CDS_{AU}
Mean	1.104	-1.347	13.399	3.462	84.316	106.964
Median	0.800	-2.000	10.000	2.990	75.894	98.340
Maximum	56.800	97.500	177.800	7.315	279.670	446.500
Minimum	-99.500	-140.600	-91.900	0.723	28.880	23.250
Std. Dev	25.066	40.850	39.503	1.837	38.245	63.155
Skewness	-0.706	-0.332	0.368	0.573	1.738	2.011
Excess Kurtosis	1.377	-0.137	0.555	-0.910	4.194	6.044
Jarque-Bera χ^2	561.450***	66.312***	122.580***	309.440***	4285.900***	7614.200***
Observations	3467	3467	3467	3467	3467	3467

Table 50: Descriptive Statistics of Control Variables

Note. The following table displays the descriptive statistics for each of the control variables. The Jarque and Bera (1980) test examines whether the third and fourth moments of the data match those of the normal distribution. The levels of significance are defined as follows: '***' implies significance at the 0.1% level, '**' implies significance at the 1% level, and '*' implies significance at the 5% level.

	Levels					
	SUR_G	SUR_{US}	SUR_{AU}	OIS_{AU}	CDS_{US}	CDS_{AU}
SUR_G	1.000					
SUR_{US}	0.660***	1.000				
SUR_{AU}	-0.074***	-0.162***	1.000			
OIS_{AU}	0.142***	-0.020	0.030	1.000		
CDS_{US}	-0.415***	-0.210***	0.085***	0.175***	1.000	
CDS_{AU}	-0.499***	-0.200***	0.057***	-0.044**	0.926***	1.000

Table 51: Pairwise Pearson Correlation Matrix of Control Variables

Note. The following table displays the Pearson correlation coefficients across each pair of control variables. The levels of significance are defined as follows: '***' implies significance at the 0.1% level, '**' implies significance at the 1% level, and '*' implies significance at the 5% level.

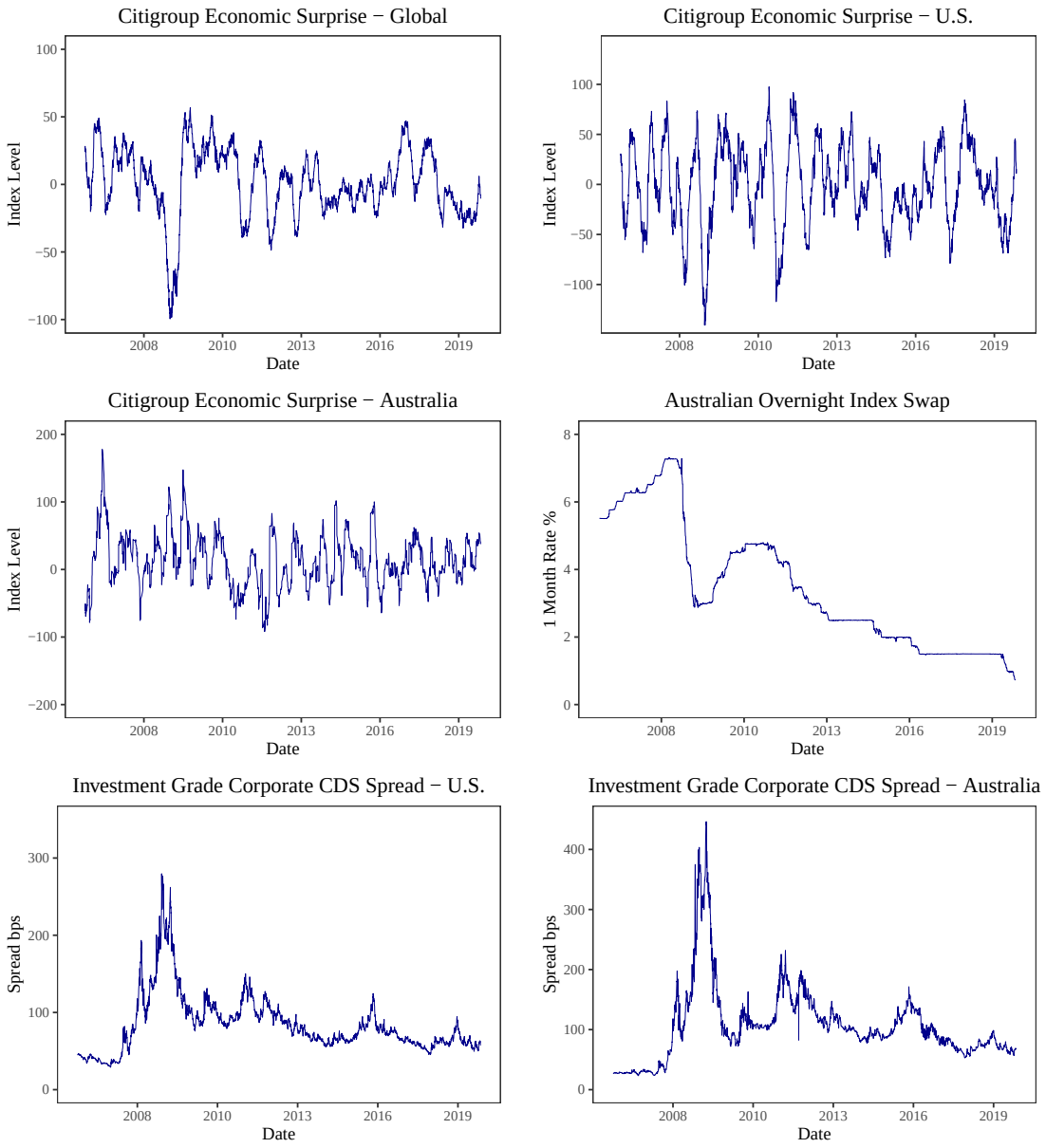

Figure 25: Control Variable Charts

Note. The following charts illustrate each of the six control variables used in the regression models to test the influence of the Federal Reserve's QE programs on volatility spillovers.

Appendix E: Descriptive Statistics of Pairwise Volatility Spillover Indices

	Levels					
	VIX/MOVE	VIX/AVIX	VIX/AGSVIX	MOVE/AVIX	MOVE/AGSVIX	AVIX/AGSVIX
Mean	0.297	4.358	0.099	0.405	-0.018	0.017
Median	0.284	4.032	0.096	0.382	-0.012	0.006
Maximum	0.776	9.006	0.650	1.406	0.133	0.415
Minimum	-0.371	3.230	-0.088	-0.068	-0.609	-0.171
Std. Dev	0.095	1.109	0.067	0.250	0.037	0.030
Skewness	0.223	3.008	2.638	1.758	-6.891	4.284
Ex. Kurtosis	10.117	8.364	11.778	3.927	93.613	38.248
JB χ^2	14815***	15333***	24059***	4013***	1293374***	221930***
Observations	3467	3467	3467	3467	3467	3467

Table 52: Descriptive Statistics of Volatility Spillover Indices

Note. The following table displays the descriptive statistics for each of the recursively constructed volatility spillover indices with an H-step-ahead forecast horizon of 12 days. The Jarque and Bera (1980) test examines whether the third and fourth moments of the data match those of the normal distribution. The levels of significance are defined as follows: '***' implies significance at the 0.1% level, '**' implies significance at the 1% level, and '*' implies significance at the 5% level.

	Levels					
	VIX/MOVE	VIX/AVIX	VIX/AGSVIX	MOVE/AVIX	MOVE/AGSVIX	AVIX/AGSVIX
VIX/MOVE	1.000					
VIX/AVIX	-0.479***	1.000				
VIX/AGSVIX	0.378***	-0.246***	1.000			
MOVE/AVIX	-0.677***	0.932***	-0.283***	1.000		
MOVE/AGSVIX	-0.177***	0.130***	0.171***	0.167***	1.000	
AVIX/AGSVIX	0.228***	0.391***	-0.121***	0.152***	-0.297***	1.000

Table 53: Pairwise Pearson Correlation Matrix of Volatility Spillover Indices

Note. The following table displays the Pearson correlation coefficients across each pair of the recursively constructed pairwise volatility spillover indices with an H-step-ahead forecast horizon of 12 days. The levels of significance are defined as follows: '***' implies significance at the 0.1% level, '**' implies significance at the 1% level, and '*' implies significance at the 5% level.

Appendix F: Structural Break Significance Testing

To test for structural breaks, each F statistic is aggregated into a holistic test statistic. There are three methods used in this study to aggregate the sequence of F statistics and are based on the work of Andrews (1993) and Andrews and Ploberger (1994). The first method involves aggregating the F statistics as an arithmetic average:

$$Average\ F = \frac{1}{T}\sum_{i=1}^{T} F_t \tag{41}$$

Where T represents the number of observations. Similarly, the supremum of the F statistics, equal to the minimum upper bound, is employed:

$$Supremum\ F = sup\,(F_t) \tag{42}$$

Finally, the exponential F statistic is the natural logarithm of the average of half the exponentiated individual F statistics and constitutes the third aggregation method:

$$Exponential\ F = \ln\left(\frac{1}{T}\sum_{i=1}^{T} e^{\frac{1}{2}F_t}\right) \tag{43}$$

The approximate asymptotic p values of each aggregate statistic are derived by Hansen (1997) and permit testing of the null hypothesis of no structural breaks.

Appendix G: Charts of First–Differences

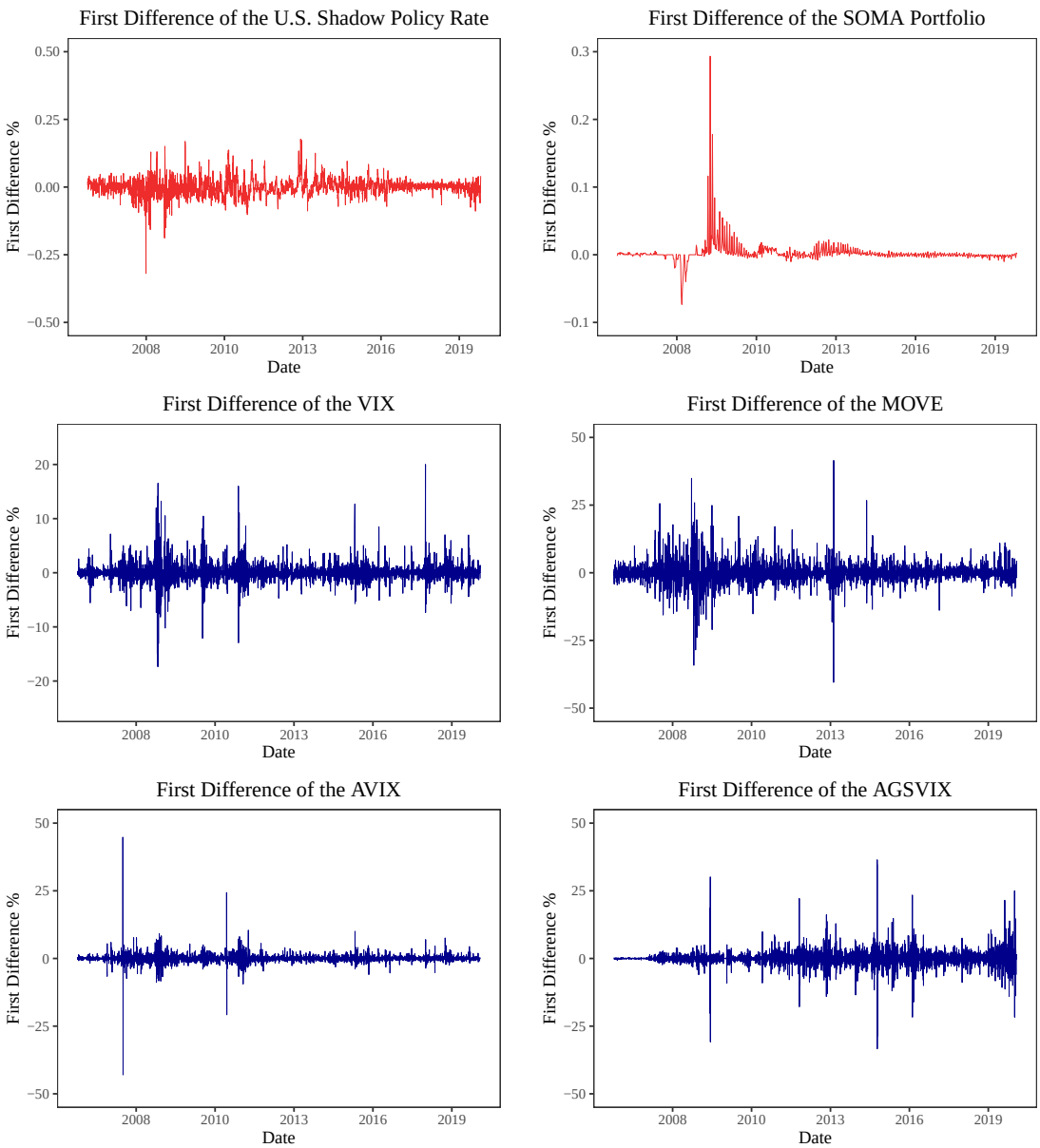

Figure 26: First Differences of the QE Instruments & Implied Volatility Indices

Note. The following charts illustrate the first differences of the QE instruments and implied volatility indices. Since the Federal Reserve's SOMA portfolio is expressed as the weekly change in total asset holdings, it is already in first difference format. As such, no further manipulation is applied.

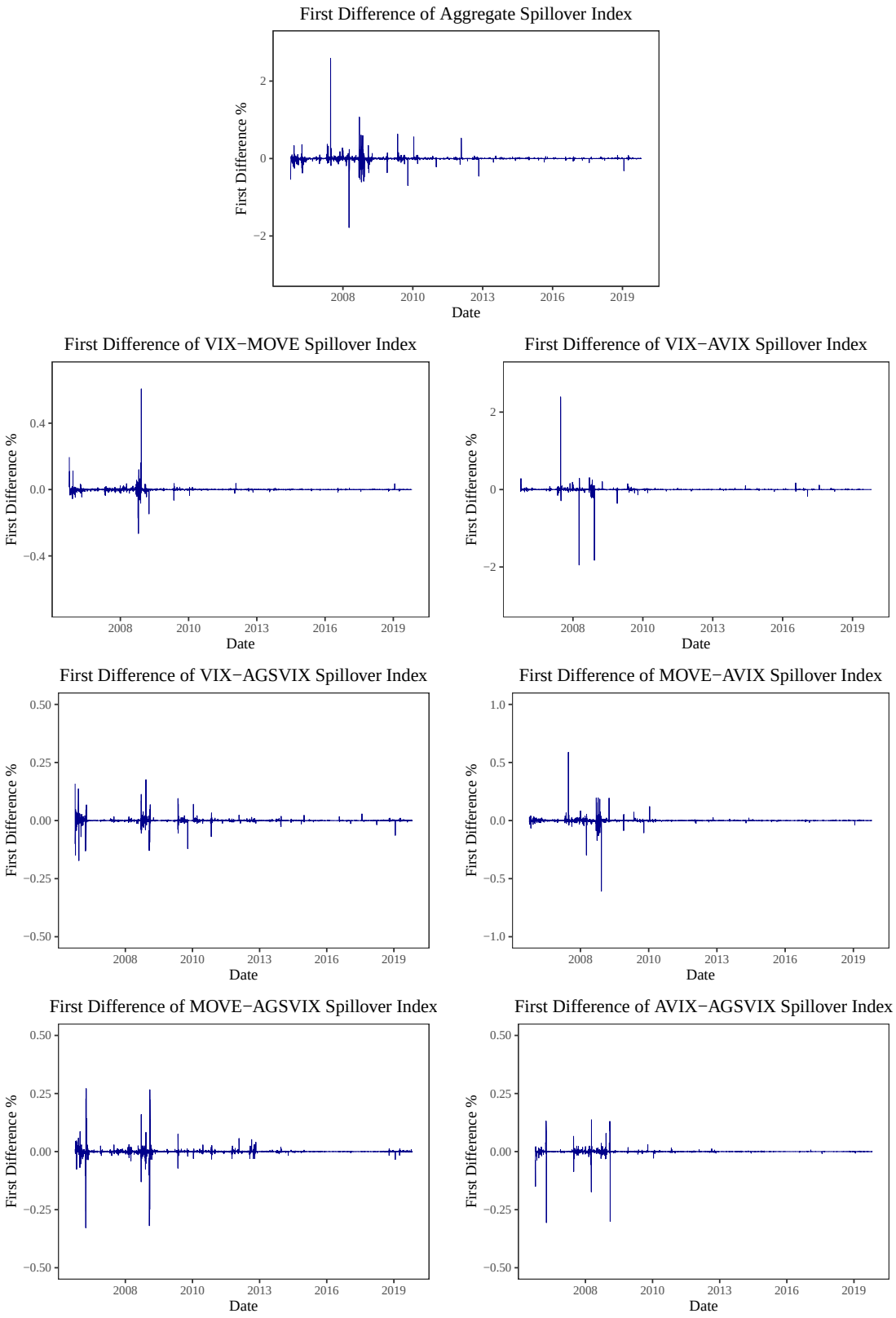

Figure 27: First Differences of the Volatility Spillover Indices

Note. The following charts illustrate the first differences of each volatility spillover index throughout time.